



The Radio and Electronic Engineer

Journal of the Institution of Electronic and Radio Engineers

COUNCIL OF THE INSTITUTION

President:

H. E. DREW, C.B., C.G.I.A., FIERE

Past Presidents:

Professor W. A. Gambling, D.Sc., Ph.D., F.Eng., FIERE

D. W. Heightman, FIERE

Professor W. Gosling, D.Sc., B.Sc., FIERE

Vice-Presidents:

Colonel W. Barker, FIERE

L. A. Bonvini, FIERE

Professor J. R. James, B.Sc., Ph.D., D.Sc., FIERE

P. K. Patwardhan, M.Sc., Ph.D., FIERE

Major-General H. E. Roper, C.B., B.Sc.(Eng.), FIERE

D. L. A. Smith, B.Sc.(Eng.), FIERE

Group Captain J. M. Walker, FIERE

Ordinary and ex-officio Members:

P. Atkinson, B.Sc., MIERE

L. W. Barclay, B.Sc., FIERE

P. V. Betts, MIERE*

W. R. Crooks, B.A., MIERE*

F. G. C. Gunningham, B.Sc., B.A., MIERE*

E. R. Hack, MIERE*

D. J. Houlston, MIERE*

P. J. Hulse, AMIERE

J. J. Jarrett, MIERE

D. J. Kenner, B.Sc., M.Sc., MIERE

R. Larry, FIERE

P. W. Lee, MIERE*

G. A. McKenzie, B.Sc., FIERE

V. Maller, M.A., FIERE

B. Mann, M.Sc., FIERE†

L. March, FIERE*

R. B. Michaelson (Companion)

C. L. Munday, MIERE*

Professor K. G. Nichols, B.Sc., M.Sc., FIERE

B. J. Stanier, MIERE*

K. R. Thrower, MIERE†

Professor R. A. Waldron, M.A., Sc.D., FIERE*

D. E. O'N. Waddington, FIERE*

T. Whiteside, MIERE*

R. H. Whitlock, MIERE*

A. Williams, B.Sc., MIERE*

M. W. Wright (Associate)

* Chairman of a Local Section in the UK

† Ordinary member of the Council who is also a Chairman of a Local Section

Honorary Treasurer

S. R. Wilkins, FIERE

SECRETARY

Sinclair M. Davidson, C.B.E., FIERE

EDITORIAL

Television Systems for DBS 311

IERE NEWS AND COMMENTARY

MAC—Multiplexed Analogue Component Signals 312

Extended PAL Video Coding 312

R. V. Jones Elected an Honorary Fellow 313

Members' Appointments 314

New Books Received 330, 357

Book Review:

The Kingdom of Sand 338

Standard Frequency and Time Service: April 1982 358

Contributors to this Issue 358

Conferences, Courses and Exhibitions 1982-83 iii

PAPERS

Radio Receivers

A reappraisal of h.f. receiver selectivity 315

R. A. BARRS (Rediffusion Radio Systems)

It is pointed out that better front-end selectivity is vital in the improvement of the performance of h.f. communication receivers. Some 10 factors are identified and quantified as hindering good reception and it is then shown how distribution of selectivity between front-end and i.f. amplifiers can lead to considerably improved performance.

Radio Modem Design

An improved 'Piccolo' m.f.s.k. modem for h.f. telegraphy 321

J. D. RALPHS (Foreign and Commonwealth Office)

The changes which have been made to the original Piccolo are described and the advantages discussed, particularly with reference to the improvements it gives in synchronization. The Send and Receive circuits are described as well as the various refinements to error indication and the remote calling system.

Editor:
F. W. Sharp, FIERE

Production Editor:
J. I. Secluna

Subscription Rates (1983)
Annual Single Copies
United Kingdom and Ireland
£44.00 £3.66

Overseas
£50.00 £4.16

North and South America
§(US)106 §(US)8.83

Subscribers outside the British Isles receive
copies by Accelerated Surface Post.

Sworn statement of average monthly
circulation:
January–December 1981, 13,393



Member of the Association of
Learned and Professional
Society Publishers

Papers published in *The Radio and
Electronic Engineer* are listed or
abstracted as follows:

Title listings: 'British Technology Index';
'Current Papers'; 'Topics'; Current
Contents'; 'Science Citation Index'; ASCA.

Abstracted fully: 'Science Abstracts';
'Referativni Zhurnal'.

Abstracted selectively: 'Chemical
Abstracts'; 'Computing Reviews';
'Acoustic Abstracts'; 'Solid State
Abstracts Journal'; 'Nuclear Science
Abstracts'.

The Institution is not, as a body,
responsible for expressions of opinion
appearing in its publications, unless
otherwise stated.

ISSN 0033-7722

All Advertisement Enquiries to
Electronic Engineering
Publications Ltd.
PO Box 29 STEVENAGE, Herts
SG1 1HJ

Telephone: 0438 727371

Published monthly by the
Institution at

99 GOWER STREET
LONDON WC1E 6AZ

Telephone: 01-388 3071

Telegrams: INSTRAD LONDON
WC1

The Radio and Electronic Engineer, Vol. 52, No. 7

Industrial Management

How complex a learning curve model need we use?

331

Professor D. R. TOWILL (UWIST)

The model advocated is the simplest possible and represents normal smooth increase in performance with each significant deviation from the curve separately accounted for. If actual performance deviates from the model curve, the characteristic of the deviation can be interpreted by management to indicate the cause and thereby initiate action.

Digital Magnetic Recording

A simple model of longitudinal digital magnetic recording

339

W. R. NAYLAND

The basic theory for the recording process can cope with more parameters than can be determined experimentally and the paper suggests that the replay performance at optimum record current is related to the magnetic characteristics of the medium and its thickness. Specifications for the medium can thus be written in terms of the readily measurable parameters and can be employed in quality control procedures.

FORTHCOMING ISSUES OF THE JOURNAL

The August and September issues of *The Radio and Electronic Engineer* which will be combined and be published at the end of August, will contain twelve papers on the University of Surrey Satellite, *UOSAT*.

© The Institution of Electronic and Radio Engineers 1982

This publication is copyright under the Berne Convention and the International Copyright Convention. All rights reserved. Apart from any fair dealing under the UK Copyright Act 1956, part 1, section 7, whereby a single copy of an article may be supplied, under certain conditions, for the purposes of research or private study, by a library of a class prescribed by the UK Board of Trade Regulations (Statutory Instruments, 1957, No. 868), no part of this publication may be reproduced, stored in a retrieval system or transmitted in any form or by any means without the prior permission of the copyright owners. *Multiple copying of the contents of the publication without permission is always illegal.*

The appearance of the code at the bottom of the first page of a paper in this journal indicates the copyright owner's consent that copies of the paper may be made in the USA for personal or internal use, or for the personal or internal use of specific clients. This consent is given on the condition, however, that the copier pay the stated per-copy fee through the Copyright Clearance Center, Inc., for copying beyond that permitted by Sections 107 or 108 of the US Copyright Law. This consent does *not* extend to other kinds of copying, such as copying for general distribution, for advertising or promotional purposes, for creating new collective works or for resale. Copying fees for pre-1978 papers are the same as those shown for current papers.

Authority is however freely given to copy titles and abstracts of papers on condition that a full reference to the source is made.

Inquiries should be addressed to the Editor.

(ii)

July 1982

Founded 1925

Incorporated
by Royal Charter 1961

*To promote the advancement
of radio, electronics and kindred
subjects by the exchange of
information in these branches
of engineering*

Volume 52 No. 7

July 1982

The Radio and Electronic Engineer

The Journal of the Institution of Electronic and Radio Engineers

Television Systems for DBS

EARLIER this year a joint announcement was made by British Aerospace, Marconi and British Telecom of their intention to launch a Direct Broadcasting Satellite into a geostationary orbit in 1986. The Government's approval of the project was linked with an initial statement that two of the five channels allotted to the UK by the WARC agreement would be used by the British Broadcasting Corporation which subsequently stated that it would use these for a Subscription Channel (funded in an as yet undetermined manner by its subscribers) and for 'Window on the World' (to feature programmes from overseas and second showings of British programmes). At that stage, and subsequently, the intentions of the Independent Broadcasting Authority were not indicated in such specific terms.

Putting aside any reservations which one may have as to the value, viability and need for such additional sources of programmes—and plans have also been announced by the Government for the encouragement of an extensive cable network to the home which could well produce even more channels of 'entertainment', in addition to, it is fair to say, information and enlightenment — the technical background details of DBS are of considerable interest. They are also important in their implications for the radio and television industry as well as operationally. During May, both BBC and IBA unveiled their respective schemes for modifying the present television broadcasting system to work most efficiently with DBS transmissions and an account of these proposals and some comment is timely.

Both organizations point out that there are certain shortcomings in the performance of the present PAL system and that these — notably crosscolour effects and noise in areas of heavily saturated colour — could be avoided or at least considerably reduced in the process of designing the systems which would be required to operate successfully with DBS. On power considerations the satellite will of necessity use not a.m. but f.m., for which encoding of conventional PAL (and SECAM) is rather inefficient. It is stressed that now, before DBS comes into being, is the time for adopting a new system, particularly as the international agreement on the adoption of multichannel digital sound for DBS is due to be reached in Spring 1983.

The proposals by BBC and IBA diverge considerably when it comes to the system to be adopted. IBA favour a 'multiplex analogue component' (MAC) system in which chrominance and luminance are separated in time, instead of being interlaced in frequency as at present. The BBC's 'Extended PAL' filters off high frequency luminance components above about 3.5 MHz and shifts them to a higher band (above 8 MHz).

The aim of the MAC system is essentially a new European standard and the BBC fear that, judging from past experience, this is likely to prove enormously difficult to agree upon. Extended PAL is suggested as being much closer to the standard which is already used for terrestrial broadcasting throughout all of Europe except for France, and hence does not call for nearly the amount of technical negotiation (and minimal political bargaining!).

On the other hand the IBA believe that the restrictions on luminance in Extended PAL will cause deterioration in picture quality for those viewers with current receivers and the full luminance will only be obtained with appropriate new receivers. It is stated that MAC has an inherently better noise performance.

The respective advantages and disadvantages of the two systems are not easy to balance: both performed very acceptably in recent demonstrations to the industry and the technical press, the reduction of crosscolour and saturated colour noise being especially noticeable.

Many of the pros and cons for MAC and Extended PAL are contingent on the ease of design of the aerial/adaptor/receiver chain and in the relative cost of special circuits. It is not unfair to say that the broadcasters are not necessarily fully experienced in the implications of the development of special integrated circuits and the economies of mass production whether of add-on adaptors or complete sets. In the receiver is really the crux of the matter: a Britain-only standard limits the sales potential of the British television receiver manufacturing industry to this country, whereas if a single European standard can be agreed the market for British-made sets in Europe is potentially vastly greater. Already there is an unfavourable factor in that French and German receiver manufacturers must have their sets ready for sale a year before the UK as their satellites will

be operating in 1985.

It would be a major technical calamity if the choice of systems were to be seen as a BBC versus IBA 'battle'. We may perhaps draw some encouragement from the eminently satisfactory compromise which was worked

out for CEEFAX and ORACLE—with the close collaboration of the industry. The moral should, we hope, be obvious to all three parties and to the Government Departments necessarily involved.

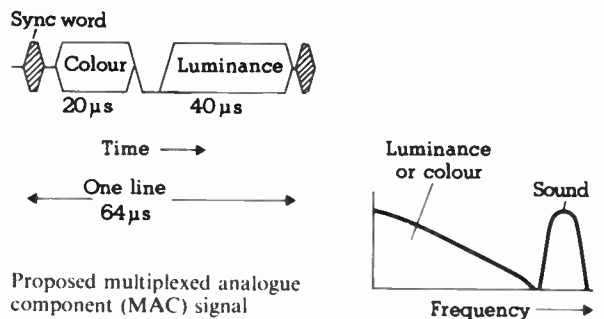
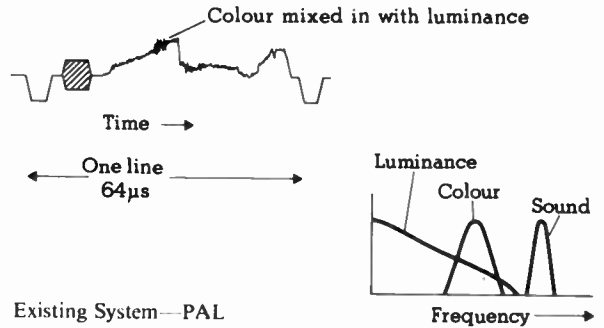
F.W.S.

MAC—Multiplexed Analogue Component Signals

The 625-line picture format is retained, but every television line of separate colour and brightness information is processed to 'shrink' each signal in time, so that within the time taken to transmit a conventional picture line of 'mixed up' colour and brightness information it is possible to transmit first the colour information and then the brightness information. This 'shrinking' process increases the amount of detail that needs to be transmitted, but this is within the capability of the satellite transmission channel. F.m. transmission of this format makes maximum efficient use of the satellite channel bandwidth, and significantly reduces the problem of noise or grain on coloured areas of the picture that is experienced with f.m. transmission of conventional colour television signals. This also leads to the possibility of reception on a slightly smaller dish aerial than would otherwise be the case. A small amount of fairly straightforward processing in the indoor satellite converter would restore the colour and brightness signals to their original form.

Conventional 625-line television signals are made up of 50 complete picture scans (or 'fields') per second, each containing 312½ lines. When displayed, alternate picture scans interlace with each other, building up a total of 625 lines for each complete picture frame (made up of two picture fields). With MAC, each of the 50 picture scans every second contains all 625 lines instead of merely 312½ lines. Processing prior to transmission discards alternate lines, thereby maintaining compatibility with the present system. However, this processing can be carried out in such a way as to enable extra circuitry in a high-definition receiver to recreate the original number of 625 lines of each picture scan, at the same time doubling the amount of picture detail that can be displayed.

A certain amount of additional signal processing would be needed to re-constitute MAC signals for display on a conventional television receiver. However, this processing employs well-known technology (using charge-coupled devices) and is amenable to cheap large-scale integrated circuit



production. The additional cost to the indoor satellite adaptor would therefore be minimal.

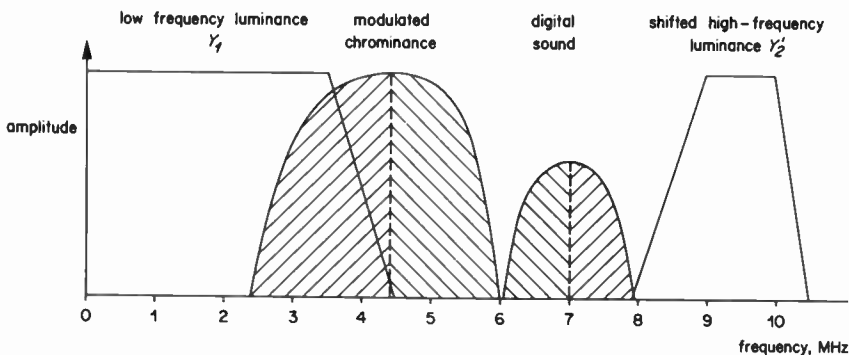
With further optional processing in digital form the MAC colour television signal can provide pictures with considerably improved definition (approximately double the resolution of existing 625-line pictures), suitable for a large screen display.

IBA Engineering Information Service

Extended PAL Video Coding

Extended PAL involves filtering off high-frequency components above about 3.5 MHz. This gives a very slight reduction in picture definition, scarcely noticeable on present-day display-tubes, but virtually eliminates crosscolour effects.

In a wider-bandwidth satellite or cable channel there is room to transmit the filtered-off high-frequency luminance components separately. The high frequencies (3.5 MHz upwards) are shifted in frequency to a higher band (8 MHz



Spectrum of an extended PAL signal

upwards) and transmitted together with the original low frequencies and chrominance signals. The upper limits of the separated high frequencies could extend above the 5.5 MHz equivalent bandwidth of the present transmission channel.

A new receiver, specially designed for this wide bandwidth transmission system would shift transmitted high frequencies back to their original values (3.5 MHz upwards) and hence display a much enhanced degree of fine picture detail. The new receiver would of course also be virtually free from crosscolour effects, since the high frequencies would be re-inserted after colour decoding had taken place.

In Extended PAL the high frequency luminance signal Y_2 is transmitted separately from the low-frequency luminance Y_1 and the chrominance, by shifting it by the colour subcarrier frequency. This leaves a gap in the spectrum which can be used for transmission of a multi-channel digital sound signal.

The Extended PAL coder is very similar to a conventional PAL coder. The extra components are a band-splitting circuit to separate the low-frequency luminance Y_1 from the high-frequency luminance Y_2 and a frequency shifter. The frequency shifter consists of a modulator similar to those used for the colour signals, and a high-pass filter.

In the Extended PAL decoder the composite signal is split into its three components, low-frequency luminance, Y_1 , shifted high-frequency luminance Y_2' signal and chrominance, by filters. The Y_2' signal is shifted back to its proper spectral position by a demodulator similar to those used for the chrominance and unwanted signal components are removed by a lowpass filter. The chrominance is demodulated in the usual way. Thus Extended PAL uses only simple additional circuitry, similar to that already used in today's television receivers.

BBC Engineering Information Department

R. V. Jones Elected an Honorary Fellow

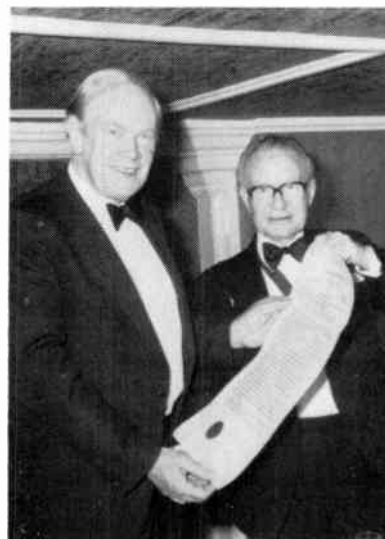
On May 20th, the President of the Institution, Mr Harry Drew, five Past Presidents and senior members of the present Council, gave a dinner party in London in honour of Professor R. V. Jones. The occasion was to mark the presentation of the Scroll of Honorary Fellowship of the IERE to Professor Jones and his signing of the Roll. The citation recording the election as inscribed in the Roll is given below.

Professor Jones recently retired from the Chair of Natural Philosophy at the University of Aberdeen which he has occupied since 1946. As is recorded in the citation, he gave the Clerk Maxwell Memorial Lecture last year and a fuller, less formal, biographical note accompanies the Lecture in the November/December 1981 issue of *The Radio and Electronic Engineer*.

MEMBERS OF THE COUNCIL OF THE INSTITUTION OF ELECTRONIC AND RADIO ENGINEERS assembled in London on the twenty-ninth day of October One thousand nine hundred and eighty-one unanimously resolved that REGINALD VICTOR JONES, Companion of the Most Honourable Order of the Bath, Commander of the Most Excellent Order of the British Empire, Fellow of the Royal Society, be elected an Honorary Fellow of the Institution.

For the past fifty years Reginald Victor Jones has been active in pursuit of discovery and application in the field of science and technology which is the primary concern of the Institution of Electronic and Radio Engineers. During this time he has taken a leading role in many highly imaginative projects and in many pioneer ventures in electronics, the most notable being his work on detection of aircraft by infra-red radiation in the late '30s, his outstanding contribution as Head of Scientific Intelligence for the Armed Forces during the 1939-45 war, and his post-war work as consultant and adviser to many Governmental and other bodies as diverse as the Air Defence Working Party of the Ministry of Defence and the British National Committee for the History of Science, Medicine and Technology. His continuing research interests include measurement of small displacements, and fundamental phenomena in optics such as radiation pressure and the aberration of light. He was the Institution's tenth Clerk Maxwell Memorial Lecturer in 1981.

This testimony gratefully acknowledges the debt that the profession of electronic and radio engineers owes to Reginald Victor Jones for his unique contribution to the advancement of the art, science and application of electronics from its infancy to its present dominant position in the defence of the realm and the nation's domestic, industrial and commercial life.



The President and Professor Jones examine the Scroll of Honorary Fellowship.

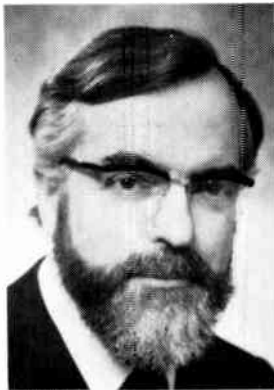


The new Honorary Fellow signs the Roll.

Members' Appointments

CORPORATE MEMBERS

Prof. W. A. Gambling (Fellow 1964) is to receive the J. J. Thomson Medal from the Institution of Electrical Engineers for 1982. The citation states that the Medal is given in recognition of 'outstanding work in electronics theory, practice, development or manufacture' and is in respect of Professor Gambling's work on low-loss optical fibres.



Professor Gambling who was President of the IERE in 1977/78 holds the British Telecom Chair in Optical Communications at the University of Southampton.

B. S. Alway (Member 1973, Graduate 1966) who has been with Cable and Wireless since 1968, has been appointed Training Manager, SANGCOM Project and is now based in Saudi Arabia.

G. Carlton (Member 1970), Telecommunications Project Group Head for the South Scotland Electricity Board since 1970, has now been appointed Telecommunications Manager.

C. J. Cole (Member 1981, Graduate 1980) has taken up an appointment as Telecommunications Coordinator with Occidental International Oil. Mr Cole was previously with Cable and Wireless where he latterly held the position of Assistant Satellite Systems Engineer.

J. A. Cox (Member 1973) is now a Senior Electronic Engineer with Sartelco, Riyadh, Saudi Arabia.

T. H. Edgar, B.Sc., Ph.D. (Member 1981, Graduate 1976) who has held the post of Senior Design Engineer with Morgan Moore Engineering of Stockton since 1979, has recently taken up employment with Stearns Roger Engineering Corporation in Denver, Colorado. Dr Edgar was for several years a member of the IERE North Eastern Section Committee and he also served on the CEI Northern Branch Committee.

J. Forrest (Member 1971) has recently relinquished his position as Managing Director, EMI (Singapore) and has returned to the UK to take up a position as Director, Distribution and Order Services, EMI Records (UK).

C. P. C. Heightman (Member 1971, Associate 1969) has transferred to Plessey Defence Systems to take up an appointment as an Assistant Sales Manager, after having spent eight years working on Project Ptarmigan, latterly as Programme Progress Officer for Plessey.

Lt Cdr D. J. Henman, V.R.D., B.Sc., RNR (Retd) (Member 1958) who recently retired from the Engineering Training Department of the BBC, is now providing consultancy services in Training Course Design for engineering personnel. In 1975/6 he was Chairman of the South Midlands Section Committee.

A. S. Kerr (Member 1967, Graduate 1963) has been appointed General Manager, British Telecom in the Preston Area. He was previously Deputy General Manager for the Glasgow Area.

J. B. McHale (Member 1971, Graduate 1967) is head of the Computer Systems and Software Group in the newly formed YARD Computer Applications Division, Glasgow. He was formerly a Project Leader with Plessey Numerical Controls, Alexandria, Dunbartonshire.

M. Obinkwo, B.Sc. (Member 1982, Associate Member 1974) has been promoted to Senior Project Engineer (XM) Zone 5 with the National Transmission Network Project, Posts and Telecommunications Area 4 in Kaduna, Nigeria.

C. Percy (Member 1967, Graduate 1964) has taken up an appointment as Sonar Manager in the Acoustics Division of McMichael, Slough. He was previously a Principal Engineer with Ultra Electronic Communications of Greenford where he led the Transducer Group.

A. Sedgwick (Member 1969, Graduate 1960) has been appointed managing director of Drallim Industries, Bexhill-on-Sea, and its manufacturing subsidiaries which between them include pneumatics, automation and electronics, together with specialized equipment for the telecommunications and transportation industries. Mr Sedgwick was formerly managing director of Thorn EMI Autopayment, Tonbridge.

K. T. Sherwood (Member 1973, Graduate 1971) is now working as Production Engineering Electrical Manager with Philips Electrical, Croydon; he was formerly Head of the Quality Engineering Group of Pye Manufacturing, Lowestoft.

A. F. Tarr (Member 1972, Student 1961) has taken up an appointment as a Design Engineer, Electronic/Telecom Instruments with Autec (Electronics), Honiton, Devon.

D. B. Trinkwon (Member 1973, Graduate 1981) has joined Northern Telecom UK Maidenhead as Manager, PBX Technical Marketing Services primarily responsible for Europe and the Middle East. Mr Trinkwon has for the past seven years been in Canada with Bell-Northern Research and Northern Telecom, prior to which he was with British Post Office Telecommunications Headquarters.

NON-CORPORATE MEMBERS

Sir Kenneth Corfield (Companion 1976) who was recently made a Honorary Doctor of Science at the University of Strathclyde, is to be awarded honorary doctorates by the University of Bath and the Queen's University of Belfast at their degree ceremonies during



the summer. Sir Kenneth, Chairman and Chief Executive of Standard Telephones and Cables, was appointed the first Chairman of the Engineering Council in July 1981.

R. Kimberley (Graduate 1973) who was a Pre-Production Engineer with Tech-Nel Data Products, has joined Systron-Donner, Leamington Spa, as a Senior Engineer.

P. J. Gutteridge, B.A. (Associate Member 1978) who was a Senior Maintenance Engineer with the BBC Transmitting Station on Ascension Island, is now a Lecturer in the Engineering Training Department of the BBC at Wood Norton.

Flt Lt A. R. Kent, RAF (Associate Member 1976) has relinquished his post as Officer Commanding Electrical Engineering Flight at RAF Cosford and has taken up the appointment of Officer Commanding Electrical Engineering Flight, RAF Akrotiri, Cyprus.

J. M. Roberts (Associate Member 1981, Associate 1979) who has been Operations Manager with Philips Consumer Service Canada in Scarborough Ontario, is taking up an appointment with Philips Electronics in Australia.

A reappraisal of h.f. receiver selectivity

R. A. BARRS, C.Eng., MIERE*

Based on a paper presented at the IERE Conference on Radio Receivers and Allied Systems held at Leeds in July 1981

SUMMARY

H.f. communication receivers have progressed towards a high level of sophistication yet a high percentage of reception failures are still due to limitations within the receiver. This paper considers the role of frequency selectivity for an ideal receiver and proposes a cost-effective approach which should noticeably reduce reception failure.

1 Design Trends

When endeavouring to advance the state of an art, it is often helpful to start by seeing how that art has changed over the years, and what motivated those changes. There has been a wide variety of circuit configurations used in h.f. communications but a definite trend may be traced.

The first professional valve receivers had front-end configurations in which r.f. selectivity and the superheterodyne oscillator were ganged to achieve a single tuning control covering a frequency range of typically 2:1. Selectivity at i.f. was by double-tuned circuits. Skirt selectivity would not have been good enough for s.s.b. reception.

The next stage was to go 'solid state'. These receivers were similar to their valved predecessors, but had now suffered a reduced dynamic range.

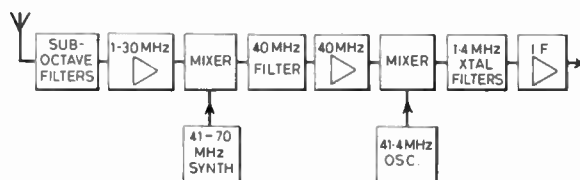


Fig. 1. Double superheterodyne with synthesizer.

The advent of the synthesizer (Fig. 1) allowed the oscillators to span the whole frequency range, i.e. 15 kHz to 30 MHz, without conventional band selection. This required some seven digital control knobs, but it was no longer easily possible to gang the frequency generation to the r.f. selectivity. To overcome this, front-end frequency selectivity was either omitted or achieved by means of octave or sub-octave filters. The wideband filtering thus provided was relatively easy to gang to the synthesizer frequency controls. In order to reduce the disadvantage of the wideband nature of the system, the dynamic range of the front-end amplifier and mixer was increased. These synthesized receivers used crystal filters at i.f. to provide the sharp skirt selectivity specified for i.s.b. and s.s.b. reception. Double superheterodynes with up-conversions were used to enable the image rejection to be obtained from the cruder front end filters. Further improvements have mainly been in the method of frequency selection by use of pushbuttons or by a rotary 'digitizer' control.

So progress has been:

- better frequency resolution (improvement $\sim 10^4$)
- improved frequency stability (improvement $\sim 10^4$)
- sharper skirt selectivity by about one order
- more facile control system

But front-end selectivity had worsened and market surveys indicated that improvement was needed.

2 Design Reappraisal

The time had come for a reassessment and this was prompted by both technical and commercial pressures.

Technical Aspects

A loss of selectivity at the receiver front end had occurred

* Rediffusion Radio Systems Ltd., Research and Development Laboratories, 15/17 Crompton Way, Manor Royal, Crawley, Sussex RH10 2QR

Difficulties had existed in ganging the synthesizer to the r.f. selectivity due to their laws being arithmetic and geometric respectively. (This constraint could be removed by microprocessor control.)

The use of synthesizers, double-superheterodynes and clocks had worsened the self-generated spurious signals.

Compared with wide bandwidth modes (3 kHz), the narrow bandwidth operational modes (300 Hz) have a lower noise level and therefore need a greater dynamic range. Some designs had tended to ignore this.

Market Aspects

- Traffic density is increasing
- Greater demand exists for a receiver that will be unaffected by co-location with transmitters. This includes mobiles.
- Need to reduce price of receivers
- Need for reduction of operator skills.
- Greater resistance to 'jamming' required.
- E.m.p. protection needed.

Bearing these aspects in mind a specification for selectivity will now be devised but it will be subjected to constraints imposed by the usual forms of spurious reception. As the objective is to eliminate receiver-caused reception failures, we will consider worst-case parameters which are encountered as hindrances to good reception.

3 Hindrances to Good Reception

The main culprits are:

- Adjacent signals.
- Reciprocal mixing.
- Transmitter noise, close-in, of adjacent signals.
- Co-located transmitter signals.
- Wideband noise of co-located transmitters.
- Cross-modulation.
- Blocking.
- I.f. breakthrough.
- Image signal reception.
- Intermodulation of unwanted signals.

The first three of these are all interferences which will be close to the wanted frequency passband. They can only be rejected by the sharp selectivity of the i.f. filtering and will therefore determine the skirt selectivity requirement of the i.f. filters.

The remaining forms of interference require some rejection from r.f. filtering.

Very large signals (greater than 1 volt) are only encountered by receivers which are co-located with transmitters. In such cases it is usual to ensure that operational frequencies are scheduled so that the transmitters do not cause interference by adjacent signals and noise, reciprocal mixing, i.f. breakthrough or image. These forms of interference are subject to signal amplitudes and densities which are due to the normal r.f. traffic.

Each of the above forms of interference will now be considered in turn.

4 Adjacent Signal Rejection

The object of selectivity is to allow reception of a wanted signal and reject all other signals by means of filtering. Figure 2 shows a typical traffic density plot for the h.f. spectrum.¹

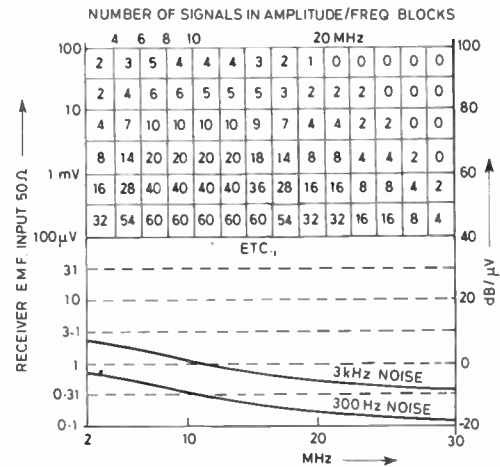


Fig. 2. Traffic density and atmospheric noise.

Superimposed on this are curves representing the combined atmospheric and galactic noise at the receiver input for 3 kHz and 300 Hz bandwidths and a receiver source impedance of 50Ω. These curves are for a quiet site and represent the lower quartile noise statistics.² The selectivity should be such as to allow reception of signals at or near noise level, while all interfering signals of up to 100 mV should be attenuated to at least 3 dB below the noise. This must apply equally to the narrow bandwidth modes and to the wide bandwidth modes. Thus for signals which lie outside the passband the maximum attenuation needed with a 300 Hz bandwidth is 107 dB to 118 dB from 1.6 to 30 MHz, and with a 3 kHz bandwidth it is 97 dB to 108 dB from 1.6 to 30 MHz as shown on curve A in Figs 3(a) and 3(b). The worst case is at 20 MHz and this may be deduced from Fig. 2.

5 Reciprocal Mixing

This form of spurious reception is caused by the noise spectrum which surrounds the synthesizer/oscillator signal. Not only does the synthesizer signal mix with the wanted signal during frequency conversion, but the noise sidebands of the synthesized signal will also mix with unwanted signals and thereby allow them to be spuriously received.

Assume that a wanted signal at 12 MHz was being converted to 1.4 MHz i.f. by the synthesizer output at 13.4 MHz. Say that at 13.41 MHz a 3 kHz slice of the synthesizer noise was 93 dB below the fundamental. This would cause an unwanted input signal at 12.01 MHz to be spuriously converted to a 3 kHz noise band at 1.4 MHz, and thus spuriously received. As the noise was 93 dB down it could be expected that the spurious signal would also be 93 dB below that attributable to an equal level wanted signal. In fact it would be 99 dB lower. This is because the mixer has a 6 dB discrimination against the conversion caused by a very small signal which appears together with the wanted synthesizer/oscillator signal.⁴ Curve 'A' of Fig. 3(a) shows that the selectivity

requirement against adjacent interfering signals should be 108 dB. This would be pointless in the example just quoted (for 10 kHz off tune) where the adjacent signal is spuriously received with an attenuation of only 99 dB. Therefore the filter attenuation need only be, say, 3 dB greater than the reciprocal mixing figure. So in this example it would be 102 dB at 10 kHz off tune.

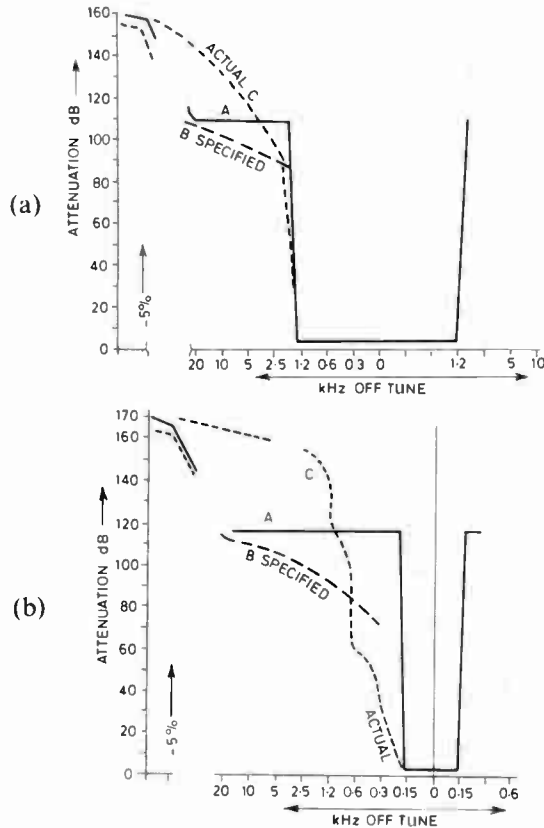


Fig. 3. Selectivity curves (a) 3 kHz bandwidth. (b) 300 Hz bandwidth.

The following Table shows the reciprocal mixing that could be achieved with the use of a high quality synthesizer.⁵ It also shows the related relaxation which may therefore be placed on the selectivity requirement. The curves 'B' in Fig. 3 reflect this.

	Frequency from centre of passband (kHz)						
	0.3	1	1.5	3	5	10	50
Reciprocal mixing with a 3 kHz passband (dB)	—	—	—	88	94	99	103
Acceptable selectivity for 3 kHz passband (dB)	—	—	—	91	97	102	106
Reciprocal mixing with a 300 Hz passband (dB)	70	85	90	98	104	109	113
Acceptable selectivity for 300 Hz passband (dB)	73	88	93	101	107	112	116

This degree of skirt selectivity can only be provided by i.f. or a.f. filters.

6 Transmitter Noise—Close-in

Although the effect of reciprocal mixing in a receiver is often discussed and specified, the close-in noise of the interfering transmitter tends to be forgotten. In the example given under 'Reciprocal Mixing' a 10 kHz off

tune signal was being spuriously received with an attenuation of 99 dB. It would probably be the case that the 10 kHz removed noise sidebands of the interfering signal (i.e. coincident with the receiver's passband) would also be about 99 dB below the interfering signal. So the interfering signal is being spuriously received by reciprocal mixing at -99 dB while the interfering signal's noise is also being received at -99 dB. Thus the two effects are rather like vertically and horizontally inverted mirror images and are problems of the same magnitude. By taking reciprocal mixing into account we also cover the problem of close-in transmitter noise.

Having considered these first three forms of interference it is now possible to define the skirt selectivity of the i.f. filters. These are shown in Fig. 3(a) and 3(b) as curves B and are bounded by the region of ± 20 kHz from the centre frequency. These specifications are far more stringent than those which are normally seen.

7 Co-located Transmitter Signal Rejection

Co-location of receivers and transmitters having closely-spaced aerials and simultaneous operation is not usually acceptable at transmitter powers much above 1 kW. Assume that the coupling of power between a 1 kW transmitter and co-located receiver is as unfavourable as -26 dB, (and this is probably a worst case condition), then the receiver will have an input e.m.f. of 22.4 V. Transmit and receive frequency spacing in this situation is not random, but is normally allocated by a station schedule which ensures a 5% separation. The attenuation needed to push this 22.4 V signal into the noise with a 300 Hz bandwidth will be 154 dB to 167 dB from 1.6 to 300 MHz; and with a 3 kHz bandwidth it will be 144 dB to 157 dB from 1.6 to 30 MHz for frequencies greater than 5% off tune. This is shown on curves 'A' Fig. 3 for the worst case which occurs at 30 MHz.

The required selectivity cannot be achieved at r.f. and it is not necessary to do so. By splitting the selectivity between r.f. filters and the i.f. filters it would be possible to come close to this ideal response. Also when coherent or quasi-coherent demodulation is used (e.g. s.s.b.), further filtering is obtained at audio frequency. This is not so for such forms of non-coherent demodulation as envelope detection. However, before considering how best to distribute the selectivity throughout the receiver it is known that there are other processes which restrict the receiver's performance. They either impose further limits, or allow relaxations to the curves 'A' which have been constructed. These processes will now be considered.

8 Wideband Noise of Co-located Transmitters

Special care is needed in the design of transmitters which are to be used for closely-spaced co-location with receivers. Ideally the noise generated by the transmitter at the receiver's frequency should not increase the receiver's noise level. Low-noise transmitters normally have several stages of r.f. filtering in front of the power amplifier output stage to reduce the off-tune noise. State-of-the-art for 1 kW transmitters is for the noise to be

130 dB to 140 dB below the rated transmitter power in a 3 kHz bandwidth at 5% off tune.

The upper limit could safely be considered as -150 dB/1 kW for a 3 kHz bandwidth and -160 dB/1 kW for a 300 Hz bandwidth as anything better will rarely be encountered. Assume that this situation exists and that a receiver is operating on a 5% frequency spacing and experiencing this level of transmitter noise. Receiver selectivity can do nothing to reject this noise as it falls within the received passband. It is therefore only necessary for the receiver to have enough selectivity to attenuate the transmitter signal to a level which is 3 dB below the transmitter's 5%-off-tune noise.

The limits on curves 'A' can therefore be relaxed accordingly, to those on curves 'B' in Fig. 3 at the 5% off tune points, i.e. -153 dB and -163 dB respectively.

9 Cross-modulation

This is the process by which an interfering signal transfers its modulation onto the wanted signal due to non-linear functions within the receiver. The worst case will again be that of a co-located transmitter and receiver where, as previously seen, the interfering signal can arrive at the receiver input at 22.4 V e.m.f. A well-designed single-superheterodyne receiver will have a cross-modulation performance such that without the aid of front end selectivity an input 30% modulated interfering signal of 300 mV e.m.f. will cause cross-modulation to a wanted 30 μ V e.m.f. signal by some -40 dB, so it will not degrade the signal-to-noise ratio of the wanted signal. 30 μ V is chosen because it is about the level of input signal at which the maximum signal-to-noise ratio will be achieved. Also front-end a.g.c. attenuators will not be acting to reduce the interfering signal. The first really non-linear element in the receiver is the first mixer. If selectivity precedes the mixer and provides sufficient attenuation, 37 dB, to reduce the 22.4 V e.m.f. input level to an equivalent 300 mV at 5% off-tune then cross-modulation will not be a problem.

This provides the first indication of the amount of selectivity needed to precede the first mixer.

10 Blocking

This effect is caused by large interfering signals overloading the amplifiers or mixers. Their gain is thereby reduced and their non-linearity increased to the detriment of the wanted signal. A good receiver, without the aid of front-end selectivity, should be able to withstand signals of at least 300 mV without noticeable blocking. As stated above when considering cross-modulation, signals in excess of 300 mV are only normally encountered as a result of co-location. Thus by achieving the necessary degree of selectivity to reduce the effects of cross-modulation, the requirement for blocking is also satisfied.

11 I.F. Breakthrough

If a strong signal is received whose frequency coincides with the receiver's i.f., it must be attenuated to below noise level, otherwise the interference caused will persist irrespective of the frequency of tune.

The attenuation requirement is again found from Fig. 3 and it is almost the same as for adjacent signal rejection with a 300 Hz bandwidth: -107 to -120 dB from 1.6 to 30 MHz. This attenuation must come before the i.f. filter. If a double-balanced first mixer precedes the i.f. filter we can expect at least 30 dB of rejection due to its balance. This leaves 77 to 90 dB from 1.6 MHz to 30 MHz to be obtained from the front-end tuning.

12 Image Signal Rejection

Spuriously-received image signals will be at a frequency which are twice the i.f. above the wanted signal. Again the image signal can only be rejected by selectivity in front of the first mixer. In order to avoid intermodulation and co-location interference, it has already been established that the front-end selectivity has to be -37.5 dB at 5% off tune. This represents a high degree of filtering which it is hoped should also be capable of providing image rejection. If the main frequency coverage is 1.6 to 30 MHz it will be convenient to have a 1.4 MHz i.f. which is just outside the reception band. The image will then be 2.8 MHz above the wanted signal. Figure 2 shows that the interfering signal levels are lower at the top end of the frequency band. This is convenient because the 2.8 MHz image spacing becomes a lower off-tune ratio as frequency increases and is accompanied by a reduction in filter attenuation. Because no image rejection is obtained from the i.f. filter it will only be necessary to consider the most stringent 300 Hz narrow bandwidth requirement.

The attenuation requirement based on signal levels given in Fig. 2, the use of a 300 Hz bandwidth, and the image being reduced to 3 dB below ambient noise, is as follows:

1.6 to 16 MHz image attenuation	-117 dB
16 to 21 MHz image attenuation	-108 dB
21 to 23 MHz image attenuation	-99 dB
23 to 25 MHz image attenuation	-89 dB
25 to 30 MHz image attenuation	-80 dB

13 Intermodulation Products

This is one of the worst forms of interference. Once more the first mixer is the major culprit in causing interfering signals to produce intermodulation products which fall within the wanted passband. A good receiver will have an intermodulation (i.m.) performance of about 90 dB μ V, i.e. two input signals at 10 kHz and 20 kHz off-tune and at a level of $+90$ dB referenced to 1 μ V e.m.f. will produce 3rd-order intermodulation products (i.m.p.) of less than 1 μ V e.m.f.

Consider three different front-end filtering configurations

- (a) Assume that there was no selectivity before the first mixer and the receiver i.m. performance was 90 dB μ V. In order to simplify things, consider the effect of only the 100 mV e.m.f. signals at the input (Fig. 2) which number 28.

These 28 signals produce:³

14 644 i.m.p.s up to 3rd order at $+30$ dB μ V e.m.f.
 175×10^6 i.m.p.s up to 7th order at $+10$ dB μ V e.m.f.

84×10^{12} i.m.p.s up to 15th order at -10 dB μ V e.m.f.

These products cover a wide frequency band and their effect would be to increase the noise floor to about $+15$ dB μ V e.m.f. and also give a high probability of interference for input signals up to $+30$ dB μ V e.m.f.

- (b) Next consider that a sub-octave filter with a bandwidth of $10-15$ MHz was used at the front-end of the receiver. There would now be 10 signals of 100 mV e.m.f. which would produce:

670 i.m.p.s up to 3rd order at $+30$ dB μ V e.m.f.

150×10^3 i.m.p.s up to 7th order at $+10$ dB μ V e.m.f.

70×10^6 i.m.p.s up to 15th order at -10 dB μ V e.m.f.

The effect would be to increase the noise floor to about $+5$ dB μ V e.m.f. and to give a high probability of interference for input signals up to $+20$ dB μ V e.m.f.

- (c) Finally, consider the use of a narrow band tuned front-end filter. What front-end selectivity is needed to overcome the i.m. problem?

Consider a filter which has at least 20 dB attenuation outside a bandwidth of $\pm 2.5\%$. Beyond this point the 100 mV e.m.f. signals will be attenuated to less than 10 mV e.m.f. which is 10 dB below the previously stipulated 90 dB μ V i.m. tones inputs. This 10 dB reduction improves the 3rd-order i.m.p. performance by 20 dB so that the 3rd-order i.m.p. is now less than 110 dB below 10 mV. This is -30 dB μ V e.m.f. and is below the noise in a 300 Hz bandwidth. Within the $\pm 2.5\%$ bandwidth there will only be one or two signals at the 100 mV e.m.f. level (Fig. 2).

Assume that there are two signals without attenuation in the band, then the i.m.p.s will be:

6 up to 3rd order at $+30$ dB μ V e.m.f.

14 up to 7th order at $+10$ dB μ V e.m.f.

30 up to 15th order at -10 dB μ V e.m.f.

This will result in a negligible level of interference. Therefore the filter requirement is for 20 dB of attenuation at $\pm 2.5\%$ from tune. The filter must precede the first mixer.

It is well known that r.f. selectivity is essential for receivers co-located with transmitters. What is seen from this Section is that r.f. selectivity is equally essential for normal operation if the sensitivity of the receiver is not to be degraded.

14 Distribution of Selectivity—Front-end

The examination of hindrances to reception has enabled a specification for selectivity to be produced. Let us now examine a practical configuration which has been used in an endeavour to achieve this ideal.

It has been argued in the preceding Sections that the front-end selectivity should provide attenuation of 37.5 dB at 5% from tune and 20 dB at 2.5% from tune. It was decided that four ganged tuned circuits would be used for the r.f. filter, each circuit having a working Q of 30 to 40 (Fig. 4). This gives attenuations of 40 dB to 50 dB at 5% from tune and 20 to 27 dB at 2.5% from

tune. The i.f. rejection is 78 dB to 106 dB from 1.6 MHz to 30 MHz against the requirement of 77 dB to 90 dB. Additional rejection could be easily obtained from a 1.4 MHz notch filter after the first amplifier.

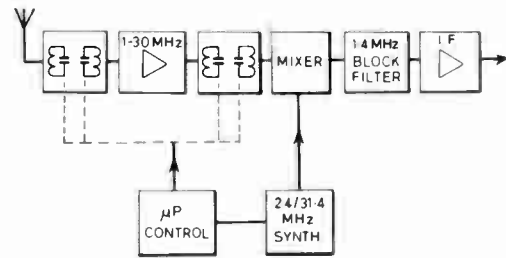


Fig. 4. Single superheterodyne—proposed.

For image rejection there is an average shortfall in attenuation of 17 dB from 20 MHz to 30 MHz and 8 dB from 5 MHz to 20 MHz (measured results, not calculation). Using the information in Fig. 2 it was calculated that this would result in increasing the probability of reception failure due to image interference from zero to 0.08% . Having fully met all the other requirements for co-located working, cross-modulation, blocking, inter-modulation and i.f. breakthrough, it was not considered justifiable to add the cost of another tuned section for such a small improvement.

The r.f. filter has been manufactured and it uses a four-section ganged variable capacitor with a 1% matching accuracy. An error of 1% in one of the capacitors will cause a frequency error of 0.5% . This is quite acceptable due to the relatively low working Q s which give a 3 dB bandwidth of $\pm 1.5\%$. The capacitors are motor driven by a servo which is controlled from the frequency controls via a microprocessor. Errors in the gang law are corrected by the program. The use of a gang capacitor is well justified. Only an $L-C$ type filter has the ability to withstand very high input powers, have a low power insertion loss, be extremely linear and have a negligible generation of noise. Apart from the power stress caused by co-location operation there is an increasing awareness of the need for aerial input circuitry to withstand the effects of lightning and electromagnetic pulses (e.m.p.).

Consider the proposed single superheterodyne receiver in Fig. 4 and the double superheterodyne shown in Fig. 1. Compare the blocks ahead of the 1.4 MHz filter for common sections. These are, a synthesizer, an r.f. mixer and an r.f. amplifier. If these are deleted there is left in Fig. 4, a four section r.f. filter with its microprocessor control. In Fig. 1 there is left a sub-octave filter block, a crystal 'roofing' filter, an amplifier, a mixer and a crystal (or synthesized) oscillator. From this it is estimated that the configuration of Fig. 4, with its r.f. selectivity, is a little less costly than that of Fig. 1.

15 Distribution of Selectivity—I.F. Filtering

Modern professional receivers provide various bandwidth service options. In general, each of these options is implemented by a separate crystal filter as in Fig. 5. It was decided that a better approach would be to integrate the filters into one block.⁶ Filter sections would

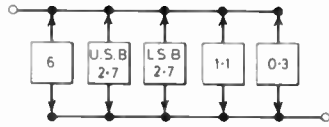


Fig. 5. Conventional crystal filter bank.

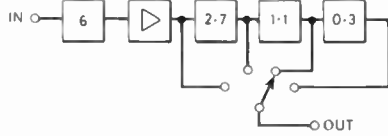


Fig. 6. Block filter configuration.

be cascaded as shown in Fig. 6. Bandwidths of 6 kHz, 2.7 kHz, 1.1 kHz and 300 Hz would be selectable. Because the filters were cascaded, the sections after the 6 kHz filter would only have to provide close-in attenuation. Attenuation further from the selected passband would be provided by the preceding sections. This would enable the two narrowest filters to be very simple. Redundant crystal filter sections would no longer be needed. This block filter has been manufactured and has shown a cost saving of some 30% over the conventional approach. It has also provided skirt selectivity (curves 'C', Fig. 3) much closer to the proposed requirement (curves 'B' Fig. 3) than previously obtained. A further advantage has been a small improvement in differential group delay. This is due to the fact that the narrow filters need less sections to provide the close-in skirt selectivity. This results in less differential delay at the band edges where it is normally worst. The 'surrounding' wider filters have little effect because their group delay is sensibly constant over the selected narrower band.

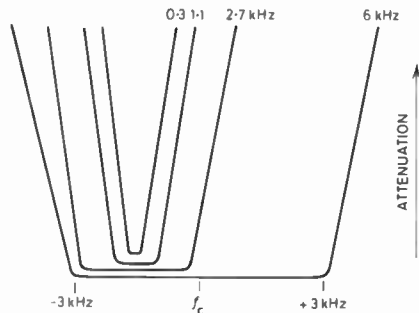


Fig. 7. Block filter frequency plan.

A long standing irritant to Production and Sales staff has been the different specifications for s.s.b. filters needed for marine and for other applications—the passbands referenced to carrier being 350 Hz to 2700 Hz and 250 Hz to 3000 Hz respectively. The 2.7 kHz filter used in the block filter is shaped to meet both of these specifications. It is also symmetrical so that it can be used for upper sideband, lower sideband or as a centralized filter (Fig. 7). Use of a single filter for the three modes is not novel. However, by microprocessor programming of the synthesizer and reinsertion oscillators, it is now possible to select the three modes without making difficult offsets to the frequency setting.

16 Front-end Attenuators

One method of improving receiver performance is to use variable front-end resistive attenuators. This can be very effective when manually controlled by an expert operator. As it has been one aim of this study to reduce operator skills and enable multiple (remote or local) control of receivers to be implemented, it has been assumed that this palliative will not be acceptable.

17 Conclusion

The requirement for this 'ideal' receiver has been based on the atmospheric noise levels experienced in quiet temperate zones. But for 'noisy' receiver sites the front-end selectivity requirement would not alter appreciably.

The selectivity has been partitioned into a front-end tuning module and a novel form of block i.f. crystal filter module. Plots of the selectivity which result are shown as curves 'C' in Fig. 3. These curves are a very close fit to the specified curves 'B'. Front-end tuning has fully met all the requirements postulated to prevent reception failure from co-located transmitters, cross-modulation, blocking, intermodulation and i.f. breakthrough. This is true for narrow-bandwidth operational modes (300 Hz) as well as the 3 kHz bandwidth. The image rejection although not perfect is quite adequate. The attenuation margins which have been obtained should provide for further increase in traffic density. The i.f. block filter comes close to meeting the ideal selectivity and appears to offer a significant improvement in performance/cost ratio.

Implementation of both selectivity blocks has been assisted by the use of microprocessor control with an accompanying improvement in man/machine interfacing.

Finally, while aiming for improved selectivity it has been possible to revert to the simpler topology of a single superheterodyne receiver. This has cost benefits, and allows an improvement in reliability and a reduction in spuriously generated whistles.

18 Acknowledgments

My thanks are due to Mr C. S. den Brinker, Mr R. F. Clarke and Mr. C. W. Higginbotham for their assistance with this paper.

19 References

- 1 Sosin, B. M., 'Performance of H.F. Receiving Systems', *Marconi Rev.*, 39, no. 20, 1st Quarter 1976.
- 2 'World Distribution and Characteristics of Atmospheric Radio Noise', Report 322 C.C.I.R. Geneva 1963.
- 3 Wass, C. A. A., 'A table of intermodulation products', *J. Instn Elect. Engrs.*, 95, pt. 111, pp. 31-9, January 1948.
- 4 Gardiner, J. G. and Yousif, A. M., 'Distortion effects in switching diode modulators arising from local-oscillator interference', *Proc. Instn Elect. Engrs.*, 118, no. 2, pp. 339-48, February 1971.
- 5 'Noise in Frequency Generators', Application Note, Adret Electronique 1979 Equipment Catalogue, Trappes, France.
- 6 Barrs, R. A. and Higginbotham, C. W., 'Multi-bandwidth Filter U.K. Patent Application No. 80/12528.

Manuscript received by the Institution in final form on
11th January 1982
(Paper No. 2033/Comm 343)

An improved 'Piccolo' m.f.s.k. modem for h.f. telegraphy

J. D. RALPHS, B.Sc., C.Eng., MIERE*

SUMMARY

The Piccolo system of multi-frequency signalling has been in operation on the h.f. telegraphy network of the UK Foreign and Commonwealth Office for almost 20 years and has proved extremely effective. A new generation equipment has now been designed which is smaller, more reliable and more flexible than previous models, and incorporates a number of parameter changes and additional facilities suggested by experience and more detailed mathematical analysis. It allows operation in the ITA-2 code at 75 or 50 bauds, and in the ITA-5 code at a 110 bauds. The new parameters have enabled the bandwidth to be considerably reduced and the stability required from the reference source to be relaxed. The improved synchronizing system will pull in to synchronism in less than 3 seconds and remain synchronized over long periods of poor or lost signal. Special provision is made for operation on continuous cryptographically-protected data streams. The unit also includes a selective calling system and an optional error indicating code. Four telegraph channels can be frequency division multiplexed into a 2 kHz bandwidth. The availability of the system under poor-signal conditions is a considerable improvement over orthodox binary techniques.

* Communications Engineering Department, Foreign and Commonwealth Office, Hanslope Park, Hanslope, Milton Keynes MK19 7BH.

The 'Piccolo' multiple frequency shift keying (m.f.s.k.) telegraphy system originated from experimental work carried out in the early fifties by Mr H. K. Robin, then the Chief Engineer of the Diplomatic Wireless Service, which later become the Communications Engineering Department of the UK Foreign and Commonwealth Office (FCO). The first experimental version, the Mark 1¹ went into service in October 1962 and the subsequent production design, Marks 2 and 3, has for the last 17 years formed the basis of the FCO h.f. radio network from UK to more than fifty Embassies.² These units employ germanium transistors and discrete components, the tone filter and generator circuits being based on resonant circuits using ferrite-cored inductors. The equipment is now obsolescent and will be replaced over the next few years by the Mark 6 unit which is the subject of this paper. The new design employs c.m.o.s. logic for all timing and audio synthesis circuits, but retains analogue processing in the signal path of the receive circuits, the matched filter tone detectors being realized by synchronous detection with f.e.t. analogue switches driven by synthesized waveforms.

The basic principle of m.f.s.k. signalling is a departure from the orthodox practice of binary (2-state) signalling. By using a larger number of tones, each tone element conveys more information and therefore each element period can be increased (for constant data rate). This considerably increases the immunity to multipath propagation, and by integrating energy over a longer period, increases the resistance to noise. The result is a significant improvement in circuit availability over binary systems.

The earlier Piccolo units (Marks 1, 2 and 3), employ a 32-tone system, in which each tone frequency represents a single character of the ITA-2 alphabet, but subsequent mathematical work^{3,4} suggested that although this system gives a very high level of accuracy in the face of noise, the use of fewer tones could give a better compromise between performance and bandwidth occupancy together with greater flexibility and reduced capital cost. The Mark 6 system therefore uses two 50 ms elements per telegraph character, selecting from 6 tones for the ITA-2 code and from 12 tones for the ITA-5 code. Although this sacrifices about 2 dB in signal-to-noise ratio over the 32-tone system this is still marginally better than the performance of an 'ideal' coherent binary demodulation system. The bandwidth is reduced to less than half that of the Mark 3 (for ITA-2) giving better availability in crowded bands, and since the signal element period is halved, a corresponding relaxation may be allowed on the accuracy of the reference crystal oscillator.

The Mark 6 unit also incorporates a versatile selective calling system and an optional error indicating code which may be extended by an external unit to give an error correction capability (either forward error correction (f.e.c.), or automatic request for repeats (ARQ).

2 Modem Characteristics

2.1 Telegraph Modes

The Mark 6 Piccolo operates in either of two modes:

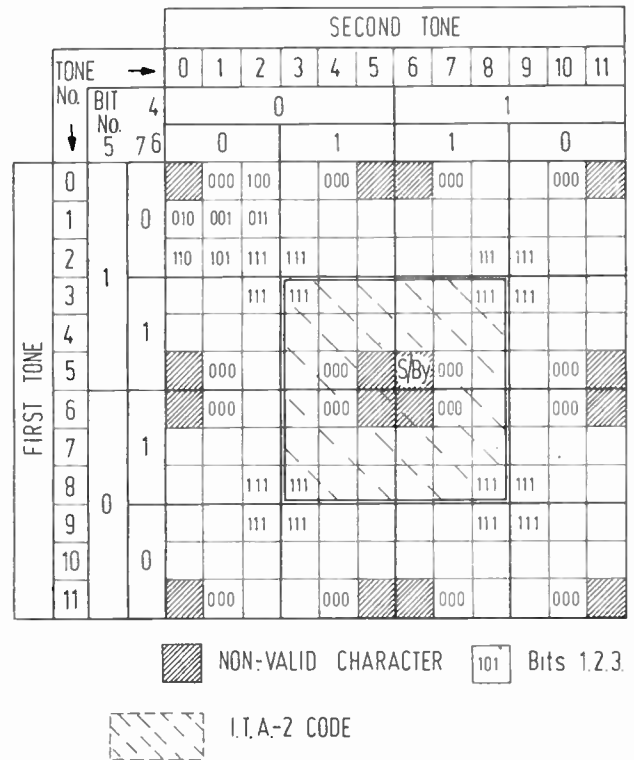
- (a) ITA-2 code in 7 or 7½-unit serial format at 75 baud, each character being transmitted as a sequence of two audio tone elements of 50 ms duration, the tones being selected from six frequencies spaced at 20 Hz intervals.
- (b) ITA-5 (ASCII) code in 10- or 11-unit 110-baud serial format, each character being transmitted as a sequence of two tone elements of 50 ms duration, the tones being selected from 12 frequencies spaced at 20 Hz intervals.

In addition a 50-baud facility has been provided (with some limitations) in which two data characters are transmitted as in (a) above, interspersed with one stand-by (or 'idle') character.

The input data may be in standard start-stop format to normal commercial tolerances on modulation rate, etc., the only additional restriction (inherent in the synchronous operation of the Piccolo system) is that the mean long-term input character rate must not exceed 10.0 characters per second. Warning and control functions are provided to facilitate this (see Sect. 3).

2.2 Character Codes

Operating in the ITA-5 code, a serial input character is first converted to an 8-bit parallel format, seven of the bits representing the data and the eighth bit the 'idle' or 'stand-by' condition which is transmitted at all times when no input data are available. The parity bit which is normally included in the ITA-5 character is ignored for Piccolo purposes. In the ITA-2 code, serial-to-parallel conversion is carried out in the same way (with a suitable change of clock rate) and stored in the same format, except that bits 6 and 7 are always in the 'mark' condition. Throughout the rest of the system the ITA-2 character is therefore considered as a special case of the ITA-5 alphabet and the need for differentiation between the two codes only arises again in the clock rate of the final parallel to serial conversion in the receive system and in minor control functions. This simplification can be achieved because of the construction of the Piccolo code itself, which is shown in the code chart of Fig. 1. Each small square of the matrix is a single character which is located by its binary representation, and transmitted as a sequence of two tone frequencies, identified by the row and column number. It can be seen that all binary numbers ending with the combination '11' are contained within the central matrix of 6×6 combinations. This means that the complete alphabet of ITA-2 characters is transmitted by using the tones 3 to 8 inclusive, the other tones never being generated in the transmit system and the equivalent filters being disabled in the receive system. Thus the dual-code operation of the unit is achieved mainly by switching the clock frequencies to the telegraph input and output circuits, and disabling half the tone filters in the ITA-2 mode.



Note.—For binary coding purposes MARK = 1, SPACE = 0. Bit 1 is transmitted first.

Fig. 1. Piccolo code chart

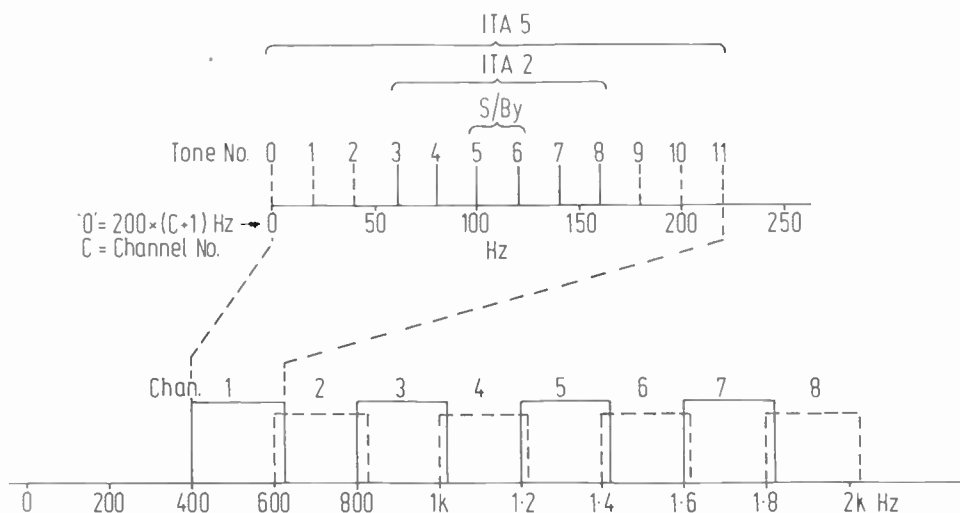
The conversion of telegraph characters to tone numbers, and the reverse process in the receiving system, can be accommodated in a single p.r.o.m. (programmable read-only memory) so that alternative codes may be achieved if necessary simply by a change of program.

2.3 Stand-by and Non-valid Characters

Two selections from 12 tone frequencies would give 144 possible combinations, of which 128 are required for the ITA-5 alphabet, and one other is transmitted for all stand-by periods. The other 15 combinations cannot be generated by the send system and are classified as 'non-valid characters' (n.v.c.). Similarly in the ITA-2 mode, 36 tone combinations are available, 32 of them being used for ITA-2, the same combination as before being used for stand-by, and the other three being n.v.c. Although an n.v.c. cannot be generated by the send system, it may be received as a result of transmission errors. When this occurs it is output to line as an 'all space' character (NULL in ITA-5 or character 32 in ITA-2).

2.4 Tone Frequencies and Frequency Multiplexing

The direct relationship between the 50 ms element length and the 20 Hz tone spacing has been previously discussed¹ and will not be repeated here. In the standard mode of operation (Channel 1—see below), the 12 tones are spaced from 400 Hz to 620 Hz inclusive, the stand-by signal consisting of the tones 500 and 520 Hz. In the ITA-2 mode the three lowest and three highest frequencies are not used, the signal then occupying the band 460 to 560 Hz as shown in Fig. 2. Both the



NOTE:- For Multiplex Operation use ODD numbered Channels ONLY

Fig. 2. Arrangement of tones and channels

'necessary' and 'occupied' band widths⁵ may conveniently be assumed to extend not more than two tone intervals (40 Hz) above and below the highest and lowest tone frequencies,³ giving a bandwidth of less than 180 Hz in ITA-2 and 300 Hz in ITA-5. Provision is included for off-setting the transmitted and receiving frequency bands upwards in increments of 200 Hz to a maximum of 7 steps, thus allowing provision for transmission in any one of 8 audio channels. The lowest (Channel 1) uses tones from 400 to 620 Hz as described above, while Channel 8 uses 1800–2020 Hz. A combiner unit is under development to allow four Piccolos set to Channels 1, 3, 5 and 7 (i.e. at 400 Hz spacing in a 2 kHz band width) to be operated in frequency division multiplex.

3 Send System

An outline block schematic of the send system is shown in Fig. 3. An incoming data character is converted into an 8-bit parallel byte as described above and stored in a 32-byte f.i.f.o. register, which is read out into the

modulator at 10.0 characters per second, a stand-by character being transmitted if the store is empty. An output 'excess data' control line is set high if the contents of the register exceed 16, the state being cancelled 800 ms after the contents have dropped below 16. This control line may be used in conjunction with an audible alarm or lamp to allow manual control of a tape reader. If the line is used to control the clutch of a suitable tape reader which is running slightly fast, the store contents will build up slowly to 16 then empty rapidly to 8. The same control function is also available as a 10 Hz pulse which is disabled under excess data conditions, thus enabling the accurate control of the data rate of a pulse-released source.

The 8-bit parallel byte is fed through a bus system to the modulator, other functions having input or in/output access to the bus as shown in the Figure. The p.r.o.m. in the modulator converts the telegraph data into a BCD representation of the required tone frequency, which is available to key a direct-keying radio frequency synthesizer. Alternatively, the BCD states are used to

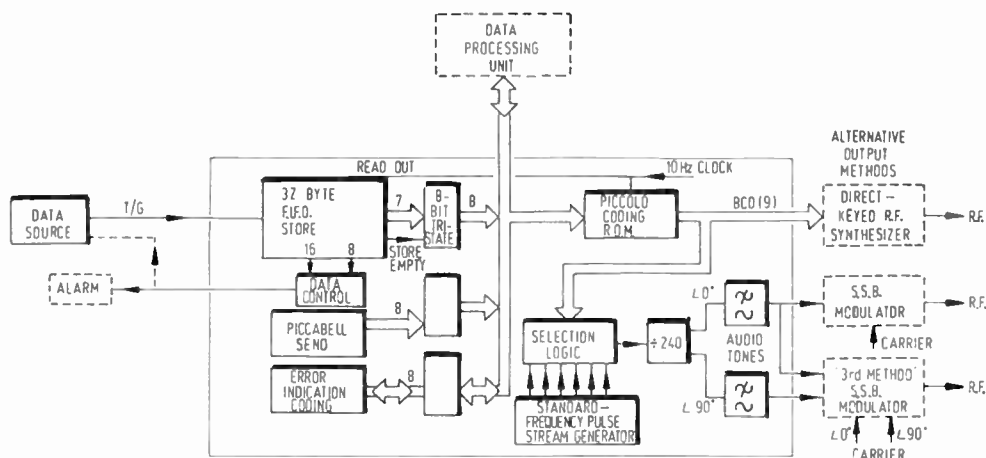


Fig. 3. Send system—block schematic

add the frequencies of standard pulse streams to synthesize the required audio frequencies as described in Section 4.4 The method of waveform synthesis used gives an output having no appreciable harmonic content below the 7th harmonic, which in many cases may be used directly with the minimum of filtering. A second audio output is synthesized in quadrature with the first, so that s.s.b. modulation onto a sub-carrier may be easily and cheaply accomplished by the 'third method'.

4 Receive System

4.1 Audio Inputs

A simplified schematic of the Receive system is shown in Fig. 4. The Piccolo modem is designed to operate in dual diversity, accepting two audio inputs (in most cases from two radio receivers with spaced-diversity or polarization-diversity aeriars). Two inputs, at a preset level of nominally 0 dBm are amplified and then peak limited by Zener diodes. The gain is such that clipping just begins to occur on a signal at the nominal input level. Since the fundamental component of a square wave is only 2 dB above that of a sine wave with the same peak-to-peak amplitude, the dynamic range of signals above the median level is drastically reduced, and since such signals may be assumed to be at a reasonably high signal-to-noise ratio, this amplitude compression is achieved without appreciable signal-to-noise deterioration.

Each audio signal feeds in parallel 12 tone filters (or 6 in an ITA-2 only version) and the synchronizing system.

front panel indicator as a measure of the frequency error in the signal, and may be used to adjust the reference crystal oscillator to agree with that at the sending end. The 10 Hz extracted modulation is passed to a second phase locked loop which pulls in a local 10 Hz clock to a fixed phase relationship with the modulation.

An independent 10 Hz clock generated by direct division from the frequency standard controls the tone detectors and decoding. When the whole synchronizing system has pulled in accurately to the phase of the incoming modulation it outputs a single 'lock pulse' which instantaneously pulls this clock into the same phase.

No lock pulse can be generated until a series of checks have been satisfied which ensure that:

- The centre frequency of the incoming signal is 510 ± 7 Hz.
- The phase modulation on the incoming tone is 10 ± 0.4 Hz.
- The 10 Hz modulation is at adequate amplitude (equivalent to a stand-by signal greater than -2 dB on the nominal level).
- The error signal from the second p.l.l. is below a level equivalent to about ± 1.5 ms timing error.

The satisfaction of all these criteria is a sufficiently tight constraint on the incoming signal as to make it most unlikely that a spurious lock pulse will be generated by interference, by ionospherically generated corruption of the signal, or by a data signal.

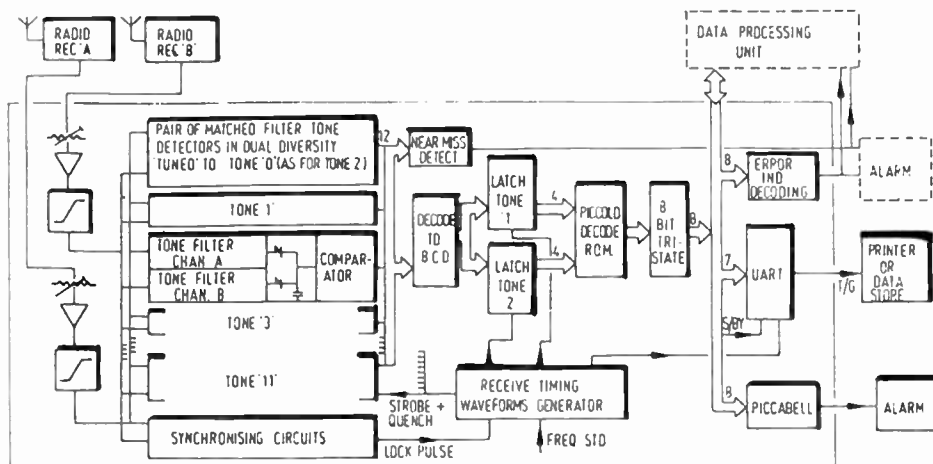


Fig. 4. Receive system—block schematic

4.2 Synchronizing System

The synchronizing system operates on the stand-by signal which is transmitted when no data are available, and consists of alternate 50 ms elements of 500 and 520 Hz. This may be regarded as a 'carrier' frequency of 510 Hz, phase modulated $\pm 90^\circ$ with a 10 Hz triangular waveform. In the synchronizing circuits this phase modulation is extracted in a phase-locked loop with a pull-in range (for a modulated signal) of about ± 7 Hz and a response to phase modulation resonant at 10 Hz. The mean d.c. output from this loop is available on a

However, the setting of a lower limit for a viable synchronizing signal does mean that a newly acquired signal which remains well below the nominal level may be of adequate quality to print but be printed incorrectly because of failure to synchronize. The possibility of this occurring is considerably reduced by the use of dual selection diversity, the synchronizing system switching alternately between the two diversity paths at about 0.5 second intervals, locking onto either channel only if it meets the first three criteria above.

The second p.l.l. is designed to give a very fast pull-in

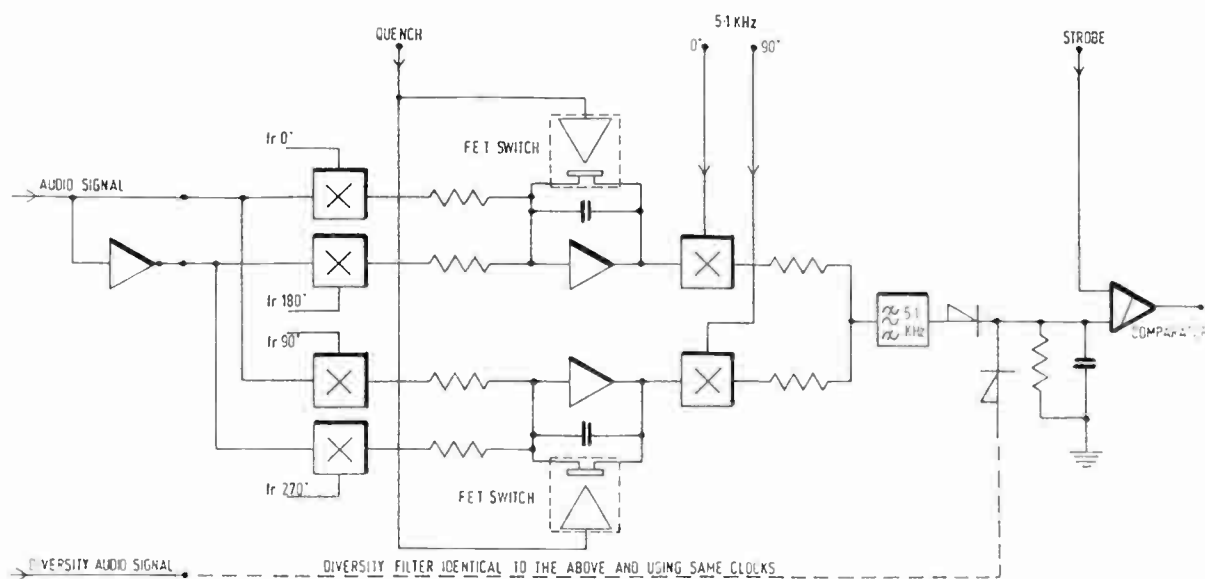


Fig. 5. Matched filter for tone element

for large errors, and on a clean signal at nominal level will pull in and output a lock pulse in less than 3 seconds. The total variation in the lock pulse timing with worst case fading and noise is normally no worse than ± 2 ms.

4.3 Tone Filters

The tone filters used in Piccolo operate on the 'integrate-and-dump' matched-filter principle. Those used in the early versions¹ consist of an LC resonant circuit to which positive feedback is applied to give effectively infinite Q , the circuit being 'quenched' at the end of each element by momentarily short-circuiting with a transistor. In the Mark 6 version this has been replaced by the quadrature-detection matched filter circuit shown diagrammatically in Fig. 5. A chopping waveform at the required filter frequency is synthesized as described in Section 4.4 and used to chop the incoming audio signal, the resultant then being integrated. The current into the integrator capacitor is directly proportional to the mean of the signal component in phase with the chopping waveform. A second waveform in quadrature with the first similarly extracts the quadrature component of the signal. The two integrators are reset to zero at the beginning of each element by discharging the integrator capacitors to zero through analogue f.e.t. switches, so that the root mean square of the two integrator outputs, measured at the end of the element, is proportional to the mean of the input signal component at the frequency of the filter. The frequency response and bandwidth of this arrangement is the same as that of the resonant circuit system.

The generation of the r.m.s. of the two bipolar voltages is conveniently carried out by using each source to modulate one of two quadrature square waves at the auxiliary frequency of 5.1 kHz (the precise frequency is of no significance). The two components are then linearly added, filtered to remove harmonics, and peak detected. The d.c. voltage on the peak detector is then the output

of the matched filter system. Two such filters are employed at each tone frequency, one on each of the diversity channels, the two peak detectors sharing a common detector load so that the output follows the higher of the two.

At the end of each element the detector outputs of all the filters are compared and the highest selected as described in section 4.5, and the d.c. voltages on the integrator capacitors are then discharged rapidly to zero in readiness for the next element. The total process of comparison and discharge occupies about 1.5 ms. Note that since the detector outputs are not relevant except at the instant of comparison, there is no need to discharge the detector capacitors and the relatively high auxiliary frequency of 5.1 kHz allows the detector voltage to follow accurately the peak value of the waveform without excessive ripple.

The limiting process on the audio input to the tone filters is reinforced by hard limiting the detected outputs from the filters, at roughly the same input level. The overall result is a matched filter having an effective dynamic range of at least 30 dB below and 10 dB above the nominal limiting level, which eliminates the need for any audio a.g.c.

4.4 Audio Frequency Synthesis

The chopping waveforms which determine the response frequency of each filter are synthesized by selecting from a number of standard pulse streams those appropriate for the required frequency, the actual repetition frequencies of the pulse streams being $240 \times$ the audio frequencies required, which are the 'channel frequency' (i.e. the lowest audio frequency in the channel—see Fig. 2) and binary multiples of 10 Hz up to 160 Hz.

These streams are generated in such a manner that no two pulses are co-incident, so that a single stream at any required frequency can be obtained by applying the appropriate standard streams to a single multiple-input

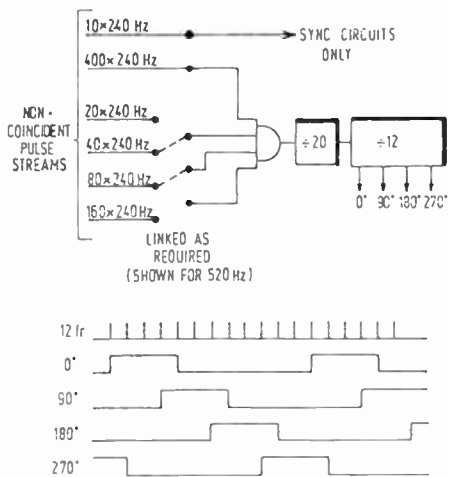


Fig. 6. Derivation of tone filter detection waveforms

gate, and then dividing by 240 as shown in Fig. 6. The high division ratio ensures that the timing jitter on the resulting audio frequency is negligible. Selection of the appropriate frequencies for each tone filter is carried out in the wiring of the mother board, so that all tone filter p.c.b.s are identical and the effective frequency of each filter is determined by the position of the board in the unit.

Each binary output waveform from a divider chops the incoming signal in an analogue f.e.t. switch. A disadvantage of this method (compared with a four-quadrant linear multiplication process) is that if the incoming signal contains harmonics, these will be acted on by the equivalent harmonics of the chopping waveforms and produce spurious d.c. components in the output, and since the peak limiting process previously described will generate distortion products on the signal (principally third harmonic), the chopping waveforms are deliberately designed to have no third harmonic, higher harmonics being negligible. This is achieved by generating from a clock frequency at 12 times the required audio, four 1:2 ratio waveforms in quadrature and using these to chop opposite phases of the incoming signals as shown in Fig. 5.

The same basic techniques are used to generate the reference frequency for the first p.l.l. in the synchronizing circuit (Sect. 4.2). A continuously variable frequency from 490 to 530 Hz is required, and this is produced by adding the pulse streams for 490 Hz, and also the '40 Hz' pulse stream gated by a variable mark/space ratio. Control of this ratio thus controls the frequency between the required limits.

The audio output from the modulator in the Send system is also generated from the standard pulse streams, each component except the 'channel frequency' being gated by a BCD control line from the r.o.m. In this case three 50/50 waveforms at the final audio frequency are generated at 45° intervals, then added in a resistive weighting network to produce a stepped waveform with no 3rd, 5th or even harmonics. An advantage of this method of synthesis is that no phase discontinuities are generated at the frequency transitions.

4.5 Comparison and 'Near Miss' Indication

The output from each tone filter is a d.c. voltage equal to the peak of the higher of the two diversity signals at each tone frequency. There are thus twelve such voltages (or six in the ITA-2 mode). Each of these outputs is applied to one input of a voltage comparator, the other input being connected to a single 'strobe' waveform. This is held high during the integration period, and at the end of the element is discharged towards zero with a short (approximately 0.2 ms) time-constant. When the strobe voltage equals the highest of the detected outputs, the corresponding comparator generates a transition which identifies which output has been selected. The strobe voltage is allowed to continue to fall to about 90% of this amplitude, and is then returned rapidly to its high condition and the quench pulse which discharges the integrator capacitors is initiated. If a second filter output is more than 90% of the highest, two comparator outputs will be high at the same time, and although this does not affect the subsequent decoding (based on the filter first chosen), it indicates that there is a lack of confidence in that choice, and each such occurrence is indicated to the operator by the momentary illumination of a 'poor signal' legend on the front panel. The pulse is also available externally. The threshold of the 'near miss' detection circuit is adjusted so that under typical conditions of poor signal the number of such events is approximately equal to the number of character errors in the output data. Since the indication occurs very frequently if the input signal consists only of noise, static, speech interference, etc., or falls below -30 dB on the mean, it is also a good general guide to the operator on the viability of the input signal.

4.6 Decoding

The input to the decoding system consists of a pulse every 50 ms on one of 12 wires from the comparators at the outputs of the tone filters. This is converted by logic into a binary representation of the number of the selected tone which is then stored in latches. When the second tone of a character has been similarly identified, the 8 latch outputs are decoded in a p.r.o.m. into the 7-bit telegraph character required. The p.r.o.m. decoding is slightly more complex than the send coding, since it must also distinguish three other conditions, namely:

- (a) Standby.
- (b) Any of the other three combinations (tones 5.5 : 6.5 : 6.6) which may be received in error when receiving the stand-by signal with the receive timing out of synchronization. This is used in the synchronizing circuit to give additional protection against false operation.
- (c) All the other non-valid characters. (See Sect. 2.3.)

If any of these three states is identified, this information is separately stored and all 7 data bits are forced to zero.

The 7 data bits, and stand-by on the 8th bit are latched on a tri-state bus system for 50 ms before being loaded into a u.a.r.t., converted to serial format at the appropriate telegraph rate and output from the equipment. The data bus is accessed by the error indication system, the Piccabell system, and by rear

panel connections which allow the control by an external data processing unit. If any of these sources wishes to block or modify the output data this may be done during the 50 ms period for which the data is held. These facilities will allow the implementation of an f.e.c. or ARQ system in conjunction with the error indication system described in Section 7.

5 Data Source Control

It is becoming common practice to use cryptography to protect the security of data in transit. Many such systems convey information by a continuous stream of apparently random characters and it is imperative that the received data should be kept in exact step with a locally generated 'key stream', the addition or subtraction of a single character being sufficient to upset the decyphering process. This problem is catered for in the Piccolo by providing two alternative modes of operation of the receiving system according to the data source control at the sending end.

5.1 'Normal' Operation

If the data rate of the source is reasonably accurate, no additional stand-by characters will normally need to be inserted into the continuous data stream. This means that at the receiving end, if a stand-by character is received it may be assumed in the first instance that this is a transmission error, and a NULL character is output to line so that the character is not deleted. If four successive stand-by characters are received it is evident that this is the termination of a data stream and the data output is held at steady mark. However, if pulse-release operation is not used, and the data source is slightly slow, the store will eventually empty and the inserted stand-by characters will be added to the output stream, causing character slip. To reduce this occurrence to a minimum, the input store is arranged to start from a 'reserve' of four characters, so that a typical data rate accuracy of 10^{-5} will permit at least 10 hours of continuous data without slip.

5.2 'Slow source' Operation

If the sending end data source has a wide tolerance on the data rate, manual control or clutch release operation will prevent the input store from over-filling, but if the source is slow, the store will empty periodically and stand-by characters will be inserted.

If stand-by were output from the Receive Piccolo as a data character, as in Section 5.1, a failure of the decrypt system would occur each time the sending store became empty. To avoid this all stand-by characters must be deleted from the output stream. Under such circumstances, if a transmission error causes the corruption of a data character to stand-by, a character will be omitted from the output stream and loss of cypher synchronization will result. This will occur theoretically about once every 36 character errors, which is an acceptable risk in most cases. As a rule of thumb, if the expected character error rate is worse than eight times the data rate tolerance, the 'normal' mode is preferred, as giving the maximum mean period without character slip.

6 The Piccabell System

After the initial introduction of the early Piccolo units into the FCO network a remote calling system actuated by the output data was designed and installed as an additional item. This facility has become such a vital part of network operation that a system fulfilling the same function, but with greater flexibility, has been incorporated in the new version.

The Send circuits of the Piccabell system will, on demand, generate a single or repeated cycles of the 'Piccabell call' consisting of a 14.4 second sequence as follows:

- (a) 9.6 seconds of stand-by.
- (b) 16 repetitions of a single character (the 'call' character).
- (c) 16 repetitions of the 'all mark' character to initialize a teleprinter.
- (d) 4 repetitions of a 4-character 'sending station identification'.

The call character and the four identification characters are independently programmable by switches on the Piccabell p.c.b. The Piccabell receiving system is active at all times, and all received data (whether or not it is printed) is scanned to detect the sequence of a long period (at least 3.2 seconds) of standby, followed immediately by continuous repetition of the 'response character' (which is also programmable). When the correct call sequence is identified it actuates the 'call received' state, which is available externally for an audible alarm, and also enables the printer for 5 seconds, allowing the identification of the calling station to be printed. Note that if the identification is not required, the call can be simply generated from the data source, for instance by using the 'run out' facility on a teleprinter keyboard.

There are several refinements of the circuit which are potentially useful in operating a network in which high priority traffic may need to be handled outside normal schedule hours. For instance, it is proposed that the operator's control system will allow the initiation of a Piccabell call either from a local button, or from a remote button (which may be associated with a remote alarm at the nightwatchman's or security guard's post) or automatically on the receipt of a call, the latter case acting as an automatic acknowledgment of 'call received'. Furthermore, at the end of transmission of a Piccabell call sequence, the data input store and data source is interrogated, and if a stored message is available, this is transmitted completely before the Piccabell call is considered terminated. This means that a base station may call an unmanned outstation and if the acknowledging call is initiated automatically or remotely, the stored data are read out.

The actual identification of the Piccabell call sequence is based on the 'counter race' system described in the Appendix. The system is effective even under conditions of very poor signal. With a character error rate as high as 50%, the probability of correct actuation remains better than 80% (i.e. 4 calls out of 5 will be successful), while the possibility of false operation by any spurious signal is negligible.

7 Error Indicating Coding

From past experience the error rate obtained on a typical Piccolo h.f. circuit under reasonable signal conditions is more than adequate for normal telegraphy purposes (typically better than 1 in 3000 characters). However, the growing use of automatic message switching, particularly for security classified traffic, means that some automatic system of error detection is essential. Such a system must primarily satisfy two requirements:

- (a) It must identify the collapse or deterioration of signal quality below an acceptable level, preferably within a matter of seconds, on a cryptographically protected (pseudo-random) data stream.
- (b) It must detect the occurrence of individual errors, particularly in routing instructions, with a very high degree of confidence.

It has been established⁶ that the use of binary error coding on a multi-level signalling system may be extremely ineffective, and therefore an error detection system for use with the new Piccolo should operate in either Modulo-6, Modulo-32 or Modulo-128. Since it was considered preferable to operate on the data in binary form, before tone coding and after tone decoding, a Modulo-128 parity check system³ has been developed which automatically reverts to Modulo-32 in the ITA-2 mode. The circuit allows a choice of two block lengths, either 8 or 16 characters. Each character is allocated a weight equivalent to the one's complement of its binary format, e.g. the character 1110011 is given the weight 0001100 (the '127s complement'). The 7 data characters in a block are then added and the sum (Modulo-128) is output as the parity character of the block. In the receiving system all 8 characters are complemented and added, and in the absence of errors the output is 1111111. When operating in ITA-2 the last 2 bits are always forced to '1'. It can be shown^{3,7} that this code is very effective, detecting all blocks containing a single error and more than 99% of all multiple-error blocks (more than 96% in ITA-2). When operating in ITA-2 with an 8-character block, with 3% input character error rate some 21% of the blocks are marked as containing errors, while the probability of an unmarked block containing an error is less than 10^{-3} .

The primary intention is that this code should be used in conjunction with an automatic message switch to allow completely automated processing of the majority of traffic, an 'error block detected' pulse causing a message to be diverted to a v.d.u. and the suspect block indicated by flashing. However, should a completely automatic system be required it is envisaged that the facilities available for an external data processing unit will allow the implementation of an f.e.c. or ARQ system. In the former case it is proposed that each code block (as described above) will be repeated immediately or after an interval of a few blocks. The message stream in the receiving system will be stored off the 8-bit bus until both versions of a block are available. If both blocks are marked as containing errors, two disagreeing characters are interchanged between blocks and the parity check on both is repeated, the process continuing

for all disagreements between the two blocks until a version is reached which satisfies the parity check. This is then output from the system down the 8-bit bus. The undetected error rate of this code should be the same as that of the original error indicating system.

Similarly an ARQ system may be implemented in which the decoded data at the receive end are output if they satisfy the block parity check, but if not the offending block is stored in the data processing unit and a repetition asked for by a return route. If, when the second version of the suspect block is received, it too contains an error the two blocks are compared as described above for the f.e.c. code. This process should result in a very low level of undetected errors and a good through-put, the number of second repetitions (i.e. three versions of the same block) required being negligible.

8 Mechanical Data and Performance

The equipment is housed on a single 5.25 in (133 mm) rack panel unit, which provides full duplex operation of a single telegraph channel complete with all the facilities described above. A mains power supply is included, and provision is also made for operation from a 24 V battery or the connection of such a battery to maintain a 'no-break' supply through mains failures. No special hybrid or custom-designed chips are used. The unit is designed for extended operation from an operator's control panel, but the front panel carries comprehensive system operation indications and diagnostic facilities. The design is such as to facilitate servicing down to module level in the field by a non-specialized technician using the minimum of test equipment.

The theoretical performance (in ITA-2 code) for single-path reception of a non-fading signal in white Gaussian noise is almost identical to that of an ideal coherent detector of binary p.s.k. signals, and some 3.5 dB better than that of an ideal non-coherent detector of f.s.k. signals.

The performance of the system has been measured on an h.f. channel simulator⁸ and shown to be within 1 dB of that calculated, except under fast fading conditions where the divergence from theory is qualitatively explicable.³

9 Acknowledgments

The Piccolo series of m.f.s.k. systems has been developed in the Development Section of the Communications Engineering Department of the Foreign and Commonwealth Office and the author would like to acknowledge the effort and dedication of his colleagues in the Section.

The Mark 6 unit has been designed for production by Racal Communication Ltd, Bracknell, under an MOD Development Contract and the manufacturers are licensed to exploit the design commercially, as Racal Modem No. LA1117.

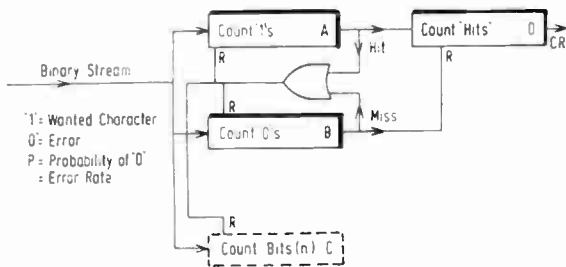
The author is grateful to the Director of Communications of the British Foreign and Commonwealth Office and to the Controller of HM Stationery Office for permission to publish this paper.

10 References

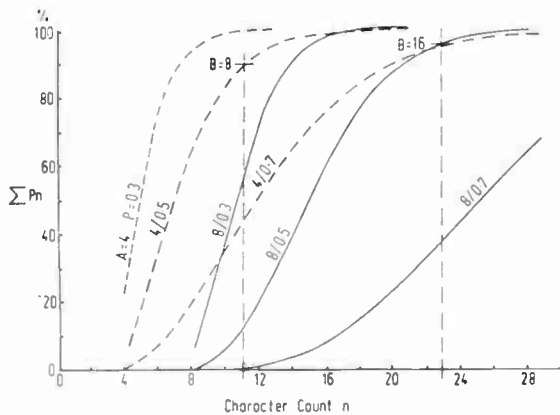
- 1 Robin, H. K., Bayley, D., Murray, T. L. and Ralphs, J. D., 'Multi-tone signalling system employing quenched resonators', *Proc. Instn Elect. Engrs* **110**, no. 9, pp. 155-4, September 1963. (IEE Paper 4204E).
- 2 Bayley, D. and Ralphs, J. D., 'The Piccolo 32-tone telegraph system in diplomatic communications', *Proc. Instn Elect. Engrs*, **119**, no. 9, pp. 1229-36, September 1971. (IEE Paper 6750).
- 3 Ralphs, J. D., 'The application of m.f.s.k. techniques to h.f. telegraphy', *The Radio and Electronic Engineer*, **47**, no. 10, pp. 435-44, October 1977.
- 4 CCIR, 'Multi-frequency-shift-keying techniques for h.f. telegraphy', Report 702, Vol. III, Kyoto, 1978, p. 171.
- 5 CCIR, 'Spectra and Bandwidths of Emissions', Rec. 328-3, Vol. 1, Geneva, 1974.
- 6 Bell, D. A., 'Piccolo 32-tone telegraph system in diplomatic communications' (correspondence), *Proc. Instn Elect. Engrs*, **120**, no. 8, pp. 851-2, August 1973.
- 7 Vincent, C. J., 'Modulo-M parity check in m.f.s.k. techniques', *The Radio and Electronic Engineer*, (Letters), **48**, no. 5, p. 248, May 1978.
- 8 Ralphs, J. D. and Sladen, F. M. E., 'An h.f. channel simulator using a new Rayleigh fading method', *The Radio and Electronic Engineer*, **46**, no. 12, pp. 579-87, December 1976.

11 Appendix: Piccabell 'Counter Race' Circuit

The receiving circuit for the selective calling system can be simplified for analysis as in Fig. 7(a). If counter A accumulates a total count of A correct characters, it outputs a 'hit'. Similarly the Counter B outputs if it accumulates a total count of B errors, referred to as a 'miss'. A third (hypothetical) counter C accumulates the total number n of characters received. The final 'Call



(a) Equivalent circuit for analysis



(b) Theoretical performance

Fig. 7. Counter race circuit

Received' output is energized if a total of D hits are scored. A hit resets A, B and C to zero. A miss resets all counters to zero.

Consider the system without any resetting and, starting with all counters at zero, let m be the number of 'ones' (correct characters) in a sequence of n characters, then:

- (a) If $m \geq A$, a hit will have been recorded at some point in the sequence.
- (b) If $n - m \geq B$, a miss will have been generated.

Note that when $n = A + B - 1$, one or the other event must occur in the sequence, but both cannot occur and so the resetting process limits each cycle to a maximum of $A + B - 1$. Therefore the resetting process does not affect the probability of success for each cycle although it may increase the number of attempts in a given time. The probability P_n of a Hit on a specific count n is given by:

$$P_n = (\text{probability of there being exactly } (A - 1) \text{ ones in } (n - 1) \text{ characters}) \times (\text{probability that the } n\text{th character will be a one}).$$

Note that if n is limited to $(A + B - 1)$, this equation implicitly excludes any previous or subsequent hits or misses in the sequence.

P_n is zero if $n < A$ or $n > (A + B - 1)$ and so if the probability of a character error is p the total probability P_h of a Hit in a sequence is

$$\begin{aligned} P_h &= \sum_{n=A}^{A+B-1} P_n \\ &= \sum_{n=A}^{A+B-1} C_{A-1}^{n-1} (1-p)^{(A-1)} \cdot p^{(n-1)-(A-1)} \cdot (1-p) \\ &= \sum_{n=A}^{A+B-1} \frac{(n-1)!}{(A-1)! (n-A)!} (1-p)^A \cdot p^{(n-A)} \end{aligned}$$

Note that B only occurs in P_h in the upper limit of n. It follows that if the summation is plotted for values of A and p as in Fig.7b, the value of B merely curtails the curve at the point $n = (A + B - 1)$ and the cumulative probability at this point is P_h .

The final probability of the call being received successfully is the probability of D successes in a row, and this is $(P_h)^D$.

11.1 Practical Parameters

In any practical system the parameters must be chosen on the basis of a compromise between the possibility of the call failing due to a high error rate, and the possibility of a false alarm as a result of noise, interference, or data input. The tentative target specification assumed was that a call should have a better than 50/50 chance of success when the character error rate was about 50%. Preliminary experiments and circuit convenience suggested a total of 5 cycles, the first 4 counting 'stand-by' characters and the last one counting 'call' characters, so that $D = 5$, and $P_h \geq 0.85$. From the curves of Fig. 7(b), it can be seen that the conditions would be satisfied by $A = 4, B = 8$, or by $A = 8, B = 16$. The first was rejected on the grounds that such a short selective

call could be prone to false alarms when working a net. The second case gives a performance rather better than the target, with a probability of success of about 80% at 50% errors, and 10% at 65% errors. A random noise input in ITA-2 mode gives an 'error rate' of 35/36, when the probability of a single 'hit' is about 1 in 8.4 million, or once in almost six months of continuous running, so the probability of five hits in succession may safely be assumed negligible.

A single hit sequence cannot take longer than 2.3 seconds so the limitation of the stand-by period to 9.6 seconds will not curtail the worst-case successful call.

The practical circuit must allow for an arbitrary period of stand-by from the completion of the first four 'stand-by' cycles to the beginning of the call character sequence and the system switches to the 'call character' mode after the receipt of two call characters following successful receipt of four stand-by hits. This modifies the operation slightly from that described above but not enough to affect the performance.

*Manuscript first received by the Institution on 9th November 1981 and in final form on 18th January 1982.
(Paper No. 2034/COM344)*

New Books Received

The following books which have been received recently have been placed in the Institution's Library and may be borrowed by members resident in the British Isles.

Digital Logic Design

B. HOLDSWORTH (*Chelsea College*)
Butterworths, Sevenoaks, 1981
14 x 22 cm, 338 pages, £17.95 (Hardback)

CONTENTS: Boolean algebra, Karnaugh maps and function simplification, NAND and NOR logic, Combinational logic design, Single-bit memory elements, Counters, Shift register counters and generators, Clock-driven sequential circuits, Event driven circuits, Digital design with MSI, Hazards, An introduction to microprocessors.

Essentially an undergraduate text, it should be useful to all practising engineers who have had no formal education in digital techniques.

Wave Propagation Theory

JAMES R. WAIT (*University of Arizona*)
Pergamon, Elmsford, New York, 1981
16.5 x 24 cm, 348 pages.

CONTENTS: Notation and some basic ideas, Reflection from stratified media, Magnetotelluric fields, General surface impedance, The Zenneck Wave, Excitation of the layered half-space—The Green's function, On the excitation of the Zenneck surface wave, Surface impedance of a spherically stratified conductor, Excitation of the h.f. surface wave by vertical and horizontal apertures, Fields of a dipole over an homogeneous anisotropic half-space, Fields of an horizontal dipole over a stratified anisotropic half-space, Asymptotic evaluation of the field of a vertical dipole over an impedance plane surface, Fields of a circular loop of current buried in a two-layer earth, Transmissions in an idealized Earth crust waveguide, Reflection from inhomogeneous media with special profiles, Approximate methods for inhomogeneous media, High frequency electromagnetic coupling between small loops, Reflection of VLF radio waves from an inhomogeneous isotropic ionosphere, Reflection from a lossy magnetoplasma half-space, EM propagation in the Earth-ionosphere waveguide, Guiding of microwaves by an elevated tropospheric

layer, Scattering from an isolated irregularity in a tropospheric duct, Coupled mode analysis for a non-uniform tropospheric waveguide.

Drawn from the author's lectures over the past 20 years, the book provides a comprehensive, up-to-date overview of electromagnetic wave propagation with special reference to terrestrial environments. It is intended that the material should provide a useful reference to engineers and scientists who are concerned with radio propagation both above and below the Earth's surface.

Discrete Electronic Components

F. F. MAZDA (*Rank Xerox*) Cambridge
University Press, 1981 18 x 25.5 cm, 177 pages, £18.00.

CONTENTS: Discrete semiconductors, Optoelectronic components, Resistors, Capacitors, Magnetic components, Peripheral components, Quartz, ceramic, glass and selenium, Power sources.

Electronic components come in many different sizes and shapes and in this book the author concentrates on components which are normally mounted on a printed wiring board. The book is primarily aimed at electronic engineers in industry, although parts of it should prove useful to postgraduate and undergraduate students. The book is basically a user's guide which describes the construction and applications of the whole range of devices currently available.

Solid State Circuit Files: Volumes One and Two

EDWARD M. NOLL Sams, Indianapolis, 1981
21 x 27.5 cm, Volume 1 89 pages, £5.15,
Volume 2 104 pages, £7.75.

CONTENTS: Vol. 1 Bipolar Transistor, FET and Linear IC Circuits Vol. 2 TTL and CMOS Circuits.

A collection of useful and tested circuits.

Minds and Mechanisms: Philosophical Psychology and Computational Models

MARGARET A. BODEN (*University of Sussex*)
Harvester Press, Hassocks, 1981
14 x 22.5 cm 311 pages, £20.00.

CONTENTS: Explanation and computation, What we have in mind, Psychologists ancient and modern, Values and psychological theory.

The essays contained in this book are concerned with four closely related questions. These explore in depth matters explained in the author's earlier books on artificial intelligence and therefore forms an important complementary work. The essays form a vital and comprehensive contribution to cognitive science—the interdisciplinary study of the mental representations and transformations that mediate thinking, action and experience.

How to Troubleshoot and Repair Microcomputers

JOHN D. LENK Reston, Reston, Virginia,
1980 15 x 23 cm, 290 pages, £5.55.

CONTENTS: Peripheral equipment and how it works, Microcomputer troubleshooting equipment, Troubleshooting typical microcomputer circuits, Microcomputer troubleshooting approaches.

Concentrates on basic approaches to microcomputer troubleshooting which can be applied to any microprocessor/stored program system.

Principles of Transistor Circuits (Sixth Edition)

S. W. AMOS (*Formerly British Broadcasting Corporation*) Butterworths, Sevenoaks, Kent, 1981 14.5 x 21.5 cm 331 pages, £12.50.

CONTENTS: Semiconductors and junction diodes, Basic principles of transistors, Common-base and common-gate amplifiers, Common-emitter and common-source amplifiers, Common-collector and common-drain amplifiers, Bias and d.c. stabilization, Small-signal A.F. amplifiers, Large-signal amplifiers, D.c. and pulse amplifiers, I.f. amplifiers, Sinusoidal oscillators, Detectors, frequency changers and receivers, Pulse generators, Sawtooth generators, Digital circuits, Further applications of transistors and other semiconductor devices.

A further edition, fully updated, of a well known work first published in 1959.

(Contd. on p. 357)

How complex a learning curve model need we use?

Professor D. R. TOWILL, D.Sc.(Eng.Prod.),
C.Eng., MIProdE, FIERE*

Based on a paper presented at the IERE Conference on Industrial Applications of Learning Curves and Progress Functions held in London in December 1981

SUMMARY

In using learning curves for management control in a typical industrial environment, we seek to identify a number of patterns in the basic data, each of which is an important source of information to be fed into the decision-making machinery. These patterns may be classified as follows:

- A trend-line, which in some 'best' sense, can be used for predicting future output. This trend-line can be influenced by proper design and planning of the product line.
- 'Normal' scatter about the trend-line, which constitutes a natural and acceptable variation, and which can be used for setting upper and lower bounds predicted output.
- 'Abnormal' scatter about the trend-line, which results in an unacceptable variation. It indicates an avoidable loss in production which can be traced to an assignable cause and hence eliminated by management control.
- 'Deterministic' changes in the trend-line. These may be long or short term, and have an assignable cause. An example of a management-induced cause is a planned change in the size or constitution of the direct labour force.

To derive a learning curve model which will cope with these four patterns simultaneously is a complex problem. The author believes there are considerable advantages in selecting the simplest model which is adequate for the purpose of efficient management control of a particular enterprise and will review a procedure for doing so. We are, after all, dealing with huge cost savings if we properly plan this activity. Understanding and implementing a simple model derived on the back of an envelope can be often more profitable for management than a sophisticated computerized model, the significance of which is difficult to grasp. The paper concentrates attention on the time constant model, and its variants, as found appropriate to 'industry learning'.

* Department of Mechanical Engineering and Engineering Production, The University of Wales Institute of Science and Technology, King Edward VII Avenue, Cardiff CF1 3NU

1 Introduction

There are many papers in the engineering and management literature which record an experience-linked improvement in task performance typically observed when plotting a suitable performance index as a function of time. These observations have been made for both long and short cycle-time tasks, and appear to apply to both individual operators and to groups of operators, and also in a wide range of industries. It is then common practice for such experimental data to be curve-fitted with an equation which it is hoped adequately describes the trend line through the inevitable scatter in results. Such curves have variously been called 'learning curves',¹ 'start-up curves',² 'progress functions',³ and 'improvement curves'.⁴ The axes used to display the data also vary widely according to the particular industry and task being studied. For example, three typical sets of data are shown in Fig. 1 and we note;

- In the first case, the axes used are quantity produced per unit time versus cumulative time spent on the task.
- In Fig. 1(b) the axes are cumulative average time per item versus cumulative number of items made (the latter plotted on a log scale).
- In Fig. 1(c) we have task time plotted versus the logarithm of cumulative number of items manufactured.

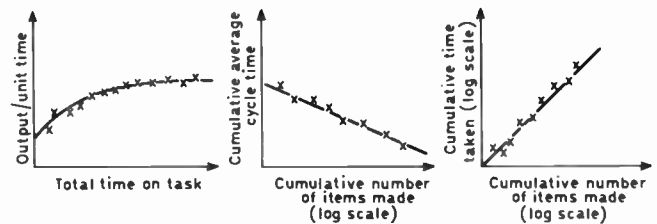


Fig. 1. Three alternative forms of learning curve graphs.

Depending on the nature of the experimental data, various 'laws' or trend equations describing the data have been proposed, these generally bearing the author's names; for example the de Jong model.⁵ As in all empirical curve fitting, the best type of equation is determined by trial and error. The best values of the equation parameters can be chosen on the basis of a computer algorithm which minimizes the least square error of the curve fit.

In general, there is no logical progression from one type of equation to another, should the initial choice be found wanting, although it is to be hoped that the progression will always start with the simplest plausible solution available. The one exception to this empirical approach is to be found in the family of models which includes as the focal point the time-constant model, and for which the data need to be in the form shown in Fig. 1(a). The vertical axis can be any convenient (but agreed and well understood) performance index which is known to increase with experience. In this paper we shall review the family of 'transfer function' models (so

designated because each member has an analogy with a physical system), thus aiding the understanding of any particular model.⁶ By progressing through the family in order of increasing difficulty, it will then become obvious when we have reached a good compromise between model complexity and accuracy of curve fitting to the data.

2 The Time-constant Model

An exponential model was first proposed at least as far back as 1950,⁷ but was restated in transfer function form with a suitable physical analogue in Ref. 8. Since then a number of studies have been published which indicate the utility of the time-constant model. If we denote $Y_{yt}(t)$ = model output at time t ; Y_c = model output at time $t = 0$; ($Y_c + Y_f$) as the model output at time $= \infty$, and τ as the model time constant, the equation relating model output to time is,

$$Y_{yt}(t) = \{ Y_c + Y_f \cdot (1 - e^{-t/\tau}) \} \quad (1)$$

which is the equation of the curve shown in Fig. 1(a). Hackett in Ref. 9 applied the time-constant model and 13 alternative learning curve laws to 88 sets of data recorded on widely different tasks. He found that the model was on average as good a curve fit as any competitor, the only model which gave a better curve fit

Table 1. Time-constant models for various industrial tasks

Industry	Task	Country	$\frac{Y_c + Y_f}{Y_c}$	τ (weeks)
Pharmaceuticals	Packaging	Japan	1.60	24
Printing	Startup of two-colour press	USA	1.23	7
Steel mill	Startup of rolling mill	USA	2.26	20
Chemical	Sampling and adjustment of product mix	UK	1.71	14
Cigar making	Leaf selection and processing	UK	2.35	3
Electrical	Switch assembly	UK	6.50	3
Watchmaking	Watch train assembly	UK	2.26	3
Heavy engineering	Anneal plates	UK	1.37	8

Table 2. Time-constant models for eight trainee operators performing electrical assembly tasks¹²

Trainee No.	Y_c (On the 0 → 100 British Standard Rating Scale)	Y_f (On the 0 → 100 British Standard Rating Scale)	τ (weeks)
1	31	81	4.6
2	30	75	5.0
3	33	57	3.5
4	35	75	7.6
5	36	54	4.3
6	36	54	4.0
7	33	77	8.4
8	35	55	4.5

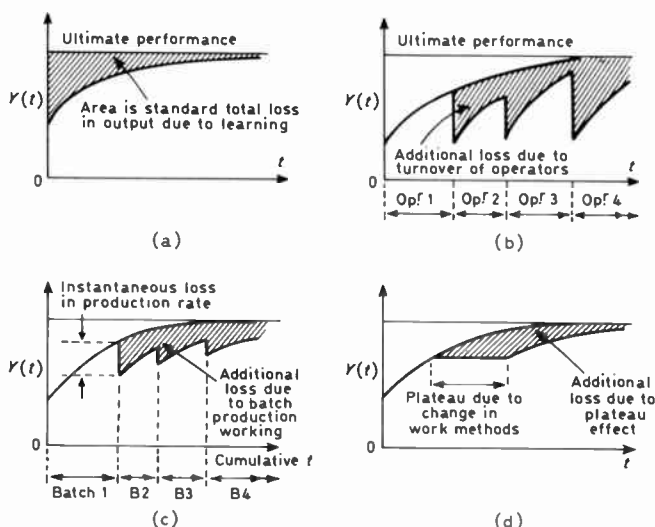


Fig. 2. Graphical interpretation of productivity losses via time-constant learning curve model.

to some sets of data failing completely in about half the test cases! Such lack of reliability for widespread use is a serious fault in any model rendering its use suspect in all but the most closely defined circumstances.¹⁰

Y_c , Y_f , and τ are functions of the task and many other variables. To give some guidance on typical ranges of model parameters, Table 1 is based on a world-wide collection of industrial case studies and is an augmented version of a previously published account.¹¹ It can be seen that the parameters vary enormously from situation to situation, suggesting that in the management of new product lines, adequate monitoring and forecasting techniques must be available,^{2,12} to help avoid the manufacturing system becoming unstable due to bad timing and bad quality decision making. Reference 2 quotes a particularly worthwhile example of this happening in the start-up of a new steel mill. Variations in model parameters are also to be expected between operators performing the same task. Table 2 is an example taken from South Wales industry in which six female operators are performing a short cycle (approximately 1 minute) electronic assembly task. In our experience, this variation between operators observed in the table is by no means unusual and must be taken account of in the design of training schemes. Bohlen¹³ has correlated the time-constant model parameters estimated for individual operators with the scores they obtained on the Purdue pegboard and five other tests. He validated his procedure by following the progress of 54 industrial operators working in Illinois light assembly industries. The results are sufficiently good to suggest consideration of the incorporation of his ideas into operator selection and training procedures.

The time-constant model has a number of interesting mathematical properties which make exploitation easy.¹² However, its practical use in management decision making can be illustrated graphically in Fig. 2, since added productivity loss resulting from a variety of industrial phenomena can be determined from the shaded area under the curve in each case. The same

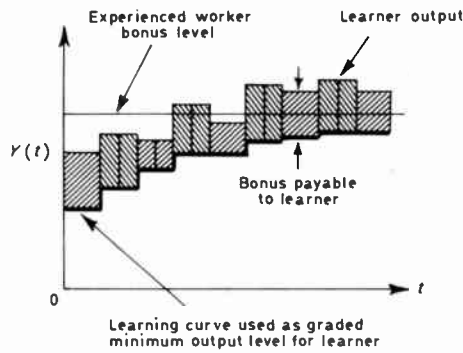


Fig. 3. Use of learning curve as a moving target for incentive scheme payments.

graphical reasoning also applies to the situation where the time-constant model is used as part of an incentive plan.¹⁴ As shown in Fig. 3, the 'learning allowance' and 'bonus output' have a simple visual interpretation.

3 Modelling Errors

Although the time-constant model has found wide application, it does not work in absolutely every case. With modification of the type suggested later in this paper, it does seem to work in most applications which may be described as 'industry learning'. The latter term is defined by Harvey¹⁵ as describing performance improvement in process or continuous flow industries as distinct from situations where the unit or production, e.g. one aircraft, is clearly apparent.

At any time t the observed data, $Y(t)$, will not agree exactly with the model output. The difference between the two is the model residual, $N(t)$, defined by

$$N(t) = [Y(t) - Y_M(t)]. \quad (2)$$

The residuals are, of course, also the curve-fit errors, which, in some curve-fit procedures, are chosen to minimize the sum of squared error calculated over all data points.^{9,13,16} In general, the lower the average

value of $(N(t))^2$ the better will be the curve fit, and the better will be any predictions made via the model.

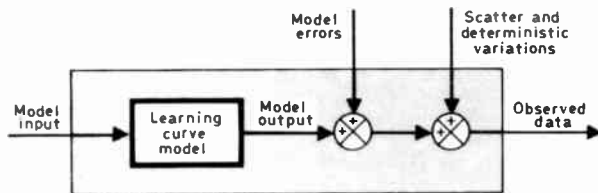
In general, there will be three main sources of prediction error,

- (i) There are errors due to 'natural' fluctuations in performance, with the fluctuations random (uncorrelated with each other) or deterministic such as a sinusoidal oscillation. Random errors usually show up as quickly varying scatter which is often Gaussian in pattern.¹⁶
- (ii) *Deterministic errors* usually vary more slowly and include plateaus, for which there may well be physiological, psychological, or environmental causes.
- (iii) A complete description of the experimental data is only achieved by taking account of *modelling errors*; that is, the form of the model may not permit adequate description of the trend line.

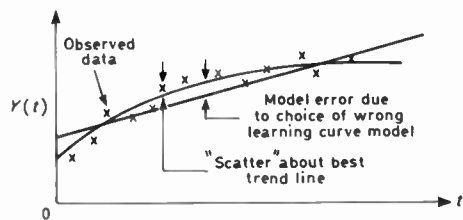
As an example of modelling errors occurring, an exponential equation could be curve-fitted to a straight line, as shown in Fig. 4. However, there will be considerable modelling error at almost every point on the curve. A statistical analysis, such as the run test¹⁷ would show up this phenomenon as a correlation between the model residuals. The block diagram also shown in Fig. 4 uses the common representation found in texts on system dynamics to represent the summation and subtraction of signals.

4 Model Selection for a Hardware System

We now digress to consider how an engineer would distinguish between these three error types, in anticipation that guidelines may thereby emerge for model selection in learning curve situations. When modelling the behaviour of physical systems the engineer will write down the differential equations governing the behaviour of the system, making such assumptions as are necessary to obtain a reasonable solution in the time available. The relevant fundamental laws such as those of Newton, Bernoulli, Ohm and Kirchhoff are enlisted for this purpose.¹⁸ Now the engineer is particularly interested in the solution of these differential equations for idealized operating conditions. The latter are usually chosen to enhance mathematical tractability of the solution and are then reproduced on the test rig at the commissioning stage of the equipment. One common method of solution of these differential equations is to use the Laplace Transform method, which may be regarded as a handle-turning exercise once the system transfer function has been obtained.¹⁹ Now the system transfer function relates system output to system input, and is the ratio of two polynomials in the Laplace Operator, s . However, the present author considers that the learning curve user does not need a formal background in Laplace Transform methods provided he appreciates the use of the transfer function as a shorthand notation which permits the solution of certain problems by analogy. Remember, *all systems with the same transfer function have the same behaviour to the same*



(a) Relating learning curve model to observed outputs.



(b) Example of model errors.

Fig. 4. Sources of variation about the learning curve model.

stimuli! Consider, as an example, the simple time-domain equation,

$$u(t) = (1 - e^{-t/T}) \tag{3}$$

which can be recognized as the time-dependent part of the time-constant learning curve model of equation (1). Equation (3) is the step response of all systems with transfer function,

$$F(s) = \left[\frac{1}{1 + Ts} \right] \tag{4}$$

The unit step stimulus which excites the system is zero until time $t = 0$, then suddenly changes at $t = 0$ to a value of unity, thereafter staying at this value. For the record, equations (3) and (4) are related via the inverse Laplace Transform,

$$u(t) = \mathcal{L}^{-1} \frac{F(s)}{s} = \mathcal{L}^{-1} \frac{1}{s(1 + Ts)} \tag{5}$$

which is solved using standard 'look-up' tables.¹⁹ The existence of these standard tables provides a powerful incentive to use transfer function analogies in learning curve modelling.⁶ Thus if the time constant model gives a large 'modelling error' term in Fig. 2, we can engage in a structured search through the tables to find a more complex model capable of yielding a better curve-fit, rather than add extra terms which have no physical analogue.

Whether or not a transfer function is a good descriptor of an actual system performance depends on the validity of the assumptions made during the analysis. For example, the hydraulic jack shown in block diagram form in Fig. 5 is described by the transfer function $[1/(1 + Ts)]$ only if the oil in the system is infinitely stiff. In practice, this is impossible, as the stiffness is certainly materially affected by any air trapped in the oil.²⁰ Thus the validity of the assumption is relative to the design of the system, and the environmental conditions under which it

operates. With finite oil stiffness, the transfer function of the hydraulic jack becomes 3rd-order, and is then somewhat more difficult to analyse, although Ref. 21 contains a number of design data sheets based on practical experience.

The practical problem resulting from infinite oil stiffness is the 'ringing' which then characterizes the jack response. This is clearly shown in Fig. 6(a) which could represent an oscilloscope trace from which the measurement noise has already been removed. The resulting equation describing $u(t)$ is then

$$u(t) \approx \{1 - e^{-10t} + e^{-5t}[\sin(5723t - 180^\circ)/9.987]\} \tag{6}$$

which has been obtained via equation (5) using the 3rd-order transfer function for $F(s)$. However, if the 'compressibility mode' is adequately damped, for example, via leakage across the piston, the ringing disappears, leaving the exponential type response of Fig. 6(b). This can be approximated somewhat crudely by a simple equation such as

$$u(t) \approx [1 - e^{-9.09t}] \tag{7}$$

For reasons which are beyond the scope of this paper, but are fully described in Ref. 21, an even better approximation to the response of Fig. 6(b) is given by

$$u(t) \approx 0 \quad \text{for } t \leq 0.01 \text{ s} \\ u(t) \approx \{1 - e^{-10(t-0.01)}\} \quad \text{for } t > 0.01 \text{ s} \tag{8}$$

which in practice is as easy to handle as the time-constant model. We would therefore conclude that in this instance the 1st-order approximation is good enough to commence the basic design of the jack, but it does not forewarn us of the possibility of oscillations in the response, which may well be a hazard as the fatigue life of the system is then affected. Under these circumstances, the engineer must design the system in sufficient depth to predict the existence of phenomena of this nature, the test rig serving to confirm the goodness of the design rather than raising questions of re-design.

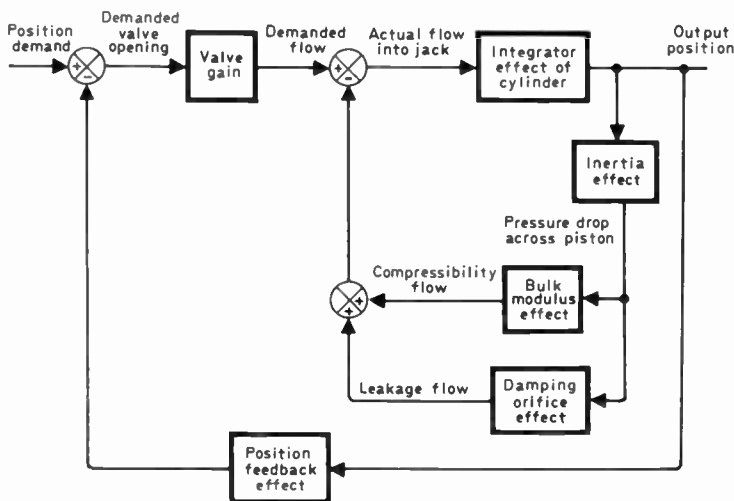


Fig. 5. Block diagram depicting physical functions in a hydraulic jack servomechanism.

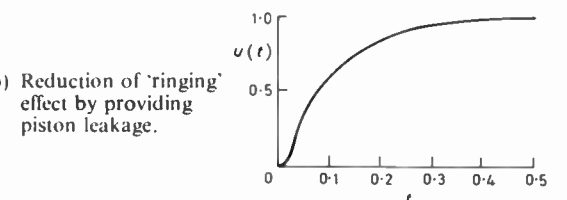
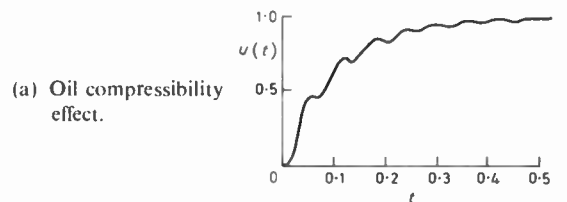


Fig. 6. Typical experimental step responses obtained for hydraulic jack servomechanism.

5 Is our Learning Curve Model Adequate?

At the test rig stage, the engineer faces a problem of interpretation. Suppose that an oscillation appears on the response of a system which was initially assumed to be 1st order. The oscillation may be a characteristic of the system under test, or it might be induced by the test rig, or it might be a characteristic of the measurement transducers. Repeatability of tests and further engineering analyses are required to resolve this situation to the satisfaction of the system user. There is, however, a similar problem facing the learning curve modeller.

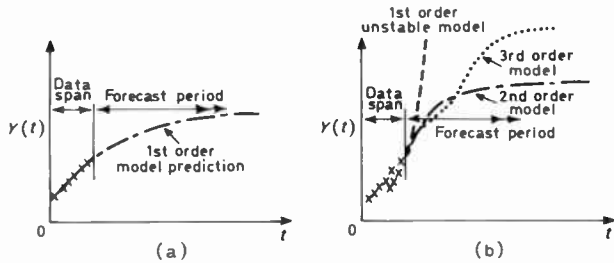


Fig. 7. Learning curve prediction problems.

- (a) Well-conditioned data (no modelling or prediction problems).
- (b) Ill-conditioned data (modelling and prediction much more subjective).

When using learning curves for forecasting purposes, we need to estimate model parameters early on in the improvement process. If the data are well behaved, as shown in Fig. 7(a) modelling and forecasting are reasonably straightforward. If the data (from the modelling point of view) are less well behaved, we may need to exercise considerable care in modelling and forecasting. For example, in Fig. 7(b), the time-constant model, religiously fitted to the early experimental data, will give a negative τ , and useless prediction. Either an 'S'-shaped curve or an oscillatory mode superimposed on the exponential would be more appropriate at this stage. Unlike the engineer concerned with hardware design and development, who has some opportunity for associating causality via the laws of physics, the learning curve analyst has little opportunity for discerning whether the oscillation is due to an assignable cause or not, or even whether it is likely to continue or die away. We also have the further complication that repeatability of human processes is more widely varied than for machinery, particularly during the improvement phase,

so that we can less readily use the conclusions from one set of data to guide the interpretation of another. Furthermore, in industrial studies, there is added difficulty in ensuring an adequate data collection scheme so that true causalities become apparent, thus running such risks as concluding that production rates are varying throughout the day, whereas the major source of variation may be due to the way in which time is spent by the operators. The true production rate (i.e. output/unit of time actually worked) is far less variable.²² Such factors mean that the time-constant model, adequate though it is for describing many improvement situations, cannot be applied totally blindly during on-line monitoring. Either we need to interact with the modelling process, or build suitable filtering into the data processing to suppress the effects of certain behaviour. When filtering is used, it is recommended that a separate estimate of variability about the trend be made and displayed. Thus the *range* of daily performance can be used to indicate the state of the process, and to suggest occasions where an industrial engineering investigation of operating practice is desirable.²³

6 Higher-order Transfer Functions

Suppose the learning curve analyst is ambitious and wishes to use a more complex model, notwithstanding the inherent difficulties likely to be encountered in curve fitting and interpretation. How can transfer functions assist in pointing the way forward? Let us turn to the problem frequently facing the engineer of describing the performance of a physical 'black box' in responding to a step stimulus. Here there is a logical path commencing as shown in Fig. 8, and which corresponds to a structured search through Laplace Transform tables. Our first assumption is that the 'black box' will faithfully transmit the stimulus undistorted and perfectly timed, thus having a transfer function of unity. The next level of assumption is to assume the 'black box' does not distort the stimulus, but delays the stimulus by a time increment τ . Then comes the time-constant model, followed by a delayed version of the previously defined time-constant model, followed by a delayed version of the time constant model. A 2nd-order model with real roots then follows. Note that this response is frequently met in behavioural science descriptions of human performance. Finally, the only 3rd-order system shown is for the case which particularly interests us. This has an oscillation of the oil compressibility type. Note that as the transfer function

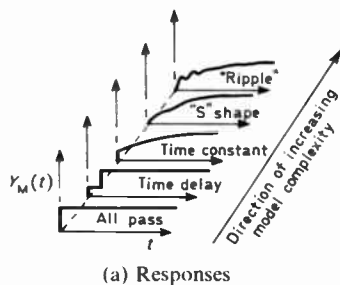


Fig. 8. Hierarchy of transfer function learning curve models.

Model	Transfer function
'Ripple'	$Y_c + \left\{ \frac{Y_f}{(1 + Ts)(1 + 2\zeta s/\omega_n + s^2/\omega_n^2)} \right\}$
'S' shaped	$Y_c + \left\{ \frac{Y_f}{(1 + T_1 s)(1 + T_2 s)} \right\}$
'Time-constant'	$Y_c + \left\{ \frac{Y_f}{1 + Ts} \right\}$
'Time delay'	$Y_c + \{ Y_f e^{-Ts} \}$
'All-pass'	$Y_c + \{ Y_f \}$

(b) Transfer functions

increases in order, the corresponding equation in the time domain for $u(t)$ becomes *very* much more involved. This increasing complexity is even more noticeable when parameter estimation is attempted. It is obvious that for the 1st-order system, only T must be estimated, for the 2nd-order system T_1 and T_2 must be estimated, whilst for the 3rd-order system, T , ζ , and ω_n must be estimated.

Methods of estimating parameters are outside the scope of this paper, but Refs. 9, 16, 24 and 25 give details of useful techniques. It is sufficient to say here that if all the learning curve data are available, i.e. $t \rightarrow \infty$ so that we are concerned with historical model building, simple graphical methods exist to estimate T in the case of the time-constant model, and T_1 and T_2 in the case of the 2nd-order model, once Y_c and Y_f are estimated by inspection (if necessary, after averaging the data around the origin and around the steady state value). Most methods which estimate Y_c and Y_f and τ early during the improvement process require the use of a digital computer or a programmable calculator, although there is a graphical technique which can be used provided the scatter is not excessive.¹⁶

7 An Example on Model Selection

To emphasize the options open to the modeller, consider the improvement curve resulting from the Crossman theory of the human operator selective process.²⁶ The data shown in Fig. 9 result from the transformation of the original Crossman calculations to the axes necessary for the transfer function approach.²⁷ By eye we can see a slight 'S' curve in evidence (Fig. 9(a)) so that a *good* curve fit attempt is with the time constant model (Fig. 9(b)), which results in large errors only near the origin, first negative, then positive in sign. The second curve fit accepts that there is more to the process than simply the time-constant model, and represents the process by a delayed time-constant model (Fig. 9(c)).

This delayed time-constant model fits the data well at the origin, and also beyond $t = (T + \tau)$, with a maximum error at $t = \tau$. The accuracy of this model increases rapidly as $T \gg \tau$. Finally, the 2nd-order model closely matches the 'S' curve, and in this case is clearly the best model to use (Fig. 9(d)). It is a matter of judgement by the modeller as to whether or not either the time-constant or the delayed time-constant models are adequate for this purpose without resorting to the 2nd-order model. It must be remembered that models are required in the first place in order to facilitate the comparison between different subjects, processes, and experimental conditions, so the simpler the better. The majority of industrial case studies available to the author do not exhibit the 'S' curve phenomena, suggesting that the time-constant model is adequate for most comparability purposes, but as suggested in Section 4, all models must be judged according to individual circumstances.

8 Sequential Transfer Function Models

Transfer function models may also be used to describe improvement processes where the plateau phenomenon is observed. This is done by using two time-constant models, one of which curve-fits the data up to the start of the plateau. A second model then curve-fits the data subsequent to the initiation of recovery, as shown in Fig. 10(a).²⁷ Often it is found that the recovery phase model time constant is approximately the same as for the initial phase model, the second curve then being simply the initial curve translated in time by the plateau length. Note that for the recovery phase model, we have the choice of time origin. We can start counting time from the recovery initiation point, calling the new time variable t' or we can count time from $t = 0$, in which case the model is only meaningful for values of time in excess of the recovery initiation point. Y_c and Y_f will, however, be different depending on which definition is used. In fact, if the recovery phase model is counted from $t = 0$, Y_{c2} may well be negative, but this of course does not mean there is a negative output at $t = 0$ for the process, since it is the initial model which is used to describe performance in this region.

The use of sequential transfer functions can be extended to the multiplateau case as shown in Fig. 10(b) since computational methods already exist for doing so.²⁷ However, the learning curve modeller needs to decide whether his purpose is better served by regarding the experimental data as represented by such a sequence of models, or by one model with periodic scatter, since the periodic scatter about the exponential trend may itself be regarded as indicative of a state of the process; witness 'stop-go' government policies of the last decade!

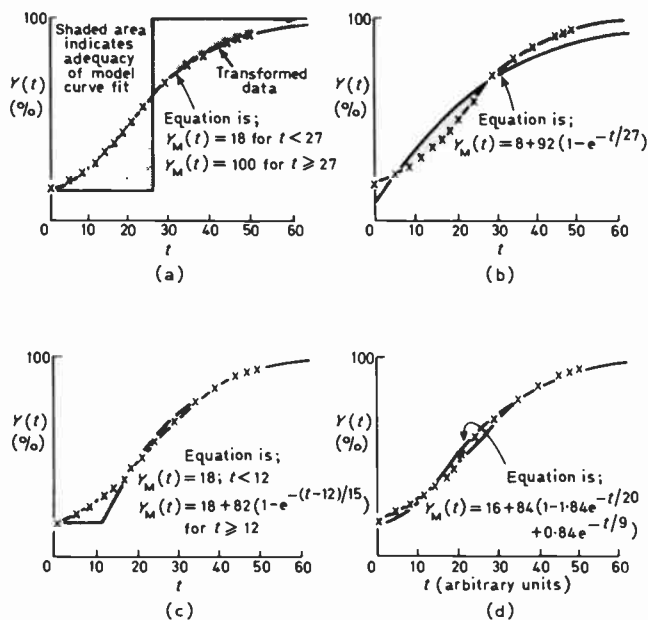


Fig. 9. Progressive stages in modelling the results obtained from the Crossman speed-skill theory.
 (a) Approximation by time delay model.
 (b) Approximation by time-constant model.
 (c) Approximation by delayed time constant model.
 (d) Approximation by 2nd-order model.

9 Event-adaptive Models

The existence of the plateau discussed in the last Section is usually attributable to a definite cause. For short-cycle repetitive tasks this can be due to the onset of a poor working pattern for an individual operator. In long-cycle tasks there may well be a change in work methods deliberately introduced at some time during the manufacturing life of the product. Ultimately there may well be a considerable increase in productivity to such changes, but in the short term there could be a definite plateau whilst new methods are bedded in. In the latter case the plateau is to be expected, so should be allowed for by the learning curve modeller. This is one of the many management-induced changes which affect performance.²⁸

Management-induced changes occur sufficiently often to justify special research into coping with their effect on the learning curve. One technique which has emerged is the so-called 'event adaptive' model wherein extra terms are added to the time-constant model, which now takes the form²⁹

$$Y(t) = \left\{ [Y_c + Y_f(1 - e^{-t/\tau})] + \sum_{i=1}^{i=m} W_i S_{it} \right\}. \quad (9)$$

Terms such as S_{it} can take only values of unity or zero, and the subscript refers to the i th event under consideration. Also S_{it} only takes the value unity for the time period appropriate to this cause. W_i is the weighting function attached to this particular cause and which can be positive or negative. It must either be estimated on-line or predicted from past records.

The advantage of using equation (9) is that it gives the learning curve modeller considerable flexibility to cope with known contingencies without recourse to a complicated model. This approach is analogous to the provision in work study of 'allowances' for known

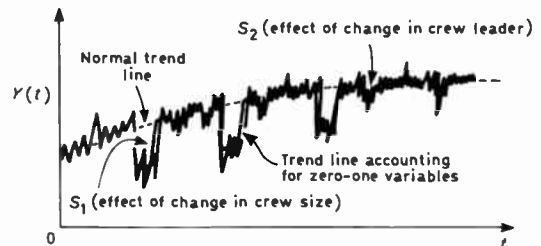


Fig. 11. Using the event-adaptive model by incorporation of 'zero-one' variables.

factors. Figure 11 shows the resulting modification to a learning curve where two zero-one events are allowed for in modelling performance of a heavy industrial group task. The two variables illustrated here are (a) a temporary reduction in number of operators composing the team and (b) a temporary change in which member of the crew is currently acting as leader. Using the event-adaptive model has led to improved output prediction and curve fitting.³⁰ It has also sharply focused on the real-time interaction between the learning curve modeller and management data information services, without which latter source the modification could not be made.

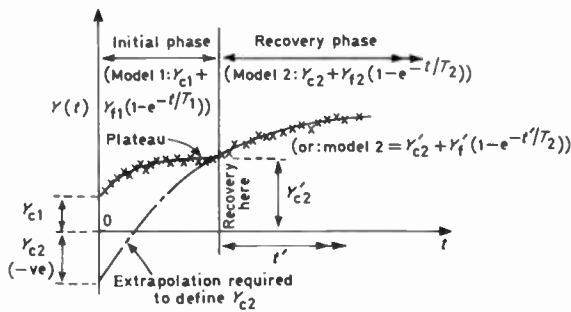
10 Recommendations

It is good management practice to install an information system which monitors 'industry learning', and compares the current rate of learning with the target value. With present knowledge this target value can only be set in one of three ways:

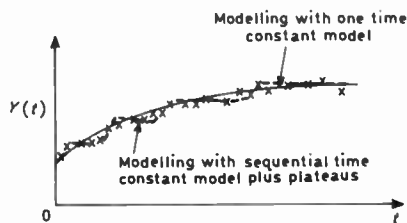
- (a) using synthetic learning curve data for individual parts of the task where such a breakdown is feasible;
- (b) from inter-company comparisons available in the open literature;
- (c) from careful use of a company data bank, in which previous performance data has been carefully annotated.

The time-constant learning curve model is frequently adequate for methods (b) and (c). Where it is not, the addition of a simple time delay is usually adequate. If periodic variations due to natural, or management induced causes, are suspected, it is suggested that these be allowed for in an additive manner, so that the simplicity of the time constant model is retained. The 'event-adaptive' model is similarly a simple way of coping with known contingencies such as absenteeism and changes in product mix.

We thus advocate the setting-up of a learning curve model which represents normal smooth increase in performance, with each significant deviation from the curve being separately accounted for. So the model can become the basis of a management control system with many different applications including costing, operator selection, etc.^{1,2} Once the proper model is in operation, deviations from target can be used to trigger management action. A plateau can suggest onset of bad work methods, a persistent fluctuation about the trend can be the result of a period-based payment-by-results



(a) Single plateau case with two time-constant models.



(b) Multi-plateau case with alternative interpretations.

Fig. 10. Application of the time-constant learning curve model to the plateau situation.

system, whilst excessive random scatter can indicate slack time standards. Management needs the simplest time-varying learning curve model which is adequate for this purpose.

11 References

- 1 Bahrick, H. P., Fitts, P. M. and Briggs, E. G., 'Learning curves—facts or artifacts?', *Psychological Bull.*, **54**, no. 3, pp. 256–68, 1957.
- 2 Baloff, N., 'Startup management', *IEEE Trans. on Engineering Management*, EM-17, pp. 132–141, 1970.
- 3 Glover, J. H., 'Selection of trainees and control of their progress', *Intl J. Prod. Res.*, **5**, no. 1, pp. 43–60, 1966.
- 4 Steedman, I., 'Some improvement curve theory', *Intl J. Prod. Res.*, **8**, no. 3, pp. 189–204, 1970.
- 5 de Jong, J. R., 'Effects of increasing skill and methods-time measurement', *Time & Motion Study*, **10**, pp. 17–24, 1961.
- 6 Towill, D. R., 'Transfer functions and learning curves', *Ergonomics*, **19**, pp. 623–38, 1976.
- 7 Knowles, A. R. and Bell, L. F., 'Learning curves will tell you who's worth training and who isn't', *Factory Management & Maintenance*, **108**, pp. 114–5, 202, June 1950.
- 8 Bevis, F. W., Finniear, C. and Towill, D. R., 'Prediction of operator performance during learning of repetitive tasks', *Intl J. Prod. Res.*, **8**, no. 4, pp. 293–305, 1970.
- 9 Hackett, E. A., CNA A M.Phil. Thesis, Middlesex Polytechnic at Hendon, 1974.
- 10 Towill, D. R., 'Low order modelling techniques: tools or toys?', Proc. IEE Conf. on Computer Aided Control System Design, Cambridge, 1973, pp. 206–12 (IEE Conf. Pub. No. 96, 1973).
- 11 Hindmarsh, G. W. and Towill, D. R., 'Theory and application of the time constant learning curve model'. Paper WA16.14, ORSA/TIMS Joint National Meeting, San Juan, Puerto Rico, 1974.
- 12 Towill, D. R. and Bevis, F. W., 'Managerial control systems based on learning curve models', *Intl J. Prod. Res.*, **11**, no. 3, pp. 219–38, 1973.
- 13 Bohlen, G. A., Ph.D. Thesis, Industrial Engineering Department, Purdue University, Lafayette, Indiana, 1973.
- 14 Turban, E., 'Incentives during learning—an application of the learning curve theory and a survey of other methods', *J. Industrial Engng*, pp. 600–7, December 1968.
- 15 Harvey, R. A., 'Analysis of contributory factors in aircraft production learning', Proc. IERE Int. Conf. on 'Industrial Applications of Learning Curves and Progress Functions', London, December 1981 (IERE Conference Proceedings No. 52).
- 16 Hitchings, B., M.Eng. Thesis, UWIST, Cardiff, 1972.
- 17 Siegel, S., 'Non-parametric Statistics for the Behavioural Sciences', pp. 52 *et seq.* (McGraw-Hill, New York, 1956).
- 18 Shearer, J. L., Murphy, A. T. and Richardson, H. H., 'Introduction to System Dynamics', chap. 5 (Addison Wesley, Reading, Mass., 1967).
- 19 Truxal, J. G., 'Control System Synthesis', chap. 1 (McGraw-Hill, New York, 1955).
- 20 Harpur, N. F., 'Some design considerations of hydraulic servomechanisms of jack type', Proc. I.Mech.E. Conf. on Hydraulic Servomechanisms, London, 1953.
- 21 Towill, D. R., 'Coefficient Plane Models for Control System Analysis and Design', chap. 2 (Research Studies Press, Forest Grove, Oregon, 1980).
- 22 Dudley, N. A., 'Work Measurement: Some Research Studies' (Macmillan, London, 1968).
- 23 Towill, D. R. and Eler, M. S., 'Performance models in a process industry', Joint National Meeting of the Operations Research Society of America/The Institute of Management Sciences, Las Vegas, Nevada, USA, TP14.8, pp. 1–1, November 1975.
- 24 Graupe, D., 'Identification of Systems', chap. 3 (van Nostrand Reinhold, New York, 1972).
- 25 Davis, W. D. T., 'Systems Identification for Self-adaptive Control' (Wiley-Interscience, New York, 1970).
- 26 Crossman, E. R. F., 'A theory of the acquisition of speed-skill', *Ergonomics*, **12**, pp. 153–66, 1959.
- 27 Sriyananda, H. and Towill, D. R., 'Prediction of human operator performance', *IEEE Trans. on Reliability*, R-22, pp. 148–56, 1973.
- 28 Kaloo, U. and Towill, D. R., 'Time-dependent changes in the production levels of experienced workers', *Intl J. Prod. Res.*, **17**, no. 1, pp. 45–59, 1979.
- 29 Cherrington, J. E., 'Event-adaptive v. sequential modelling of learning curves', Proc. V Symposium uber Operations Research, Universitat zu Koln, August 1980.
- 30 Cherrington, J. E., CNA A Ph.D. Thesis, City of Birmingham Polytechnic. (In preparation) 1981.

*Manuscript received by the Institution on 17th August 1981
(Paper No. 2035/ACS27)*

Book Review

The Kingdom of Sand: essays to salute a world in process of being born

WILLIAM GOSLING (Technical Director, Plessey Electronic Systems)

Council for Education Technology, London, 1981 14.8 × 21 cm. 98 pages, £4.50

CONTENTS: In the age of the thinking machines. The kingdom of sand. Invention, too, has a natural history. Some possible futures for the developed world. Augusta Ada and the religious education problem.

Most members of this Institution will be familiar with the writings of Professor Gosling, as distinct from his papers, which have been published in this Journal: in 1974, his Inaugural Address at the University of Bath, 'Technology at Childhood's End', and in 1980 his Presidential Address, 'Electronics—a Profession in its Golden Age'. These addresses, which aroused great interest and enthusiasm in both spoken and written form, demonstrated his wide ranging views on the problems facing the engineer today, and in particular the electronics engineer.

The present collection of essays, based on talks given to some very diverse audiences between 1978 and 1981, set out further aspects of his thinking: one lecture, 'The Kingdom of Sand', which gives its name to the book, is of course a reference to the silicon devices—and optical fibres—which have already revolutionized our discipline, and looks into the means of realization and implications of what is now known as 'information technology'.

The other four essays each take the themes broadly suggested in their titles and explore, in his characteristically forthright manner, the whole process of innovation and the nature of technological change. The 'natural history' of invention, given to a new graduate intake at Plessey, tries to show how different types of technical advance may be expected to

progress, while the forward look into trends in growth, given to senior Plessey management, calls for a greater understanding of his earlier thesis that technology is now challenged by maturity and is in fact 'at childhood's end'.

The final essay, first given at a convent, sketches out some of the relationships which are implicit regarding the human brain as a 'biological computer' only functioning 'by virtue of the incredibly sophisticated adaptive software which is stored within it.' He then touches on analogies between this software and theological concepts.

Many readers will find Professor Gosling's ideas express well what they feel themselves: a few may disagree emphatically. None however will dispute the views expressed by the Director of the Council for Educational Technology, Geoffrey Hubbard, in his Foreword, that William Gosling 'is a communicator, who speaks fluently and compellingly, and who writes with clarity and style'.

F.W.S.

A simple model of longitudinal digital magnetic recording

W. R. NAYLAND, C.Eng., MIERE*

SUMMARY

A two-dimensional theoretical distribution with many of the features observed on a 5000:1 model is developed and the field external to the medium linking the replay head is shown to be equivalent to the field from a filamentary pole parallel to the medium surface and transverse to the track direction located at the centre of each transition. Each transition is described by its pole strength per unit track width, Φ_t and its distance behind the medium surface, a . Methods for relating Φ_t and a to the magnetic characteristic and physical dimensions of the medium are developed. Prediction of the replay performance from the theory show good agreement with experimental data.

A notation for describing vectorial magnetization in two cartesian dimensions is introduced which automatically enforces the requirement that the divergence of B is zero whilst simultaneously allowing the magnetization of elements within the distribution some independence so that internal divergence of magnetization is described.

* 23 Burnt Common Close, Ripley, Surrey GU23 6HH.

1 Introduction

A popular theory of longitudinal magnetic recording assumes that the magnetization is one-dimensional and has the form $J_x = \arctan x$, $J_y = 0$, where J is the flux density of magnetization.¹ This assumption is not consistent with the experimental evidence obtained on a 5000:1 model by Tjaden and Leyten.² (See Fig. 1(a).)

The purposes of this paper are threefold. First, to develop a model magnetization distribution (Fig. 1(b)) which has many of the characteristics of the empirical distribution and which may be described by two parameters, Φ_t and a . Φ_t is a scaling parameter varying the flux density everywhere in the distribution and a is a transition width parameter for which the pulse width obtained by an ideal head in good contact with the recording medium measured at 50% of the peak replay amplitude is $2a$. Secondly, to derive reasonable approximations by which Φ_t and a may be determined with sufficient accuracy by measurements not subject to the large errors introduced by spacing loss. Thirdly, to show how replay performance may be predicted from a knowledge of Φ_t and a and the system parameters; replay head gap, relative head to medium velocity and the spacing between the replay head and the recording medium. In this context it is shown that an equivalent model of the replay process may be obtained by representing each transition by a filamentary pole located a behind the medium surface, where the pole maps as a point in the two dimensions of interest and has strength Φ_t webers per metre track width.

It is assumed that the track width is sufficiently large compared with all other relevant dimensions so that track edge effects are negligible and then the track may be regarded as a section taken from an infinite width track so that a two-dimensional treatment is justified with x as the track length dimension, y the medium thickness dimension and w the track width dimension.

SI units are used throughout and data taken from other authors' work is converted to this form. The notation used for magnetic quantities is taken from Olsen.³

2 The Model Magnetic Field Distributions

The magnetization distribution is assumed to take a functional form described by Φ_t and a . In general the dimensions involved are large compared with particle dimensions for a particulate medium so that the material properties are those measured on a large bulk sample. The material may be anisotropic with the principal directions along the track and normal to the medium surface. Consistent with the experimental results obtained by Bate,⁴ it is assumed that the material properties vary smoothly with angle.

The classical theory of magnetization is amply described in the literature for the c.g.s. system of units, e.g. Becker,⁵ but some modification is needed to account for permeability to be consistent with the SI system and further modification is made to facilitate the generalized description of magnetization with distributed divergence.

In order to translate some of the concepts discussed by Becker for three dimensions to two dimensions the following reduction is useful. Becker shows that flux

density may be represented by the curl of an arbitrary, sufficiently continuous and differentiable vector field. Let this arbitrary field be U and let the components of U in the x , y and w directions be U_x , U_y and U_w respectively and let $U_x = U_y = 0$, then $\text{curl } U$ becomes $\hat{c}U/\hat{c}y - j \hat{c}U/\hat{c}x$ and in two dimensions U may be regarded as a scalar. Becker also shows that H may be represented as minus the gradient of a scalar $= -\text{grad } v$ and in two dimensions v will be invariant with respect to w . If $V = \mu v$, then $W = U + jV$ is the complex potential discussed by Tozoni,⁶ although he reverses the normal usage in English (adhered to here) for U and V . Tozoni shows that, for all regular forms of f , if

$$W = f(z) = f(x + jy),$$

then U and V separately satisfy the Laplace equation and are connected by the Cauchy-Riemann conditions, namely

$$\frac{\partial U}{\partial x} = \frac{\partial V}{\partial y} \quad \text{and} \quad \frac{\partial U}{\partial y} = -\frac{\partial V}{\partial x}.$$

With these conditions loci of constant U are perpendicular to loci of constant V and hence loci of constant v and W is a differentiable function of z , i.e. dW/dz exists and is independent of the direction of dz . Fields free of magnetization or current always satisfy the Laplace equation so that the complex potential method is a convenient and appropriate notation for the discussion of fields outside the magnetic medium.

In the notation U is a measure of the flux per metre track width crossed when moving in the z plane from the datum $U = 0$ to the point in question and has the dimension weber/metre. Similarly v is a measure of the m.m.f. crossed when moving in the z plane from the datum $v = 0$ to the point in question and has the dimension of current (amperes). Then it can be found that

$$\begin{aligned} \mathbf{B} &= \text{curl } U = \frac{\partial U}{\partial y} - j \frac{\partial U}{\partial x} = \mu \mathbf{H} = -\mu \text{grad } v \\ &= -\mu \left(\frac{\partial v}{\partial x} + j \frac{\partial v}{\partial y} \right) = -\text{grad } V = -\left(\frac{\partial V}{\partial x} + j \frac{\partial V}{\partial y} \right) \end{aligned}$$

U is known as the stream function and loci of constant U are streamlines or lines of force and v is known as the potential function and loci of constant v are equipotentials.

The notation requires some adaption in order to describe magnetization. The recording medium is regarded as closely-packed elemental prisms with their major axis in the track width direction. This is a mathematical fiction which does not purport to describe the particulate nature of the medium which is regarded for this purpose as homogeneous with properties identical to those measured in bulk and the prisms are regarded as fitting so closely that there are no boundary effects. The magnetization in each element is taken to be normal to its major axis but may have any direction in the z plane. Because of the curvilinear nature of the magnetic recording process the magnetization of each element is regarded as independent of its neighbours so that divergence will occur internal to the medium as well as at the surfaces. If, for the sake of discussion, a prism

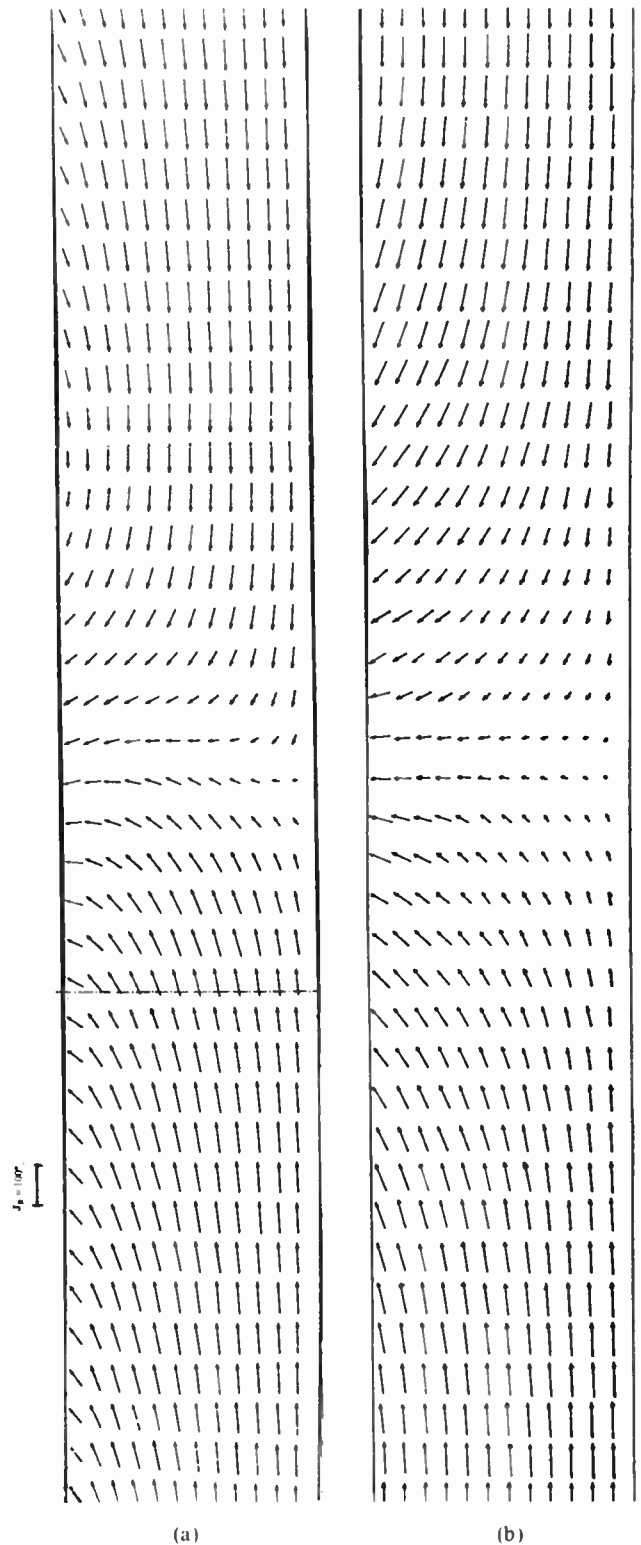


Fig. 1(a). Empirical magnetization distribution obtained by Tjaden and Leyten.² (b) Theoretical magnetic polarization distribution.

had a square cross-section with its faces normal and parallel to the magnetization then it could, in principle, be placed in a zero reluctance return path so that \mathbf{H} and hence m.m.f. would be zero everywhere and the net flux would equal the magnetization. The flux density would be totally described by \mathbf{J}_0 , the magnetic polarization.

If now an m.m.f. were induced in the return path by a suitably disposed current then a potential gradient would be established across the prism and the flux density would undergo a change proportional to μ and \mathbf{H} . In this case μ is the incremental permeability. Then the net flux through a prism may be regarded as the sum of its magnetization with no potential gradient present, \mathbf{J}_0 , and the flux due to the potential gradient. It is fundamental to our understanding of \mathbf{B} that in total \mathbf{B} exhibits no divergence, i.e. flux circulates without being either created or destroyed. (This comment is of course subject to quantum physicists proving that the isolated pole exists but it should not affect our understanding at this level.) Then, because div curl is identically zero, net magnetization flux, \mathbf{J}_m , is most conveniently and naturally described as the curl of an appropriate vector field, U_m . Nonetheless, as has been discussed, it is to be expected that individual elements will be magnetized with some degree of independence from their neighbours so that the description of the magnetization of the elements, \mathbf{J}_0 , must allow some divergence. The effect of this divergence will be to set up a potential field, v_m , which redistributes the flux to a non-divergent state. Because the net magnetization flux is fully described by U_m there will be no net flux associated with v_m so that v_m must be zero at the medium boundaries. A discontinuity in v_m would imply infinite field gradient which is unsustainable so it may be concluded that v_m is continuous. A discontinuity in U_m would imply a flux source or sink so U_m is also continuous. Otherwise there are no *a priori* constraints placed on the form taken by U_m and v_m . The flux density described by U_m is $\mathbf{J}_m = \text{curl } U_m$. The magnetization force described by v_m is $\mathbf{M}_m = -\text{grad } v_m$. The flux density through an isolated element with a zero reluctance return path is

$$\mathbf{J}_0 = \mathbf{J}_m - \mu \mathbf{M}_m = \text{curl } U_m + \mu \text{grad } v_m. \quad (1)$$

If the recording medium were surrounded by zero reluctance keepers the above expression would describe the flux distribution in its entirety. The real situation is that the external flux path has reluctance so that the passage of flux through it sets up a potential which acts to maintain the flux external to the medium and to oppose the emergence of flux from the medium. Because this field opposes the flux emergent from the medium it is conveniently known as the demagnetization field. The flux density of this field will be \mathbf{B} and the magnetization force \mathbf{H} . The potential distribution describing this field will be v which will be continuous everywhere and $\mathbf{H} = -\text{grad } v$. The associated stream function will be U which will be continuous everywhere except at the medium boundaries where the discontinuity will exactly match the discontinuity in the magnetization stream function, U_m , so that the total stream function, $U_t = U_m + U$ is continuous everywhere and $\mathbf{B}_t = \text{curl } U_t$.

Similarly the total potential function is $v_t = v_m + v$ and $\text{grad } v_t = -(\mathbf{M}_m + \mathbf{H})$.

Then

$$\mathbf{B} = \mathbf{J}_m + \mu \mathbf{H} = \text{curl } U_m + \text{curl } U \quad (2)$$

and

$$\mathbf{J}_0 = \text{curl } U_t + \mu \text{grad } v_t \quad (3)$$

Figure 2 illustrates the concepts discussed above with a simple thought experiment in which the flux is entirely perpendicular, U is a function of x only and v a function of y only.

The write process is, of course, crucial to the form taken by the recorded transition. Space limitation does not permit more than a brief discussion of this topic but fortunately there is evidence in the literature from complex numerical calculations, e.g. Potter and Schmulian,⁷ Curland and Speliotis⁸ and Ortenburger *et al.*,⁹ that the final transition shape is largely determined by permanent demagnetization which takes place when the medium is exposed to the greatest demagnetization field. This field occurs when the medium is completely removed from the vicinity of the head. Then, although the write process is to some extent asymmetric, the final transition is very much less so. Also from Potter and Schmulian⁷ the write current rise-time has only a small effect on the final transition shape. The empirical observations by, e.g. Bate and Dunn,¹⁰ Middleton and Wisely,¹¹ Davies¹² and Miyata and Hartel,¹³ that the replay amplitude and pulse width are substantially independent of write current providing it is greater than a minimum for a given set of system parameters also tend to support the same conclusions.

Earlier accounts of the write process, e.g. McCary,¹⁴ assume that longitudinal recording in the presence of the large component of the head field normal to the medium surface at the trailing edge of the gap is accounted for by anisotropy of the medium. This assumption is unnecessary and should be discussed in this context where it is assumed that magnetization can have an appreciable component normal to the medium surface.

If it is taken that regions already magnetized set up potential distributions which tend to maintain their magnetization externally at the expense of a tendency to demagnetize themselves, then an intuitive understanding of the write process may be arrived at which is presented in the sequence of Figs. 3 to 8.

Figure 3 illustrates the condition between transitions for an initially demagnetized medium. The demagnetization field distorts the head field so that a stationary potential wave is formed at the gap which the medium leaves with magnetization mainly longitudinal. As the newly magnetized region leaves the gap area the potential gradient, indicated by the closeness of the equipotentials, is so low that virtually no demagnetization takes place in this region and the medium is very close to saturation as a result.

Figure 4 illustrates the condition when the head current is zero halfway through the current switching sequence initiating a new transition. At this instant flux distribution external to the magnetized region is maintained by the demagnetization field alone and the potential gradient will be no greater than is sufficient to

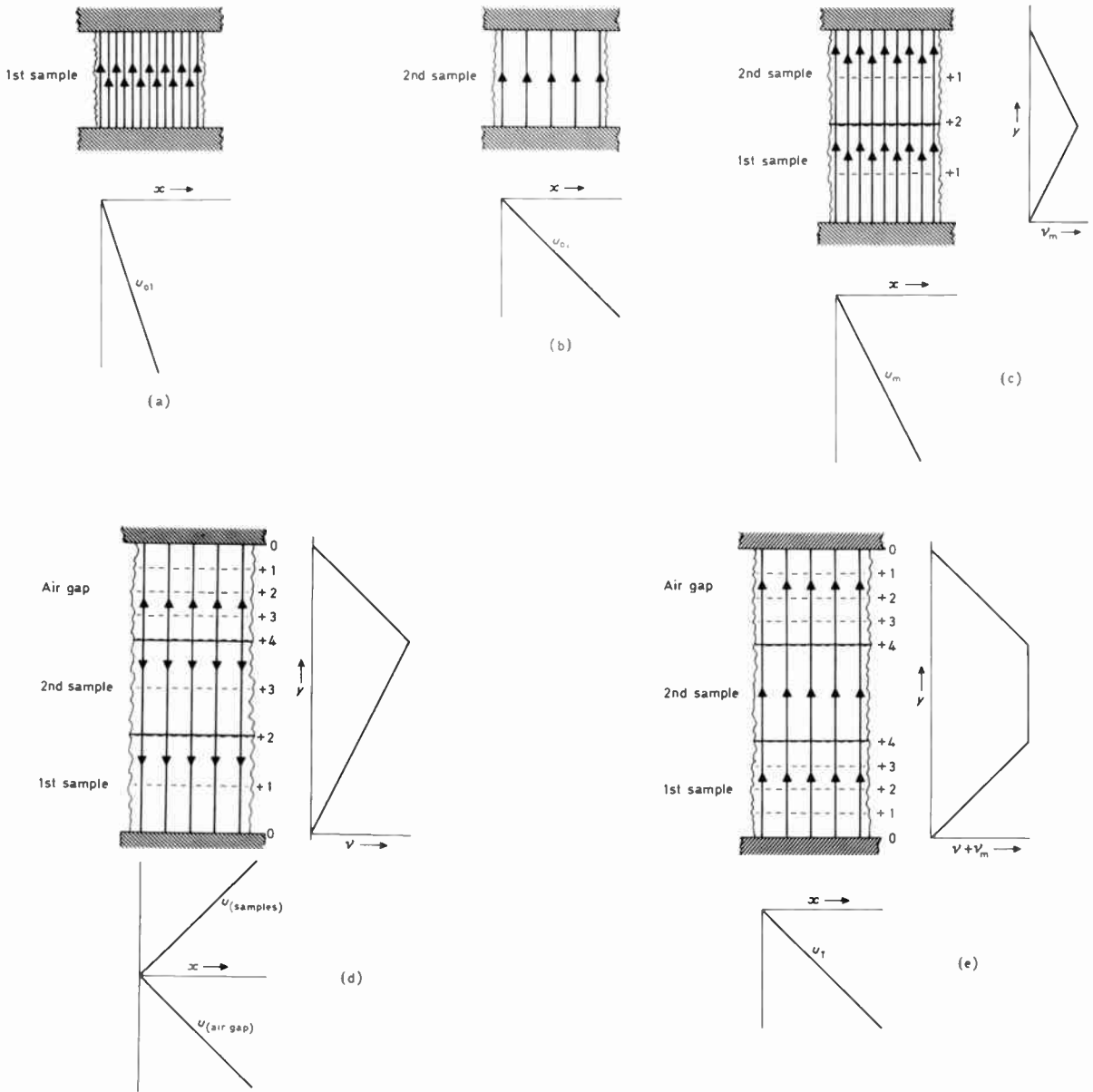


Fig. 2. Build-up of composite assembly with internal divergence to illustrate magnetic field notation presented herein. The magnetic samples are assumed to be small sections at the centre of large sheets so that edge effects can be neglected and thus the fields are uniformly distributed over the samples. The magnetic characteristics of the samples are assumed to be such that no permanent demagnetization occurs at any stage in the build-up of the assembly and the incremental relative permeability of the samples representing the slope of the minor recoil loops is assumed to be two. Stream functions (U) and potential functions (v) are illustrated except where they are zero and streamlines are plotted as solid lines at intervals of equal increments in U whilst equipotentials are plotted in broken lines for equal increments in v .

(a) 1st sample magnetized so that J_0 is 0.12 tesla. The stream function is U_{01} . The sample is shown between the poles of a zero reluctance return path (not shown) and so the potential function is zero everywhere and there are no equipotentials.

(b) 2nd sample as above but J_0 is 0.04 tesla.

(c) Two samples above of same thickness and permeability arranged in series between the poles of the zero reluctance return path so that the potential of both poles is zero. Each sample has the same cross-sectional area so that they have the same incremental reluctance. For continuity of the stream function the flux density in the first sample must reduce and that in the second sample must increase until they are

equal and for continuity of the potential function the potential at the boundary must be the same for both samples. These conditions are satisfied when J_m in both samples is 0.08 tesla which requires an equal increment of flux density in both samples and hence equal potential gradient in each sample and hence equal potential drop. These are the conditions illustrated.

(d) The demagnetization field that results when an air-gap of the same length as one sample is introduced. The combined samples have twice the length and twice the permeability of the air-gap and so have the same reluctance as the air-gap. For continuity at the boundary the potential drop is the same for the gap and the combined samples. Then the flux density due to this potential drop is the same for the air-gap and samples but in the opposite direction. Note that any sample assembly with the same overall dimensions and the same permeability with the same net stream function, U_m , giving flux injected into the sample air-gap boundary of 0.08 tesla, J_m , would result in the same demagnetization field where the flux density is 0.04 tesla. The difference of slope for the potential function in air and in the samples is due to the difference in permeability.

(e) The total field which is the sum of the magnetization fields of (c), treating the two samples as a composite assembly with internal divergence, and the demagnetization field of (d).

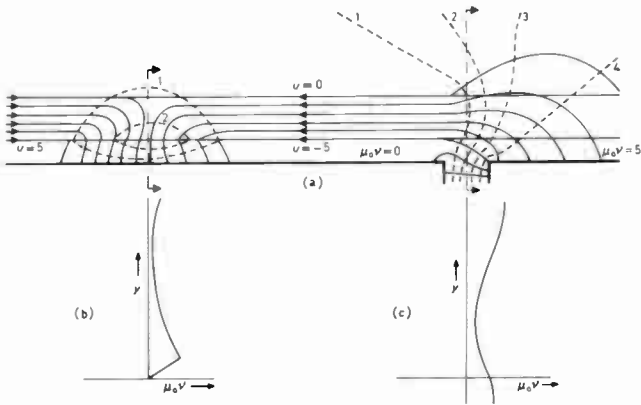


Fig. 3. Streamlines in full lines and equipotentials in broken lines mapping the field in the region of the gap immediately before the head current is switched to record a new transition. (a) Total distribution. (b) Potential distribution at centre of transition. (c) Potential distribution at gap centre.

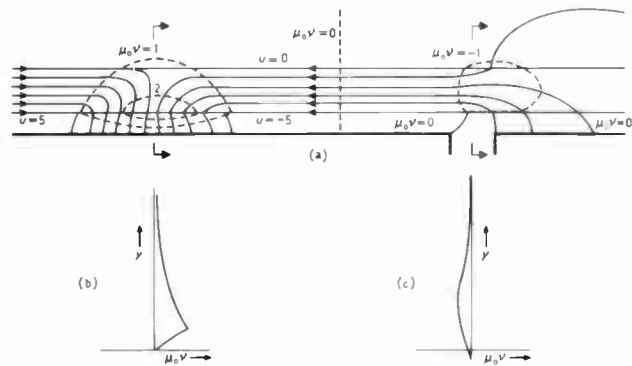


Fig. 4. Field in the region of the gap at the instant when the head current is zero halfway through the current switching sequence at the formation of a new transition.

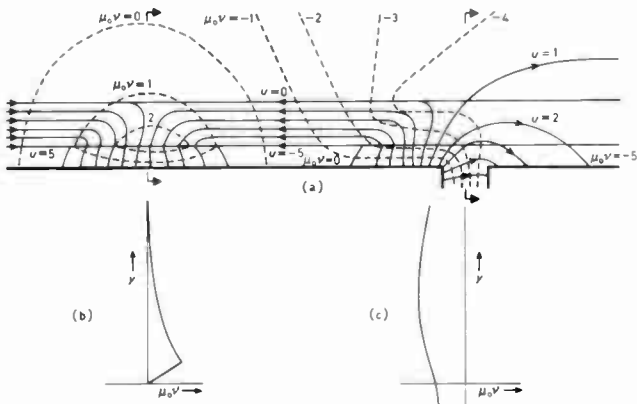


Fig. 5. Field distribution in the region of the gap as the newly formed transition nears completion.

maintain the continuity of the stream function and so will probably be more diffuse than that appropriate for Fig. 3.

Figure 5 illustrates the condition at the end of the current switching. Up to this point the head current has been growing so that there has been an increasing tendency to induce flux across the gap. On the assumption (reasonable for most longitudinal recording

systems) that an element of the medium transits the gap region in a time significantly greater than the current switching time, the sequence from Fig. 3 to Fig. 5 may be understood with little error to take place whilst the medium is stationary. Then the increasing flux density across the gap can only be achieved by magnetizing the region to the left of the gap vertically. The demagnetizing field will act to maintain as much of the prior longitudinal magnetization as possible giving the field distribution indicated with the vertical magnetization concentrated to the left of the gap. Shortly thereafter the newly established transition will move to the left of the gap and the magnetization will be best maintained if the field reverts to the form illustrated in Fig. 3.

The foregoing illustrates that it is unnecessary to postulate extreme anisotropy in order to account for longitudinal recording. Also that the demagnetization field co-operates with the head field to produce strong magnetization normal to the medium surface as the transition is formed so that it can be expected that some demagnetization will occur in the stronger demagnetization fields that will occur away from the influence of the head.

Figures 6 and 7 illustrate a different sequence which may be expected when inducing a transition in a previously magnetized medium.

Figure 6 shows the condition at the end of current switching which may be anticipated to be symmetrical and in which the transition is not fully formed.

Figure 7 illustrates the condition when the transition is nearing completion following some leftward shift of the medium so that the effect of prior magnetization of the

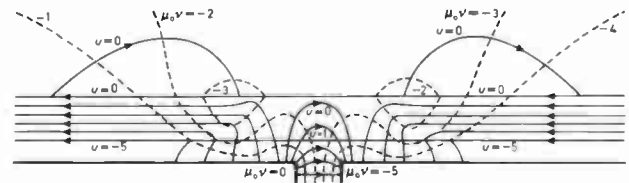


Fig. 6. Field distribution in the region of the gap at the initiation of a new transition within a medium already magnetized so that the sense of magnetization is the same either side of the gap.

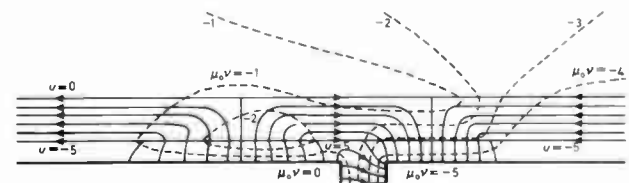


Fig. 7. Field distribution in the region of the gap at a later stage in the sequence initiated in Fig. 6.

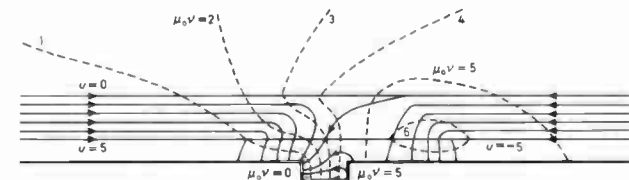


Fig. 8. Field distribution at the initiation of a transition within a medium already magnetized so that the sense of magnetization differs either side of the gap.

medium with the illustrated sense is to delay the transition giving it a rightward shift and to reduce its intensity.

Figure 8 illustrates that prior magnetization with the opposite sense will intensify the transition and give it a slight leftward shift or advance, though it will tend to be bound to the gap edge.

Thus the principal recording effects observed empirically can be accounted for on an intuitive basis by assuming two-dimensional magnetization and conservative stream functions.

The above discussion of the write process taken with the cited evidence from the literature encourages the belief that the magnetization set up by the write process in the vicinity of the write head is more intense than the medium can sustain in free space. The final transition form is dictated by demagnetization considerations. Hence it may be postulated that the resultant magnetization takes a functional form which fits the stable $J-H$ characteristic as closely as possible. The stable $J-H$ characteristic is determined for a particular sample and particle orientation by submitting the sample to a saturation H followed by unidirectional, cyclic demagnetization and hence determining the final stable state for J as a function of peak demagnetization.

Examples of this approach are available in the literature, e.g. Middleton and Wisely,¹¹ Maller and Middleton,¹⁵ Lindholm¹⁶ and Nayland.¹⁷ These examples either deal only in one-dimensional magnetization or are limited to a single transition. The treatment to be developed will be two-dimensional and will be derived for transitions of alternate polarity repeated at intervals of $\lambda/2$.

The functional form adopted takes account of the previous discussion and also the magnetization pattern discovered by Tjaden and Leyten,² part of which is reproduced in Fig. 1(a), and further the observation that the replay pulse shape has the form of the differential of the arctan transition, frequently reported in the literature, found by complex numerical calculations by, e.g. Potter and Schmulian⁷ and empirically by, e.g. Tercic.¹⁸

Examination of Fig. 1(a) shows that negligible flux emerges from the bottom surface of the medium and this may be modelled by setting a streamline $U_m = 0$ along the bottom surface.

To be consistent with the arctan assumption and a simple modelling procedure to be discussed later, the flux density emergent at the top surface is taken to have a form generated by the superposition of pulses with alternate sign and shape determined by:

$$J_y = \frac{\Phi_t}{\pi} \frac{a}{a^2 + (x - x_p)^2},$$

where x_p takes values such that the transitions are centred on a pitch of $\lambda/2$ and where Φ_t is a scaling parameter and a controls the peakiness of the pulse. This is clearly a cyclic function with fundamental wavelength = λ and it will simplify the solution for the demagnetization field if it is described as a harmonic series.

The flux density emergent at the top surface is described by $-\partial U_m / \partial x$ and it is shown in Appendix 1 that a waveform as described above has harmonic amplitudes found from:

$$h_n = -\frac{4\Phi_t}{\lambda} e^{-2\pi n/\lambda}, \tag{4}$$

where n may take any positive odd value. Also the integral with respect to x of the waveform described above is shown to be:

$$X(x) = -\frac{2\Phi_t}{\pi} \sum_{m=0}^{\infty} \frac{e^{-2\pi a(2m+1)/\lambda} \sin 2\pi x(2m+1)/\lambda}{2m+1} \tag{5}$$

and clearly U_m should take this value at the top surface. As has been discussed, the only other constraint on U_m is that it be continuous and any function of $z = X(x), Y(y)$ is acceptable providing $X(x)$ and $Y(y)$ are continuous in the region of interest. Then $X(x)$ may be set equal to (5) so that $Y(y)$ at the top surface should be unity. The choice of only two parameters to describe U_m is made for the sake of simplicity and to be consistent with the probable accuracy of the method but it does imply that there are only two degrees of freedom available when fitting the model distribution to the magnetic characteristic. This means that an exact fit can be made at only two points. The points chosen for the fit are at the peak at the medium surface where the magnetization will be entirely normal to the surface and at a quarter wavelength on the medium mid-line where the magnetization will be entirely longitudinal. This will allow some account to be taken of anisotropy.

In principle $Y(y)$ may be a polynomial of any order but it will assist the fitting process if $Y'(-\delta/2)$ is independent of the coefficients. Here δ is the medium thickness. In order to set a streamline $U_m = 0$ along the bottom boundary $Y(-\delta) = 0$. An expression that satisfies the discussed conditions is:

$$Y(y) = \frac{y - Ky^2/2 + \delta + K\delta^2/2}{\delta(1 + K\delta/2)}. \tag{6}$$

Then U_m is the product $X(x) \cdot Y(y)$ as defined in (5) and (6) above. Expressions for the flux density,

$$J_p = -X'(x) \cdot Y(y),$$

at $x = y = 0$ and

$$J_L = X(x) \cdot Y'(y),$$

at $x = \lambda/4, y = -\delta/2$ have been derived in Appendix 1 as

$$J_p = 2\Phi_t/\lambda \operatorname{cosech} 2\pi a/\lambda \tag{7}$$

$$J_L = -2\Phi_t/\pi\delta \arctan [\exp(-2\pi a/\lambda)] \tag{8}$$

and these will be useful when finding the values for Φ_t and a which best fit the model distribution to the magnetic characteristics.

The demagnetization distribution is in itself free from magnetization or current so that it satisfies the Laplace equation for both stream and potential functions and so may properly be described by functions of a complex variable, as discussed earlier. It is typical of the method that solutions are found by trial, i.e. different functions

are tried until one is found that satisfies the initial conditions. As a result the solutions when found are presented as *fait accompli* and appear without derivation.

The distribution may be divided into three zones, above the medium, within the medium and below the medium.

There are two cases above the medium. In the first case the head is present and spaced s above the medium surface whilst in the second the head is not present. With the head present the following assumptions are made. First, that the head has a very high permeability so that it may be assumed with little error to be infinite and the head reluctance zero. Then there will be no potential drop within the head and the entire head surface will be an equipotential. This equipotential is arbitrarily set to zero and the remaining potential distribution, v , calculated from this datum. Secondly, that the head may be represented in an idealized form as having zero gap length and having pole pieces that extend to plus and minus infinity. Some techniques for dealing with more practical representations of the head will be discussed later but this is a convenient starting point.

For the second case above the medium, when there is no head present, the stream function, U , and the potential function, v , are assumed to go to zero when y is infinite, i.e. at an infinite distance above the medium's surface though it should be noted that the solutions found approach zero exponentially so that the field has virtually disappeared within one wavelength of the medium's surface. The conditions at the medium's surface for both cases is that the potential distribution should be continuous across the boundary and that the discontinuity in the demagnetization stream function should complement the discontinuity in the magnetization stream function, U_m , so that the resultant total stream function, $U_t = U_m + U$ is continuous.

For the zone within the medium the conditions at the top boundary are given above. At the bottom boundary U_m has been set equal to zero by the choice of the form for $Y(y)$ so that both U and v should be continuous across this boundary. Internal to this zone it is necessary to take account of μ_r which will occur automatically if $V = \mu_0 \mu_r v$.

For the zone below the medium the boundary condition described above applies with the condition that U and v go to zero as y goes to minus infinity.

The solution for the demagnetization distribution consistent with the above discussion is presented in Appendix 2. The general solution is found for any value of the incremental permeability, μ_r but simplified formulae for \mathbf{H} and \mathbf{B} at particularly useful points are derived on the assumption that μ_r is unity, which is probably close to the truth for particulate media dispersed in a non-magnetic binder.

Then at the medium surface, at the centre of the transition, the flux and the demagnetization force are entirely normal to the medium surface and \mathbf{H}_p is found as

$$\mathbf{H}_p = -\frac{\Phi_t}{\mu_0 \lambda} \operatorname{cosech} 2\pi a/\lambda \quad (9)$$

At the quarter wavelength locus, $x = \lambda/4$, flux and demagnetization force are entirely parallel to the medium surface and \mathbf{H}_t is found as

$$\mathbf{H}_t = \frac{\Phi_t}{\mu_0 \lambda} \operatorname{sech} 2\pi(a-y)/\lambda \quad (10)$$

The replay amplitude is proportional to the rate of change of flux through the replay head winding and this in turn is proportional to the product of the track width, the relative velocity between the head and medium, and the flux density at the idealized gap. The flux density at the head surface, at the peak is found as

$$\mathbf{B}_p = \frac{2\Phi_t}{\lambda} \operatorname{cosech} 2\pi(a+s)/\lambda \quad (11)$$

The integral of the replay waveform can be a useful measure of medium uniformity. This integral is proportional to the flux crossed in the interval of integration and for the interval $0 \leq x \leq \lambda/4$, the flux crossed per unit track width is found as

$$-U_{\lambda/4} = \frac{2\Phi_t}{\pi} \arctan [\exp \{-2\pi(a+s)/\lambda\}]. \quad (12)$$

3 Fitting the Magnetization Distribution to the Magnetic Characteristic

As has been discussed, the magnetization stream function, U_m , totally describes the resultant magnetization flux brought about by the interaction of the elemental magnetization, \mathbf{J}_0 , and the magnetization potential function, v_m , where v_m is introduced to describe internal divergence.

There is evidence in the literature, from complex numerical calculations, that the bulk of the divergence is concentrated at the medium surface, see e.g. Ortenburger *et al.*⁹ and Suzuki.¹⁹ This suggests that v_m will be zero. Also better correlation has been found between replay performance as predicted by the theory and that found experimentally on the assumption that v_m is zero than is found if v_m is chosen to give a good fit to the magnetic characteristic everywhere.

By equating v_m to zero the distribution can be fitted to the magnetic characteristic along the medium surface, $y = 0$, and along the locus $x = \lambda/4$. Elsewhere the fit is close to but within the major magnetic characteristic loop except in the region $x = 0, y = -\delta$. Here the magnetization is very much less than the magnetic characteristic is able to support. That this is to be expected can be explained by consideration of the write process discussed previously with reference to Figs. 3 to 8.

In the region of poor fit, in the centre of the transition at the surface remote from the head, longitudinal streams converge from opposite directions rotating through a right angle as they do so. As is usual for streamline flow inside a corner the flux density fades to zero at the apex so that in this region a fit to the magnetic characteristic is not possible. Away from this region high flux densities are induced so that some permanent demagnetization can be expected when the medium is removed from the potential shielding effect of the head. This demagnetiza-

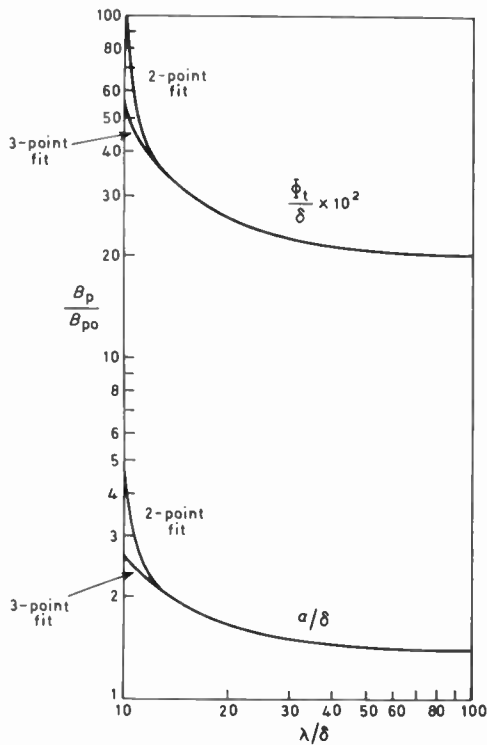


Fig. 9. a/δ and Φ_t/δ as a function of λ/δ for a typical gamma ferric oxide.

tion process will be moderated by the necessity to maintain continuity of the stream function at all epochs so that the process will be accomplished without the establishment of any great degree of internal divergence so that the assumption that v_m is zero is probably reasonable. This assumption is made in the bulk of what follows with a brief excursion to indicate the trials made for non-zero v_m . If the major stable $J-H$ loop is expressed in terms of $J/\mu_0 H$ as a function of $\mu_0 H$ then (7), (8), (9) and (10) may be used to solve for Φ_t and a , using numerical methods. Such a procedure may be generalized if the solution is made in terms of Φ_t/δ , a/δ and λ/δ since a solution for one particular set of ratios will be true at all values of δ .

Anisotropy is catered for when the magnetic characteristics in the vertical and horizontal directions are matched to the appropriate fit points. Expressing the characteristics in terms of $\mu_0 H$ qualifies the procedure for the consistent set of units for which the chosen μ_0 is appropriate.

Several tests have been made using a numerical fitting procedure outlined above and the experimental results of Tjaden and Leyten,² Bate and Dunn,¹⁰ Middleton and Wisely¹¹ and Lindholm.¹⁶ Using the Lindholm data for gamma ferric oxide, $J_r = 0.096$ tesla, $H_c = 21\ 600$ A/m and $\bar{S} = 0.791$, where \bar{S} is a parameter defined by Lindholm describing the squareness of the $J-H$ loop, the effect of the approximation involved in the form of $Y(y)$ may be assessed by comparing the solution for Φ_t/δ and a/δ as a function of λ/δ as found by the two-point fit made at $x = y = 0$ and $x = \lambda/4$, $y = -\delta/2$ and a three-point fit made at $x = y = 0$; $x = \lambda/4$, $y = 0$ and $x = \lambda/4$, $y = -\delta$. In the comparison the same general form for the

distributions are used. Then the two fit procedures will enclose a more accurate fit that might be obtained with a more elaborate form for $Y(y)$. The result of this test is presented in Fig. 9.

At short wavelengths it is impossible to fit at either two or three points because the total flux crossed along the locus $y = 0$ in the range $0 \leq x \leq \lambda/4$ is equal to the total flux crossed along the locus $x = \lambda/4$ in the range $0 \geq y \geq -\delta$. Then as the wavelength is reduced the flux density along the $x = \lambda/4$ locus tends to reduce, which is compensated for by reducing the peakiness of the distribution by increasing a/λ . This process fails when a/λ is so large that the distribution is effectively that for the fundamental alone. At this point further reduction in the peakiness of the distribution is impossible if the arctan assumption for the transition is to be retained so that a/δ found by the fitting process goes to infinity. Up to this point the harmonic content is varied by the variation in λ varying the ratio a/λ without much change in the ratio a/δ . This is consistent with the empirical observation that the pulse width is substantially constant over a wide range of wavelengths. When a/δ starts to change rapidly, the ratio a/λ is sufficiently large that the harmonic content is virtually limited to the fundamental. This marks the onset of pulse crowding. Then it is a convenient approximation to regard a/δ as a constant at its long wavelength value for all wavelengths.

As will be seen from Fig. 9, there is no appreciable difference over the useful range in the values of Φ_t and a



Fig. 10. Magnetization stream function, U_m , for the case when $r_m = 0$ when in contact with the head.

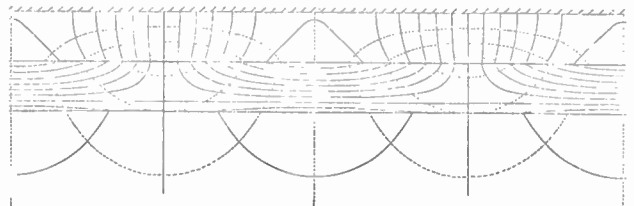


Fig. 11. Total stream and potential functions when close to the head.

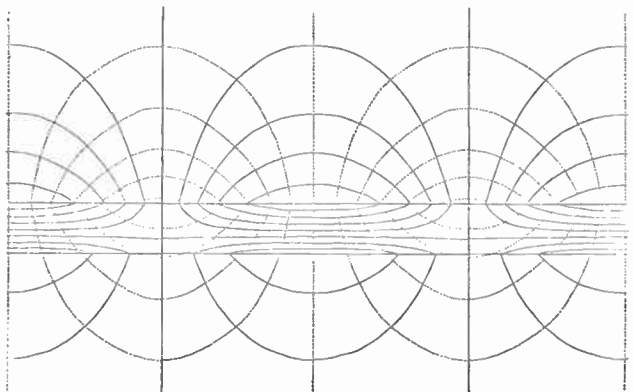


Fig. 12. Total stream and potential functions when remote from the head.

obtained by the two- or three-point fit method so that the form assumed for $Y(y)$ is justified.

Using the values of Φ_1 and a found above and assuming that the properties of the oxide used by Tjaden and Leyten² are similar, the theoretical distribution is plotted in Fig. 1(b) with a λ/δ ratio of 12 so that it may be compared with Tjaden and Leyten's empirical distribution of Fig. 1(a). It will be seen that while there is considerable agreement, the differences are in the main due to the asymmetric nature of the write process and cannot be explained in terms of the properties of the medium, considered in isolation.

The total stream and potential functions with streamlines solid and equipotentials broken for the above example are illustrated for different head to medium spacings in Figs. 10, 11 and 12, and it may be seen that continuity is maintained everywhere.

J may be plotted as a function of $\mu_0 H$ for all points in the medium and, providing all points lie within the major stable $J - \mu_0 H$ loop, the distribution may be regarded as stable. Then this plot may be known as the stability diagram, after Lindholm.¹⁶

Stability diagrams for the two- and three-point fit at $\lambda/\delta = 12$ for the Lindholm oxide already discussed are

plotted in Figs. 13 and 14. It will be seen that there is very little difference. The fit to the magnetic characteristic is good along the locus $x = \lambda/4$ and reasonable along the locus $y = 0$. The fit along the $y = 0$ locus might be improved by using one of the more elaborate transition descriptions discussed in an earlier work¹⁷ but the extra complication is not considered justified in view of the small error in the fit and the overall aim of simplicity. The fit at points away from the fit loci gets progressively worse as the point $x = 0, y = -\delta$ is approached as has been discussed previously.

Because a/δ is substantially constant, the region of poor fit may be expected to remain similarly nearly constant so that as λ/δ is increased the loci of constant x may be expected to crowd towards the $x = \lambda/4$ locus. Then the volume of the medium at or close to the stability locus will increase with increasing wavelength.

Frequency response may be calculated from (11) and this has been done for the material properties reported by Middleton and Wisely,¹¹ $J_r = 0.085$ tesla, $H_c = 19\,900$ A/m, S (an alternative loop squareness parameter described in their paper) = 0.75 and is plotted with $(s+s'')/\delta$ as a parameter in Fig. 15. Here s is the spacing between head and medium and s'' is an

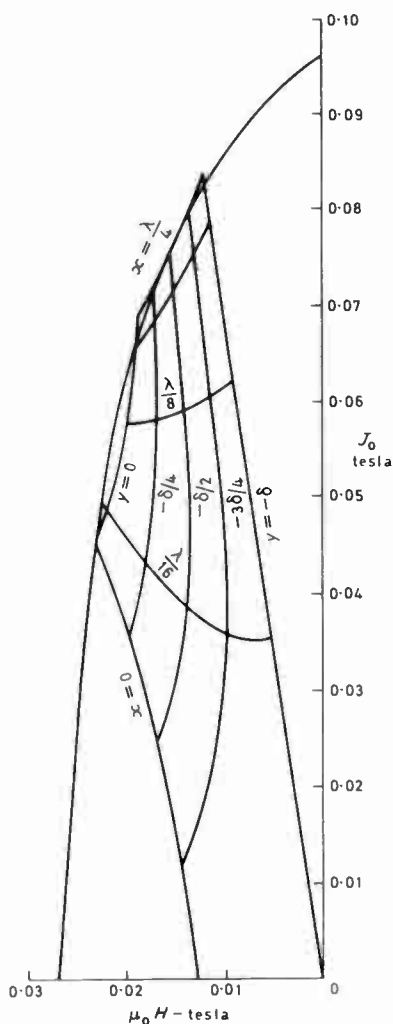


Fig. 13. Two-point-fit stability diagram.

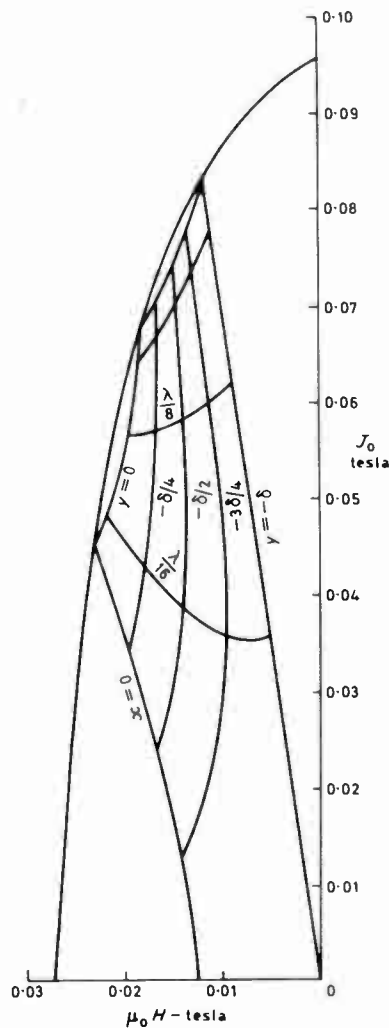


Fig. 14. Three-point-fit stability diagram.

increment introduced to account for gap loss, discussed later. For comparison the replay amplitudes at optimum write current, adjusted by an arbitrary constant to account for head gain, from Fig. 5 of the same paper are plotted, joined by a broken line, interpolated to fit the frequency response at $(s+s'')/\delta = 0.13$. From this and the quoted head-gap, $3.2 \mu\text{m}$, and medium thickness, $10 \mu\text{m}$, the head-to-medium spacing is found by a graphical method, yet to be discussed, as $0.208 \mu\text{m}$. At the low reported tape speed of 9.5 cm/s this spacing may be entirely ascribed to a surface finish of $0.07 \mu\text{m c.l.a.}$ if the head is regarded as riding on asperities 3 s.d. high.

A further check of the frequency response predictions may be made using the experimental data, $\delta = 3.75 \mu\text{m}$, $g = 1 \mu\text{m}$, of Bate and Dunn¹⁰ for chromium dioxide. Because the magnetic properties are not reported, the properties for chromium dioxide reported by Lindholm¹⁶ are substituted. This is justified by the observation that the characteristics of gamma ferric oxide examined share the same shape, except for a scaling factor, when plotted in a form suitable for the fitting method. Figure 16 is a plot of the theoretical frequency response with the experimental data interpolated at $(s+s'')/\delta = 0.3$. From this s is found as $1.035 \mu\text{m}$ and at the higher tape speed of 25.4 cm/s it is possible that some air-bearing effect is becoming apparent.

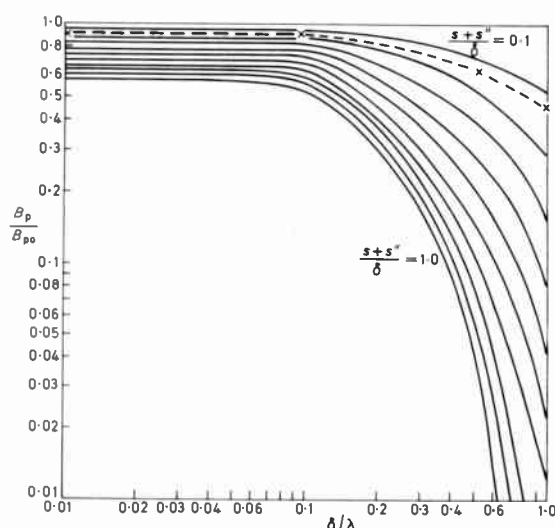


Fig. 15. Theoretical frequency response for a typical gamma ferric oxide with $(s+s'')/\delta$ as a parameter. Also shown by a broken line are the empirical data obtained by Middleton and Wisely.¹¹

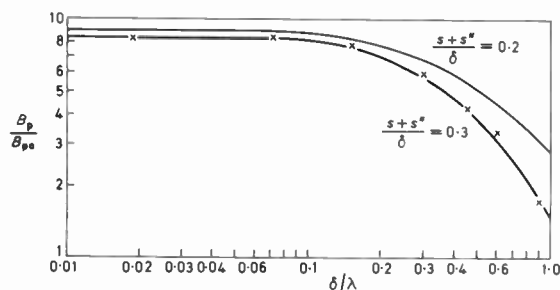


Fig. 16. Theoretical frequency response for a typical chromium dioxide tape close to a match with the empirical data reported by Bate and Dunn.¹¹

As discussed previously the distribution may be more closely fitted to the magnetic characteristic by allowing r_m to take a value other than zero. In order to make the fit to the magnetic characteristic the peakiness of U_m is increased by reducing a/δ . The fit is made for U_m considered in isolation along the $x = 0$ locus at the mean H point and at $x = \lambda/4, y = -\delta/2$ (Fig. 17). A form for r_m is needed which will close the stability diagram about the $J - \mu_0 H$ characteristic. Using a very simple form for r_m , Fig. 18 is obtained. It will be seen that a more elaborate form for r_m would improve the fit slightly without changing the fit point at the mean H along the $x = 0$ locus so that the frequency response predictions based on a fit at this point and at $x = \lambda/4, y = -\delta/2$, would not be improved.

Using methods similar to those discussed previously for Fig. 9, Φ_1/δ and a/δ for the same oxide are presented in Fig. 19; the predicted frequency response is presented in Fig. 20. The Middleton and Wisely data now fit at $(s+s'')/\delta = 0.3$, instead of 0.13 found for Fig. 15 and the fit is less well maintained outside the range of the graph. This suggests that the simple case, $r_m = 0$, offers the best predictive ability.

4 Head Gap Losses

It has been assumed that all the magnetization flux emerges at the medium's top surface so that, in the two dimensions of interest, $x + jy$, the medium may be treated as a line source with the line located at the top surface. In a system in which the head gap is well matched to the application, only one transition at a time will be in the gap region, i.e. within one gap length of gap centre. In this case the arctan transition may be further simplified to a point source in two dimensions which becomes a line source in three dimensions with the line parallel to both the medium surface and track width dimension, as follows.

The magnetization flux density normal to the surface, at the surface is found as

$$J_y = \frac{\Phi_1}{\pi} \frac{a}{a^2 + (x - x_p)^2},$$

which for a medium of unity relative permeability will be divided equally above and below the surface so that above the surface, at the surface

$$B_y = \frac{\Phi_1}{2\pi} \frac{a}{a^2 + (x - x_p)^2} \tag{13}$$

and below the surface

$$B_y = -\frac{\Phi_1}{2\pi} \frac{a}{a^2 + (x - x_p)^2}. \tag{14}$$

A point source located at the origin has a complex potential

$$W = -j \frac{\Phi_1}{2\pi} \log z,$$

from which

$$U = \frac{\Phi_1}{2\pi} \arctan \frac{y}{x} \tag{15}$$

$$v = -\frac{\Phi_1}{2\pi\mu} \log \sqrt{x^2 + y^2} \tag{16}$$

It may be found from (15) by the inclusion of suitable constants that the construction illustrated in Figs. 21, 22 and 23 has the flux densities at the surface given by (13) and (14) so that Fig. 23 illustrates an equivalent of the isolated transition.

Figure 24 illustrates how a planar change of permeability may be treated using the method of images for an isolated pole and Figs. 25 and 26 extend the method to the model of the isolated transition. Then Fig. 25 completely describes the flux linking the medium and the head when the medium relative permeability is unity. It will be seen that the flux linking the head may be modelled by a simple point source when using analogue methods of the type discussed by Tozoni,⁶ e.g. conductive paper. The method may be modified for media with relative permeabilities other than unity using

multiple point sources found by the method of images. The principal loss of the ring head occurs at the front gap and this may be modelled with the aid of the Schwarz-Christoffel transformation. Previous treatments of this loss by Westmijze²⁰ and Karlqvist²¹ have treated the medium as a constant m.m.f. source and have solved for the flux linking the replay head coil using the reciprocity theorem. Given the model of the transition as a constant-flux point source, it is more direct to solve for the rate of change of flux at the gap which is directly related to the rate of change of flux in the coil.

Figure 27 is an approximation for a cross-section of the front gap which is converted using the transform into an equivalent semi-infinite block (Fig. 28). By the transform

$$\frac{dz}{dt} = R(t-l)^{\frac{1}{2}}(t-n)^{-1}(t-p)^{\frac{1}{2}}$$

which is solved by the substitutions $n = 0, l = -p,$

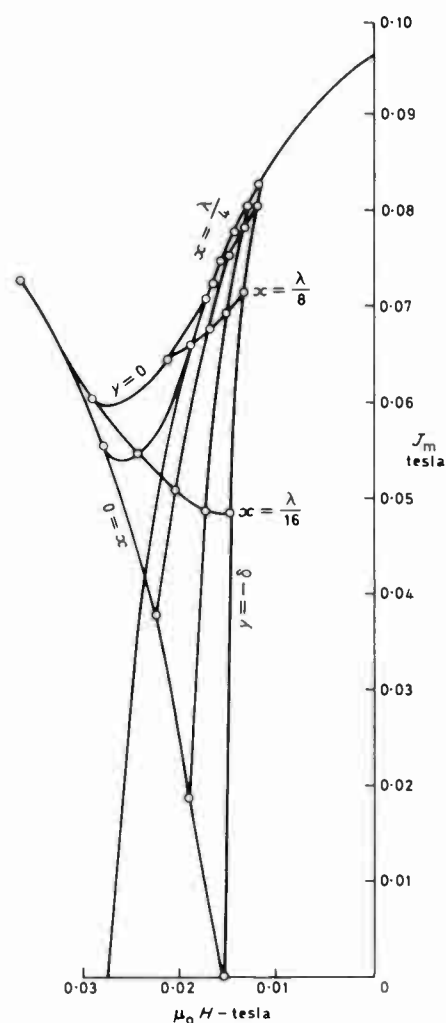


Fig. 17. J_m as a function of $\mu_0 H$ for the first quarter-wavelength with $\lambda/\delta = 12$ as fitted for a typical gamma ferric oxide. This is similar to the two-point-fit (Fig. 13) except that a potential function, v_m , other than zero, is required to redistribute the magnetic states so that all regions are close to the magnetic characteristic. This diagram shows the state prior to the application of the potential function.

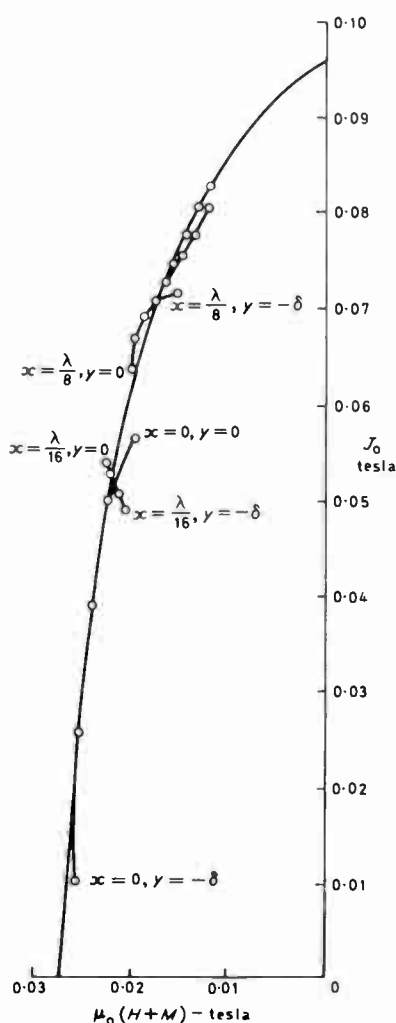


Fig. 18. J_0 as a function of $\mu_0(H+M)$. This illustrates the same condition as that shown in Fig. 17, but with the effect of the potential function now included.

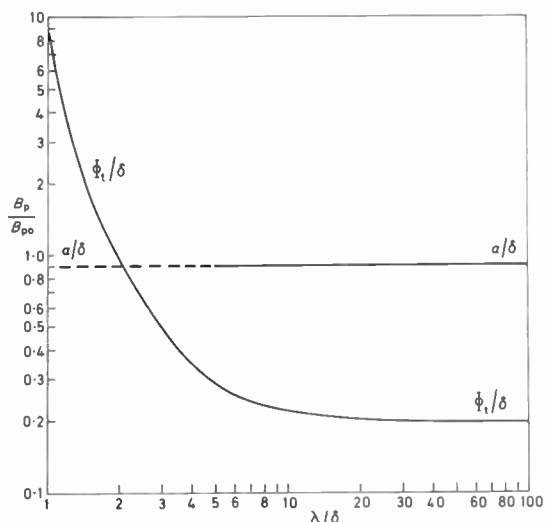


Fig. 19. Φ_t/δ and a/δ as a function of λ/δ for the fitting scheme illustrated in Fig. 18.

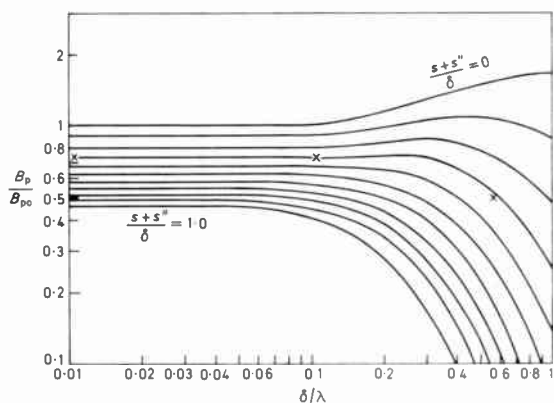


Fig. 20. Normalized theoretical frequency response for the fitting scheme illustrated in Fig. 18.

$p = g/\pi, R = 1, t = g/\pi \cdot \sec \theta$ to find

$$z = g/\pi \cdot [\tan \theta - \theta] + g/2.$$

The transform from the z to the t plane is mapped in Fig. 29 and from the t to the z plane in Fig. 30, both for 0.1g grids.

To be consistent with the model developed for a medium space a constant distance from a semi-infinite block, the medium should be mapped on a locus of constant η in t and its curved equivalent in z . The mapping will only be accurate at the gap centre in z but the inaccuracy in the region of the pole corners will, to some extent, model their lack of absolute squareness. For equivalent segments of medium at the gap centre to subtend the same angle at the pole position, the poles should be located so that a' , the distance between the pole and the medium surface in t , is equal to a . $d\zeta/dx$, where a is the distance between the pole position and the surface locus in z . Then equal amounts of flux will emerge from the surface in the equivalent segments.

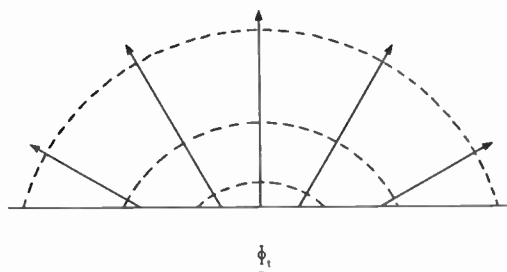


Fig. 21. Section through pole and its associated field active above the medium surface.

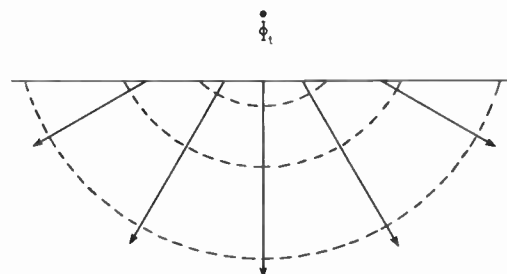


Fig. 22. Section through pole and its associated field active below the medium surface.

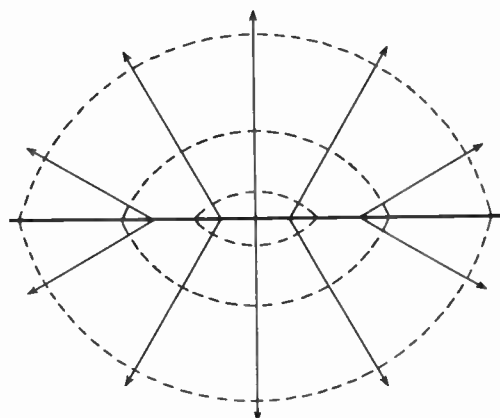


Fig. 23. Total field at a line source equivalent to the abutting of the active regions of Figs. 21 and 22.

Equal amounts of flux will always subtend equal angles at the pole positions so that a comparison of the angle subtended at the pole by equivalent points in z and t will show the goodness of fit at points away from the gap centre. Such a comparison is indicated in Figs. 29 and 30 for a pole at relatively small spacing where the mismatch is worst, but it will be seen that the fit is quite good and will improve as the spacing is increased. At the gap centre $d\zeta/dx$ may be found as $1/(1 + g^2/\pi^2\eta^2)^{1/2}$.

Having established the same flux density at the gap centre in z and t , it is necessary to apply a further correction so that the rate of change of flux at the medium surface, at the gap centre, maps properly for those cases where it is the rate of change of flux which is of primary interest, e.g. wound heads. If the velocity in z is u , then the velocity in t should be $u \cdot d\zeta/dx$. The two

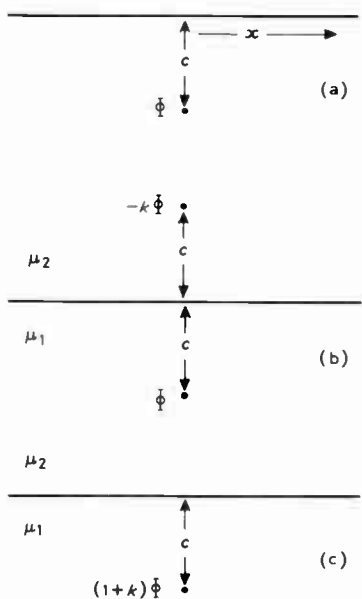


Fig. 24. (a) Section through pole and planar change of permeability. (b) Section through pole and image, both of which are active in the medium with permeability μ_1 located below the change. (c) Section through apparent pole active in medium with permeability μ_2 located above the change. Note $k = (\mu_2 - \mu_1) / (\mu_1 + \mu_2)$.

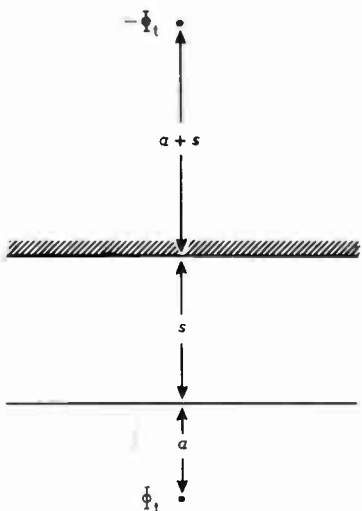


Fig. 25. Medium surface located s below semi-infinite head surface. Primary pole located a below medium surface. Image in the head for the case where head permeability is sufficiently high relative to free space that k may be taken as unity. Both pole and image are active in the region between medium and head.

corrections may be combined into one effective increase in spacing, s'' , where $s'' = s' \cdot d\xi/dx - s$, s is the spacing between medium and head at the gap centre in z and s' is the equivalent spacing in t . s''/g has been calculated and is plotted as a function of s/g in Fig. 31.

5 Recording Code Amplitude and Jitter Characteristics

Because the replay characteristics are defined by Φ_t and a , and because these are nearly constant over the small range of wavelengths involved in most digital recording

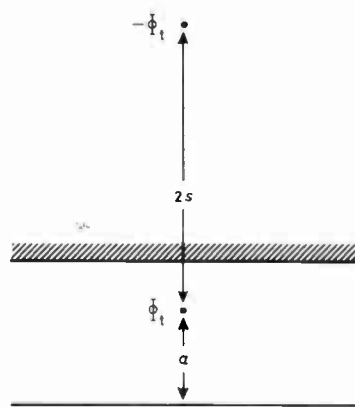


Fig. 26. Poles active in region below medium surface for the configuration shown in Fig. 25.

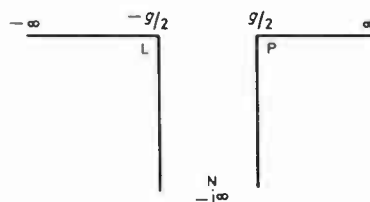


Fig. 27. The gapped semi-infinite head in $z = x + jy$.

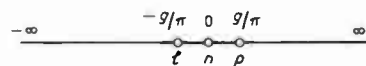


Fig. 28. The gapped semi-infinite head transformed to $t = \xi + j\eta$.

codes, it is possible to construct amplitude and jitter characteristics for particular codes. It is not possible to incorporate the mechanical jitter of a particular system within the general scheme so that this must be done as a separate exercise particular to the system involved. Apart from this the generalization allows for the comparison of different recording codes on an objective, system independent basis.

Because the medium's wavelength characteristic is defined by a and the way the system modifies this is defined by the simple addition of $s + s''$, $a + s + s''$ may be normalized in terms of the maximum wavelength present in a particular code, λ_{max} . This has been done for the Aiken two-frequency, coherent phase code as an example by simulating a representative sample of code patterns at various $(a + s + s'')/\lambda_{max}$ ratios and the results are presented graphically in Figs. 32 to 34.

6 Useful Approximations

As has been mentioned, it is a convenient approximation to regard the width parameter, a , as a constant at its long wavelength value. As the wavelength tends to infinity the longitudinal flux density at the quarter wavelength locus tends to J_r and the total flux per unit track width converging on the transition is $\Phi_t = 2J_r \delta$. At very long wavelengths (7) may be manipulated to find

$$a = \frac{\Phi_t}{\pi J_p} = \frac{2J_r \delta}{\pi J_p} \tag{17}$$

J_p is the magnetization flux density at the vertical fit-point, $x = y = 0$, and at this point it may be found from (7) and (9) that

$$J_p = -2\mu_0 H_p, \tag{18}$$

so that J_p may be found from the intercept of the locus $J = -2\mu_0 H$ and the magnetic characteristic.

For gamma ferric oxide the value of H at the intercept, $H_p \approx 0.85H_{cp}$, where H_{cp} is the perpendicular coercivity, so that an approximate value for a/δ is

$$\frac{a}{\delta} = \frac{J_r}{0.85\mu_0\pi H_{cp}} \tag{19}$$

Taking a as constant from either (17) or (19), then (9) may be rearranged to give Φ_1 at any wavelength as

$$\frac{\Phi_1}{\delta} = \frac{\mu_0\lambda H_p}{\delta} \sinh \frac{2\pi a}{\lambda} \tag{20}$$

Using values for a/δ and Φ_1/δ found from (19) and (20) in (11) to predict replay performance of the ferric oxide taken as typical, the error when compared with the results of the two-point fit procedure is less than 15% at the worst case considered, $\lambda/\delta = 10$, $(s+s'')/\delta = 1.0$. The error increases from zero at zero spacing as a function of spacing and is worst at the knee of the wavelength/frequency response characteristic as a function of wavelength. Asymptotes of the wavelength response from (11) are:

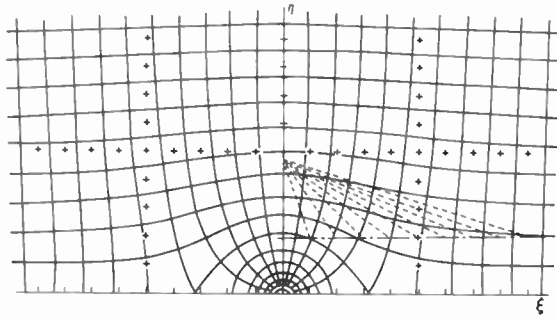


Fig. 29. 0.1g grid in z mapped into t . For comparison purposes a pole position is plotted along with the surface locus of the recording medium located so that it maps close to zero spacing at the gap centre in the z plane (Fig. 30). The pole position is joined to the surface locus at intervals of constant ξ so that the angle from the vertical may be compared with the angle made by joining equivalent positions in the z plane (Fig. 30).

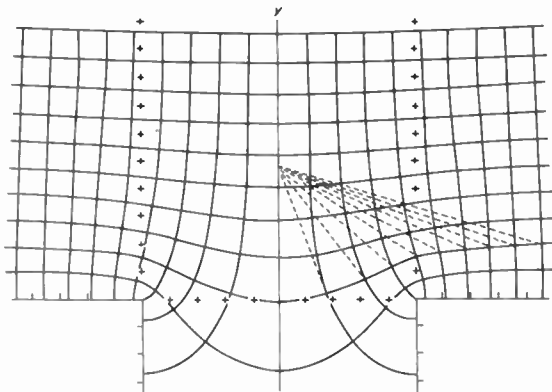


Fig. 30. 0.1g grid in t mapped into z . The equivalent pole position is joined to equivalent grid positions so that angular comparisons may be made.

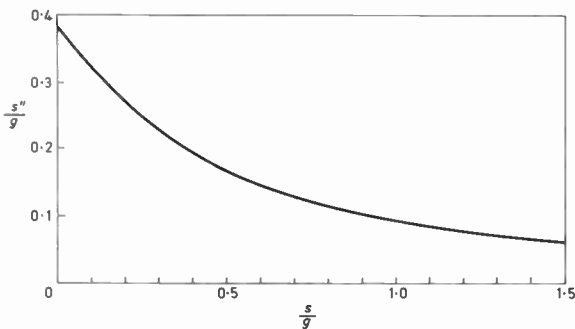


Fig. 31. Increment in spacing needed to account for gap loss, s'' , as a function of head gap, g and spacing, s .

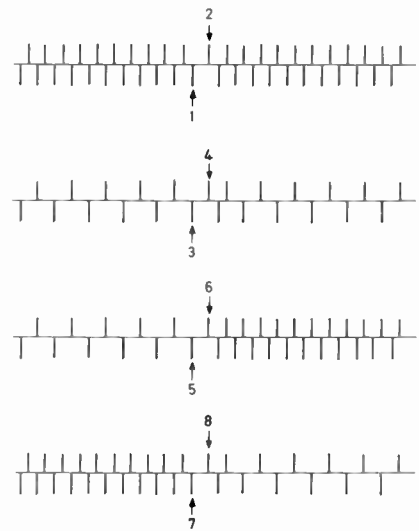


Fig. 32. Simulated recording code patterns for which the behaviour of the numbered pulses is monitored as a function of total spacing $(a+s+s'')$ scaled by bit cell length, λ_{max} with the results presented in Figs. 33 and 34.

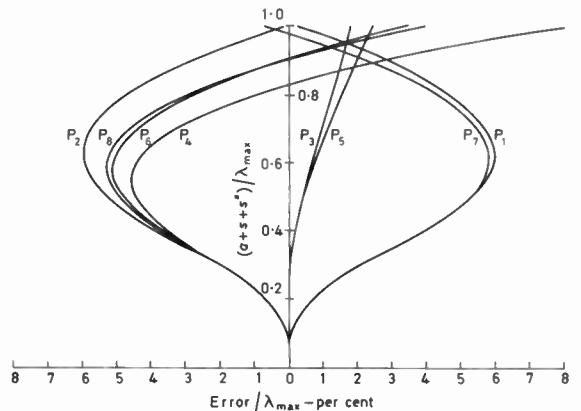


Fig. 33. Error in peak position normalized in terms of bit cell length, λ_{max} expressed as a function of $(a+s+s'')/\lambda_{max}$.

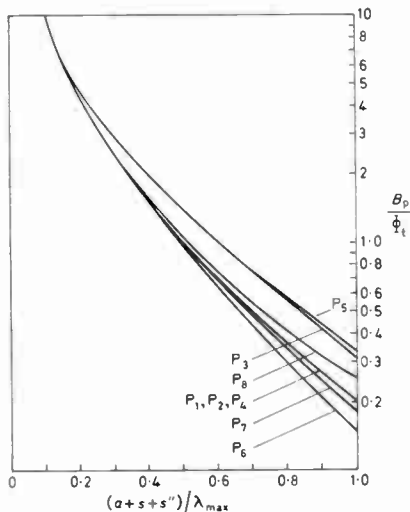


Fig. 34. Replay pulse amplitude normalized in terms of the peak flux density at the gap, B_p and Φ_1 and expressed as a function of normalized spacing $(a+s+s'')/\lambda_{max}$.

7 Measuring Medium Uniformity in the Presence of Spacing

In applications like cash/credit cards where a magnetic stripe is mounted on a stiff, non-ideal, backing the head can be forced out of contact with the medium by the asperities and deformities of the compound assembly. In these circumstances it is difficult to measure the uniformity of the magnetic stripe because of the resultant spacing loss. A useful measure in these circumstances is the integral of the replay signal which has been derived (eqn. (12)) and may be seen to be relatively insensitive to spacing loss at long wavelengths. Figure 35 illustrates the replay signal and its integral with and without spacing forced by varnish bars painted on the surface of the card. It may be seen that the integral is very much less sensitive to spacing.

8 Discussion

It is, in principle, possible to calculate the field distributions, and hence the magnetic state of the medium, for all epochs during the record-replay sequence. By repeating the calculation for every combination of write current, write head gap, spacing between medium and head, and medium properties, it would be possible to arrive at the optimum replay performance for a given medium or system. Incomplete examples of such an approach have been cited from the literature.^{7,8,9} Unfortunately the computation involved is enormous and must be repeated for every separate combination with the result that simplifications are made in order to reduce the workload. The outcome provides a valuable insight into the record-replay process but does not, as yet, represent a practical method for linking the replay performance to the physical dimensions and magnetic properties of the recording medium.

It has long been known that the replay amplitude and pulse width in longitudinal digital recording are substantially independent of write current once the write current exceeds a minimum for a given system.¹⁰⁻¹³ This strongly suggests that a limiting mechanism is operating. It is postulated in this paper that the limiting mechanism is such that magnetization flux densities established in the vicinity of the record head are greater than can be sustained when the medium moves into the stronger demagnetization fields that exist away from the shielding effect of the record head. Then, in these stronger fields, the medium suffers some permanent partial demagnetization into a sustainable state. This assumption is the basis for assuming that the final recorded distribution can be described by a functional form which lies on or within the stable magnetization loops (Figs. 13, 14 and 18).

There is much experimental evidence that the replay pulse shape is, with sufficient accuracy, in the form of the differential of the arctan function,¹⁸ and this form is used in the construction of the assumed distributions so that this well-established empirical fact is always complied with.

There is experimental evidence that in longitudinal recording negligible magnetization flux crosses the lower medium boundary² (Fig. 1(a)), and this is used in the

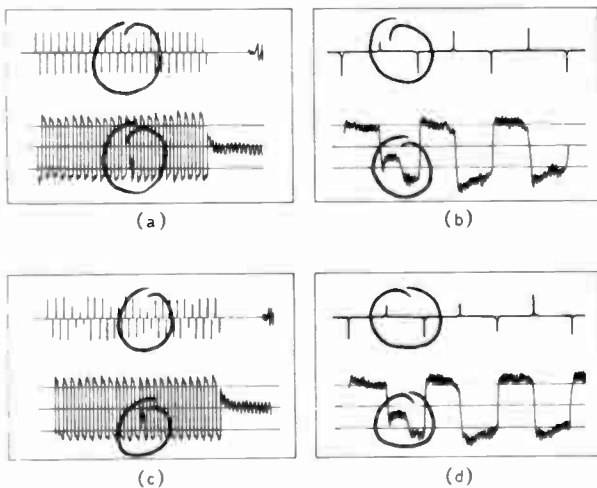


Fig. 35. (a) Replay signal (upper trace) recorded at 0.525 flux transitions per millimetre and its integral (lower trace) for a complete track on a cash credit card whilst in reasonable contact with the head. A loss of signal due to a discontinuity in the stripe is circled. Note that the same card with the same recording is retained throughout these measurements. (b) Section of same signal in region of fault on an expanded timebase. (c) and (d) Repeat of (a) and (b) after the card had bars of varnish painted across the stripe which force the head out of contact in a cyclic fashion by about 12.5 μ m. This set of measurements illustrates the sensitivity of the normal replay signal to spacing even at these comparatively long wavelengths and the relative immunity of the integral.

$$\lambda \rightarrow \infty, \quad B_p = \frac{2\mu_0 H_p a}{a + s + s''}, \quad (21)$$

$$\lambda \rightarrow 0, \quad B_p = 2\mu_0 H_p e^{-2\pi(s+s'')/\lambda}. \quad (22)$$

Although equation (22) only becomes true well into the region where transverse recording may be expected, the flux emergent from the medium surface remote from the head is so attenuated by spacing loss that the observed replay amplitude is consistent with the formula.

construction of the assumed functional form so that this experimental evidence is always complied with.

The above two assumptions lead to the forms assumed for $X(x)$ in (5) and $Y(y)$ in (6) and hence to the general form of the net magnetization stream function, U_m . The particular form assumed by U_m for a particular material completely describes the replay performance for that material. This particular form is found by a fitting process giving stability diagrams like those illustrated in Figs. 13, 14 and 18. There remains a degree of freedom for the fitting process which is closed when the potential function, r_m , describing the internal divergence, is determined. Different forms may be assumed for r_m which will give different stability diagrams and hence different particular forms for U_m for a particular material.

Two forms are assumed for r_m in this paper. The first assumes that the record process in co-operation with the subsequent partial demagnetization leaves the material in a state so that every element is on the stability locus (Fig. 18). This obviously represents the ultimate performance for the material in a longitudinal recording mode, given that no magnetization crosses the lower medium boundary. If the replay performance predicted under this assumption were found to correspond best with the available experimental evidence, it would probably be easier to accept this as the limiting case achieved at optimum record current in a head of the usual ring geometry because of the good fit everywhere to the magnetic characteristic.

In fact the second assumption provides predictions which fit the available experimental evidence better. The second assumption is that r_m is zero everywhere. This in turn implies that there is zero internal divergence. Cited complex numerical calculations^{9,19} confirm that this is so. It will be seen from Figs. 13 and 14 that the fit to the magnetic characteristic is confined to the loci $y = 0$ and $x = \lambda/4$. Away from these loci demagnetization criteria do not apply so that in these regions the distribution is, in a sense, uncontrolled except for the requirement that the net stream function, U_m , be continuous. Because no magnetization flux crosses the lower medium boundary all the flux approaching the transition across the locus $x = \lambda/4$ must also cross the surface, $y = 0$, between the limits $x = 0$ and $x = \lambda/4$. Because the fit to the magnetic characteristic is almost exact along the loci $y = 0$ and $x = \lambda/4$, the case $r_m = 0$ is typical of a class of distributions which share the same fit loci and the same replay performance although they may differ in their internal arrangement away from the fit loci. To be in the same class a distribution must also satisfy the requirement that $\text{grad } r_m$ be zero along the fit loci. Note that r_m has been defined to be zero at the boundaries for any distribution in order that U_m shall describe the net magnetization flux in its entirety. In order to generate flux distributions in this class then all that is necessary is that the record process saturates the medium longitudinally across the locus $x = \lambda/4$ and induces magnetization greater than can be subsequently sustained at the surface and that the combined effect of the magnetization process followed by the partial demagnetization process gives zero divergence near the

surface and the locus $x = \lambda/4$. Earlier discussion of the write process suggests that this is quite likely.

Experimental evidence suggesting that the theory is close to the truth comes in three ways.

(1) The detail of internal magnetization available from the Tjaden and Leyten experiment (Fig. 1(a)) is not used in the construction of the model. All that is used in the construction of the model is the fact that negligible magnetization flux crosses the lower medium boundary. Comparison of the internal detail discovered by experiment in Fig. 1(a) with the internal detail predicted from the theory using the fitting process (Fig. 1(b)) shows a considerable degree of agreement. This suggests that the experimental distribution is close to being in the same class, as discussed above, and quite close to being the same case as that used in the bulk of the theory, namely $r_m = 0$.

(2) It is assumed in the construction of the model that the replay pulse has the shape of the differential of the arctan function but its amplitude and width are left to be discovered by the fitting process. Over a wide range of wavelengths the fitting process predicts a near constant value for the amplitude and width of the replay pulse (Fig. 9) and this is consistent with often reported experimental data, see e.g. Ref. 18.

(3) The predicted replay amplitude at optimum record current is in very good agreement with that observed experimentally (Figs 15 and 16), with only minor and very plausible allowance for unavoidable spacing loss over a very wide range of wavelengths which extends well into the region of pulse crowding and possibly transverse recording. This suggests that, for the ring structure record head, longitudinal flux closure is maintained within the medium even in the transverse recording mode with longitudinal flux densities so low that they are not controlled by demagnetization criteria and replay performance is then controlled by demagnetization at the surface only. Alternatively or in complement, spacing loss for flux emergent from the lower medium surface in the transverse mode is so great that the effect of flux emergent from the lower surface may be neglected.

In order to make comparisons between theory and experiment it has been necessary to augment the available experimental evidence by making the following assumptions.

(1) That the incremental relative permeability describing the slope of the minor magnetization recoil loops is, or is close to, unity. This seems very reasonable for a particulate medium in a non-magnetic binder.

(2) To arrive at Fig. 16, Lindholm's¹⁶ data for chromium dioxide is assumed to be representative of the chromium dioxide used in the Bate and Dunn¹⁰ experiment. This assumption was made after it was observed that all the data for ferric oxide shared the same characteristic shape within a scaling factor when plotted in a form suited to the fitting process. The assumption amounts to believing that the same applies to chromium dioxide.

(3) That the shape of the stable $J-H$ loop, when plotted in a form suited to the fitting process, does not

differ substantially from that of the major $J-H$ loop in the second and fourth quadrants, except for a scaling factor. Given the dilution of the magnetic characteristic for a particulate medium suspended in a non-magnetic binder, this assumption seems reasonable.

(4) That the particle packing fraction for the materials used in the experiments was sufficiently high that anisotropy was negligible. This would follow from the work on particle packing fractions reported by Bate.⁴

The above assumptions are only made for comparison purposes and do not form part of the theoretical development, in particular relative permeabilities greater than unity are catered for as is anisotropy.

9 Conclusion

As discussed, the theory will cope with more parameters than are currently available from experiment and it may be desirable that these parameters be determined and a comparison of theoretical and practical replay performance in that light be made.

The case has been put that the replay performance at optimum record current is related to the medium's magnetic characteristics and its thickness. If this is accepted then the way is open for specifications for digital recording media to be written in terms of parameters which can be readily measured with considerable accuracy, e.g. magnetic moment per unit superficial area and coercivity, instead of current methods which rely on accurate determination of the replay amplitude, often in situations where spacing is uncontrollable and subject to considerable variation so that spacing loss is large and indeterminate. It is not necessary that the theory be perfected for this course to be adopted, it is only necessary to accept that a relationship exists. Adoption of the alternative specification method will benefit quality control procedures without affecting design procedures, which will continue to be referred to typical materials.

10 Acknowledgments

The author would like to express his gratitude to Burroughs Machines Ltd. for permission to publish the paper in its original form although this has since been modified by the author working in a private capacity. Thanks are also due to Philips Electrical Industries Ltd. for permission to reproduce Fig. 1(a) from Tjaden and Leyten's paper.²

11 References

- 1 Potter, R. I., 'Digital magnetic recording theory', *IEEE Trans. on Magnetics*, **MAG-10**, pp. 502-8, 1974.
- 2 Tjaden, D. L. A. and Leyten, J., 'A 5000:1 scale model of the magnetic recording process', *Philips Tech. Rev.*, **25**, no. 11/12, pp. 319-29, 1963/64.
- 3 Olsen, E., 'Applied Magnetism. A Study in Quantities', p. 10 (English edn) (Philips Technical Library, Eindhoven, 1966).
- 4 Bate, G., 'Angular variation of the magnetic properties of partially aligned $\gamma-Fe_2O_3$ particles', *J. Appl. Phys.*, **32**, (Supplement), no. 3, pp. 239s-40s, March 1961.
- 5 Becker, R., 'Electromagnetic Fields and Interactions', Chapter CIII, Volume 1 (Blackie, London, 1964).
- 6 Tozoni, O. V., 'Mathematical Models for the Evaluation of Electric and Magnetic Fields' (Iliffe, London, 1968).
- 7 Potter, R. I. and Schmullian, R. J., 'Self consistently computed

- magnetization patterns in thin magnetic recording media', *IEEE Trans.*, **MAG-7**, no. 4, pp. 873-80, December 1971.
- 8 Curland, N. and Speliotis, D., 'An iterative hysteretic model for digital magnetic recording', (1971 Intermag Conference), *IEEE Trans. on Magnetics*, **MAG-7**, pp. 538-43, Sept. 1971.
- 9 Ortenburger, I. B., Cole, R. W. and Potter, R. I., 'Improvements to a self consistent model for the magnetic recording properties of non-particulate media', *IEEE Trans.*, **MAG-13**, no. 5, pp. 1278-83, September 1977.
- 10 Bate, G. and Dunn, L. P., 'Experiments on the writing process in magnetic recording', *The Radio and Electronic Engineer*, **47**, no. 12, pp. 562-6, December 1977.
- 11 Middleton, B. K. and Wisely, P. L., 'The development and application of a simple model of digital magnetic recording to thick oxide media', *IERE Conference Proceedings No. 35*, pp. 33-42, July 1976.
- 12 Davies, A. V., 'Effects of the writing process and crosstalk on the timing accuracy of pulses in NRZ digital recording', *IEEE Trans.*, **MAG-3**, no. 3, pp. 217-22, September 1967.
- 13 Miyata, J. J. and Hartel, R. R., 'The recording and reproduction of signals on magnetic medium using saturation-type recording', *IRE Trans. on Electronic Computers*, **EC-8**, pp. 159-69, June 1959.
- 14 McCary, R. O., 'Saturation magnetic recording process', *IEEE Trans.*, **MAG-7**, no. 1, pp. 4-16, March 1971.
- 15 Maller, V. A. J. and Middleton, B. K., 'A simplified model of the writing process in saturation magnetic recording', *The Radio and Electronic Engineer*, **44**, no. 5, pp. 281-85, May 1974.
- 16 Lindholm, D. A., 'A phenomenological model for self-demagnetization in recording media', *IEEE Trans.*, **MAG-9**, no. 3, pp. 339-42, September 1973.
- 17 Nayland, W. R., 'Deriving the replay pulse from the physical and magnetic characteristics', *IERE Conference Proceedings No. 35*, pp. 291-300, July 1976.
- 18 Tercic, E. J., 'Superposition measurements with a flux-sensitive head in digital magnetic recording', *IEEE Trans.*, **MAG-9**, no. 3, pp. 335-8, September 1973.
- 19 Suzuki, K., 'Theoretical study of vector magnetization distribution using rotational magnetization model', *IEEE Trans.*, **MAG-12**, no. 3, pp. 224-9, May 1976.
- 20 Westmijze, W. K., 'Studies on magnetic recording', *Philips Res. Rep.*, **8**, pp. 161-83, 1953.
- 21 Karlqvist, O., 'Calculation of the magnetic field in the ferromagnetic layer of a drum', *Trans. R. Inst. Technology, Stockholm*, 1954.

12 Appendix 1: The Magnetization Stream Function— U_m

The summation of

$$-\frac{\Phi_t}{\pi} \frac{a}{a^2 + (x - x_p)^2}$$

for alternate sign poles on a pitch of $\lambda/2$ is

$$-\frac{\Phi_t}{\pi} \sum_{m=-\infty}^{\infty} \frac{(-1)^m a}{a^2 + (x - m\lambda/2)^2}$$

This expression is even and $f(x + \pi) = -f(x)$ so that there are no sine terms and no even harmonics. Then for the half-range Fourier series

$$b_n = -\frac{4\Phi_t}{\pi\lambda} \int_0^{\lambda/2} \sum_{m=-\infty}^{\infty} \frac{(-1)^m a}{a^2 + (x - m\lambda/2)^2} \cos \frac{2n\pi x}{\lambda} dx$$

With the substitutions $x = a\omega + m\lambda/2$, $dx = a d\omega$, $\omega = (x - m\lambda/2)/a$, this expression becomes

$$b_n = -\frac{4\Phi_t}{\pi\lambda} \int_{-m\lambda/2a}^{-(m-1)\lambda/2a} \sum_{m=-\infty}^{\infty} \frac{(-1)^m a^2}{a^2 + a^2\omega^2} \times \cos \frac{2\pi n}{\lambda} \left(a\omega + \frac{m\lambda}{2} \right) d\omega$$

By expanding the cosine term using the addition formula and noting that $\sin n\pi = 0$ and $\cos n\pi = (-1)^n$ (n is odd), this becomes

$$b_n = -\frac{4\Phi_t}{\pi\lambda} \int_{-m\lambda/2a}^{-(m-1)\lambda/2a} \sum_{m=-\infty}^{\infty} \frac{\cos 2\pi n a \omega / \lambda}{1 + \omega^2} d\omega.$$

It will be found that the intervals of integration are contiguous so that this becomes

$$b_n = -\frac{8\Phi_t}{\pi\lambda} \int_0^{\infty} \frac{\cos 2\pi n a \omega / \lambda}{1 + \omega^2} d\omega$$

and this expression may be evaluated by the method of differentiation under the integral sign to give

$$b_n = -\frac{4\Phi_t}{\lambda} e^{-2\pi n a / \lambda}. \tag{4}^\dagger$$

Then $X'(x)$ becomes

$$X'(x) = -\frac{4\Phi_t}{\lambda} \sum_{m=0}^{\infty} e^{-2\pi a(2m+1)/\lambda} \cdot \cos 2\pi x(2m+1)/\lambda,$$

and by integrating with respect to x

$$X(x) = -\frac{2\Phi_t}{\pi} \sum_{m=0}^{\infty} \frac{e^{-2\pi a(2m+1)/\lambda} \cdot \sin 2\pi x(2m+1)/\lambda}{2m+1}. \tag{5}$$

For the flux density at the medium surface, at the peak, $x = y = 0$,

$$-X'(x) = \frac{4\Phi_t}{\lambda} \sum_{m=0}^{\infty} e^{-2\pi a(2m+1)/\lambda},$$

which may be found equal to the expansion by the Binomial Theorem of

$$\frac{2\Phi_t}{\lambda} \operatorname{cosech} 2\pi a / \lambda = J_p. \tag{7}$$

The flux density at the second fit point, $x = \lambda/4$, $y = -\delta/2$, may be found from (5) and (6) as $X(x) \cdot Y'(y)$,

$$J_L = -\frac{2\Phi_t}{\pi\delta} \sum_{m=0}^{\infty} \frac{(-1)^m \cdot e^{-2\pi a(2m+1)/\lambda}}{2m+1} \\ = \frac{4\Phi_t}{\lambda\delta} \int \sum_{m=0}^{\infty} (-1)^m \cdot e^{-2\pi a(2m+1)/\lambda} da.$$

For $y \geq 0$, W is found as

$$W = -\frac{2\Phi_t}{\pi n} \frac{e^{-2\pi n a / \lambda} \cdot \cosh 2\pi n G_n / \lambda \cdot \sin 2\pi n(z - js) / \lambda}{\text{DEN}}. \tag{23}$$

For $0 \geq y \geq -\delta$, W is found as

$$W = j \frac{2\mu_r \Phi_t}{\pi n} \frac{e^{-2\pi n a / \lambda} \cdot \sinh 2\pi n s / \lambda \cdot \cos 2\pi n(z + jG_n) / \lambda}{\text{DEN}}. \tag{24}$$

For $-\delta \geq y$, W is found as

$$W = j \frac{4\mu_r \Phi_t \cdot e^{-2\pi n a / \lambda} \cdot \sinh 2\pi n s / \lambda \cdot \sinh 2\pi n G_n / \lambda \cdot e^{-j2\pi n z}}{\pi n [\mu_r + 1 - (\mu_r - 1) e^{-4\pi n \delta / \lambda}] \cdot \text{DEN}}. \tag{25}$$

The expansion by the Binomial Theorem of $\frac{1}{2} \operatorname{sech} 2\pi a / \lambda$ is identical with the expression

$$\sum_{m=0}^{\infty} (-1)^m \cdot e^{-2\pi a(2m+1)/\lambda},$$

and the integral may be evaluated as

$$\int \frac{e^{-2\pi a / \lambda}}{1 + e^{-4\pi a / \lambda}} da = -\frac{\lambda}{2\pi} \arctan (e^{-2\pi a / \lambda}),$$

so that J_L becomes

$$J_L = -\frac{2\Phi_t}{\pi\delta} \arctan (e^{-2\pi a / \lambda}). \tag{8}$$

13 Appendix 2: The Demagnetization Distribution

This distribution is split into three zones, $y \geq 0$, $0 \geq y \geq -\delta$ and $-\delta \geq y$. For $y \geq 0$ and $-\delta \geq y$ relative permeability is unity so that $v = V/\mu_0$. For $0 \geq y \geq -\delta$ relative permeability is μ_r so that $v = V/\mu_0\mu_r$. For $y \geq 0$ two cases exist, with and without the head present. The case without the head present may be obtained from the other case by setting $s = \infty$, where s is the head to medium spacing. The boundary conditions are that when $y = s$ and $-\infty$ the potential is zero, the potential across the two medium boundaries is continuous, the stream function is continuous across the medium bottom boundary and the discontinuity in the stream function, U , at the surface $y = 0$ is exactly matched to the discontinuity in the magnetization stream function, U_m , so that the total stream function, $U_t = U_m + U$ is continuous. The solutions are obtained and may be tested by trial, noting that $U = \mathcal{A}(W)$ and $V = \mathcal{J}(W)$ and that U_m at $y = 0$ may be obtained from (5). Also

$$G_n = \delta + \frac{\lambda}{2\pi n} \operatorname{arccoth} \mu_r,$$

and

$$\text{DEN} = \cosh 2\pi n s / \lambda \cdot \cosh 2\pi n G_n / \lambda + \mu_r \sinh 2\pi n s / \lambda \cdot \sinh 2\pi n G_n / \lambda.$$

† Numbers refer to equations in main part of paper.

With the head absent $s = \infty$ and also with $\mu_r = 1$ in the range $0 \geq y \geq -\delta$, W may be found from (24) as

$$W = j \frac{\Phi_t e^{-2\pi n a/\lambda} e^{-j2\pi n z/\lambda}}{\pi n}$$

Hence H_p at $x = y = 0$ may be found as the summation of $-\text{grad } v$ for all odd harmonics, i.e.

$$H_p = -\frac{2\Phi_t}{\mu_0 \lambda} \sum_{m=0}^{\infty} e^{-2\pi a(2m+1)/\lambda}$$

which is identical to the expansion of

$$-\frac{\Phi_t}{\mu_0 \lambda} \text{cosech } 2\pi a/\lambda = H_p \quad (9)$$

H_L at $x = \lambda/4$ may also be found as the summation of all odd harmonics of $-\text{grad } v$, i.e.

$$H_L = \frac{2\Phi_t}{\mu_0 \lambda} \sum_{m=0}^{\infty} (-1)^m e^{-2\pi(a-y)(2m+1)/\lambda}$$

which is identical to the expansion of

$$\frac{\Phi_t}{\mu_0 \lambda} \text{sech } 2\pi(a-y)/\lambda = H_L \quad (10)$$

In the range $y \geq 0$ at the head surface, $y = s$ and with $\mu_r = 1$, W may be found from (23) as

$$W = -\frac{2\Phi_t}{\pi n} e^{-2\pi n(a+s)/\lambda} \sin 2\pi n x/\lambda = U \quad (26)$$

Hence the peak flux density, at $x = 0$, linking the head is B_p , which may be found as the summation over all odd harmonics of $-\partial U/\partial x$:

$$B_p = \frac{4\Phi_t}{\lambda} \sum_{m=0}^{\infty} e^{-2\pi n(a+s)/\lambda}$$

which is identical to the expansion of

$$\frac{2\Phi_t}{\lambda} \text{cosech } 2\pi(a+s)/\lambda = B_p \quad (11)$$

The flux per unit track width going from $x = 0$ to $x = \lambda/4$ at the head surface may be found from (26) as

$$-U_{\lambda/4} + U_0 = -U_{\lambda/4}$$

and the summation over all odd harmonics is

$$-U_{\lambda/4} = \frac{2\Phi_t}{\pi} \sum_{m=0}^{\infty} \frac{(-1)^m e^{-2\pi(a+s)(2m+1)/\lambda}}{2m+1}$$

Which may be evaluated similarly to (8) in Appendix 1 as

$$-U_{\lambda/4} = \frac{2\Phi_t}{\pi} \arctan [e^{-2\pi(a+s)/\lambda}] \quad (12)$$

Manuscript first received by the Institution on 10th August 1978 and in final, revised form on 4th December 1981. (Paper No. 2036/R3)

New Books Received (contd.)

Solar Cells and Photocells

(Second Edition)

RUFUS P. TURNER (Sams, Indianapolis, Indiana, 1980) 13.5 x 21.5 cm 96 pages. £3.20.

CONTENTS: Photoelectricity simplified. Light meters. Relays and control circuits. Communications circuits. Miscellaneous circuits and devices.

Intended as an introduction to solar cells and photocells for experimenters, technicians, and anyone else interested in the subject, it provides a brief summary of the principles of photoelectric devices, their history and their possible future.

Electronics for TEC Level II

A. L. COOPER and T. R. BALL (Plymouth College of Further Education) Stanley Thornes Publishers, Cheltenham 1981 16.5 x 24.5 cm. 262 pages. £5.25.

CONTENTS: Elementary theory of semiconductors. The P-N junction. Applications of semiconductor diodes. The bipolar transistor. The small signal transistor amplifier. Waveform generators. Logic. The silicon-controlled rectifier. Integrated circuits. Thermionic devices. The cathode ray oscilloscope.

Much of the book is concerned with conventional solid-state electronics. The objectives for Electronics units at TEC Level II have been well covered.

Transmission Systems for Technicians 2

G. L. DANIELSON (Norwood Technical College) and R. S. WALKER (South London College) Butterworths, Sevenoaks 1981 18.5 x 24.5 cm. 69 pages. £4.25.

CONTENTS: Signal characteristics and frequencies. Logarithmic units. Filters. Modulation. Multiplexing. Cables. Two- and four-wire operation.

Written as a course text for Technician Education Council students who have chosen transmission systems it should satisfy and interest those intending to specialize in more advanced aspects in their later studies.

Mechanical & Engineering Principles

Volume I

KEN SMITH (North Staffordshire Polytechnic) Pitman London 1981 18.5 x 24.5 cm 172 pages. £4.50.

CONTENTS: Statics—force, resultant and centroid. Equilibrium. Effect of load on engineering components. Dynamics—Friction and machines. Motion and energy.

Presented in two volumes, this book is intended to offer students a simple and concise explanation of mechanical engineering science and mechanical science up to certificate level. The two volumes cover the mechanical principles (or mechanical science) requirements of a first technician qualifications.

Handbook of Microwave Testing

THOMAS S. LAVERGHETTA (Artech House, Dedham, Mass. 1981) 23.5 x 16 cm. 518 pages. £25.

CONTENTS: Introduction. Test equipment. Power measurements. Noise measurements. Spectrum analyzer measurements. Active testing. Antenna measurements. Automatic testing. Miscellaneous measurements.

The intention of this book is to remove the idea of complexity from the measurement of many microwave parameters and make the measurements understandable. It is essentially a practising engineer's guide.

Electrical & Engineering Mathematics

Volume 2

RICHARD MEADOWS (Polytechnic of North London) Pitman London 1981 18.5 x 24.5 cm 300 pages. £5.95.

CONTENTS: Algebra and its applications. Trigonometry: identities, equations and sinewaves. Calculus. Complex numbers. Boolean Algebra.

This book, which follows the author's first volume on basic mathematics, is written essentially for science, engineering and technology students completing their first course in mathematics. The scope of the text fully meets the needs of the Technician Education Council (TEC) levels 2 and 3 units and, in certain topics, higher level units.

Contributors to this Issue

Ron Barrs (Member 1959) joined the Development and Research Laboratory of Rediffusion Radio Systems in 1954. He was responsible for the design of a number of communications receivers, radio-telephones and terminal equipments for use at h.f. and v.h.f. Amongst these was the first fully transistored marine receiver to obtain approval by the Ministry of Posts and Telecommunications. He also helped pioneer the use of transistor h.f. transmitters. Mr Barrs became Chief Engineer of the Company's Marine Development Laboratory when it was formed as a separate group in 1963. Later the Company's Laboratories were combined and he was appointed Chief Engineer responsible for product development in 1969. He is still with RRSLS but is now responsible for advanced concepts which include research activities and major funded studies.

Bill Nayland's last appointment was as Staff Engineer with Burroughs Machines, responsible for magnetic recording standards and security algorithms for cash/credit cards. In this capacity he served on the appropriate working groups of national and international standardization bodies. He obtained his HNC in electrical and electronic engineering at Wimbledon Technical College in 1961 and was elected a Member of the Institution in 1965 following success in the Graduateship Examination in which his specialist subject was Computer Engineering. Since qualifying he has had various posts in R & D connected with computers and computer peripherals including many magnetic recording devices. Prior to qualifying he was for 5 years a Test Engineer in industry and for 5 years a Radio Mechanic with the Royal Signals.

Dennis Ralphs (Member 1969, Associate 1945) graduated from Birmingham University in 1943. During the war he worked on the development of airborne radar and ground training simulators, and subsequently on instrumentation for nuclear research. In 1947 he joined the Scientific Civil Service and since 1954 has been Head of the Development Section of the UK Foreign and Commonwealth Office Communications Engineering Department. He has been responsible for the design of successive generations of the 'Piccolo' telegraphy systems used on the FCO h.f. radio network and has studied m.f.s.k. principles and the practical application of these to poor-signal telegraphy. One of his papers on this subject, published in the Journal in October 1977, gained him the Rediffusion Television Premium, and for a previous paper (joint) on an h.f. propagation simulator he was awarded the Marconi Premium for 1976.

Denis Towill (Fellow 1970) is Head of the Department of Mechanical Engineering and Engineering Production and a founder member and Head of the Dynamic Analysis Group at the University of Wales Institute of Science and Technology



R. A. BARRS



W. R. NAYLAND



J. D. RALPHS



D. R. TOWILL

(UWIST), Cardiff. He holds the degree of B.Sc.(Eng.) from the University of Bristol and the degrees of M.Sc. and D.Sc. from the University of Birmingham. Prior to taking up the chair of Engineering Production at UWIST, he was a Senior Lecturer in Automatic Control at the Royal Military College of Science, a Consultant Engineer, and a Dynamic Analyst with the British Aircraft Corporation. He is the author of the textbook 'Transfer Function Techniques for Control Engineers' and the research monograph 'Coefficient Plane Models for Analysis and Design'. On six occasions Professor Towill has been awarded IERE premiums for outstanding papers in the Journal. He has undertaken lecture tours in the United States and the Far East, and was recently commissioned to prepare a NATO AGARDO-graph on the Dynamic Testing of Avionic Systems.

Standard Frequency and Time Service

(Communication from the National Physical Laboratory)

Relative Phase Readings in Microseconds

NPL—Station
(Readings at 1500 UTC)

APRIL 1982	MSF 60 kHz	GBR 16 kHz	Droitwich* 200 kHz
1	-10.4	34.4	60.9
2	-10.5	34.9	60.7
3	-10.4	34.7	60.5
4	-10.4	34.3	60.3
5	-10.2	34.7	60.1
6	-10.5	34.4	59.8
7	-10.3	33.9	59.5
8	-10.3	34.3	59.3
9	-10.3	34.0	59.0
10	-10.3	34.3	58.8
11	-10.5	35.1	58.5
12	-10.5	34.5	58.3
13	-10.5	34.4	58.0
14	-10.7	34.2	57.4
15	-10.7	34.2	57.0
16	-10.6	33.7	56.5
17	-10.5	34.3	56.2
18	-10.5	33.8	55.9
19	-10.5	34.4	55.7
20	-10.7	33.8	55.4
21	-10.7	34.2	55.2
22	-10.5	34.8	55.0
23	-10.5	34.4	54.8
24	-10.5	34.1	54.6
25	-10.7	33.7	54.3
26	-10.5	35.1	54.0
27	-10.7	33.9	53.5
28	-10.7	33.9	53.1
29	-10.7	34.0	52.6
30	-10.7	34.0	52.0

Notes: (a) Relative to UTC scale ($UTC_{NPL-Station} = +10$ at 1500 UT, 1st January 1977).

(b) The convention followed is that a decrease in phase reading represents an increase in frequency.

(c) 1 μ s represents a frequency change of 1.2 part in 10^{11} per day.

(d) It may be assumed that the relative stations on 200 kHz at Westerglen and Burghead will follow the day to day changes in these phase values.

Conferences, Courses and Exhibitions, 1982-83

The date and page references in italics at the end of an item are to issues of *The Radio and Electronic Engineer (REE)* or *The Electronics Engineer (EE)* in which fuller notices have been published.

The symbol ★ indicates that the IERE has organized the event.

The symbol ● indicates that the IERE is a participating body.

An asterisk * indicates a new item or information which has been amended since the previous issue.

Further information should be obtained from the addresses given.

JULY

★ **Video Revolution 12th to 15th July** *READING*
A Symposium on the Video Revolution organized by SERT, will be held at the University of Reading. Information: Conference Organizer, SERT, 57-61 Newington Causeway, London SE1 6BL (Tel. 01-403 2351)

Control 19th to 21st July *HULL*
Conference on Applications of Adaptive and Multivariable Control, sponsored by the IEEE in association with the University of Hull, to be held at the University of Hull. Information: G. E. Taylor, University of Hull, Dept. of Electronic Engineering, Hull (Tel. (0482) 46311 Ext 7113).

● **Image Processing 26th to 28th July** *YORK*
Conference on Electronic Image Processing, organized by the IEE in association with the IEEE and the IERE, to be held at the University of York. Information: IEE Conference Secretariat, Savoy Place, London WC2R 0BL (Tel. 01-240 1871).

AUGUST

★ **Software 25th to 27th August** *EDINBURGH*
Residential Symposium on Software for Real-Time Systems organized by the IERE Scottish Section will be held in Edinburgh. Information: Mr J. W. Henderson, YARD Ltd, Charing Cross Tower, Glasgow.

★ **Satellite Communication 23rd to 27th August** *EINDHOVEN*
A Summer School on Satellite Communication Antenna Technology organized by the Eindhoven University in association with IEEE Benelux and the University of Illinois will be held at Eindhoven University. Information: Dr E. J. Maanders, Department of Electrical Engineering, University of Technology, Postbox 513, 5600 MB Eindhoven, Netherlands. (Tel. (040) 47 91 11).

SEPTEMBER

★ **Aviation and Electronics 6th to 12th September** *FARNBOROUGH*
International Exhibition and Flying Display, organized by the Society of British Aerospace Companies, at Farnborough, Hampshire. Information: SBAC, 29 King Street, St James's, London SW1Y 6RD. (Tel. 01-839 3231)

★ **Microwaves 6th to 10th September** *HELSINKI*
Twelfth European Microwave Conference organized by the IEEE in association with URSI to be held in Helsinki. Information: IEEE, Conference Co-ordination, 345 East 47th Street, New York, NY 10017.

★ **BA '82 6th to 10th September** *LIVERPOOL*
Annual Meeting of the British Association for the Advancement of Science, will be held at the University of Liverpool. Information: British Association, Fortress House, 23 Savile Row, London W1X 1AB.

★ **ICCC '82 7th to 10th September** *LONDON*
Sixth International Conference on Computer Communication, sponsored by the International Council for Computer Communication, to be held at the Barbican Centre, London. ICC '82 PO Box 23, Northwood Hills HA6 1TT, Middlesex.

★ **Personal Computer 9th to 11th September** *LONDON*
Personal Computer World Show, to be held at the Cunard Hotel, Hammersmith, London W6. Information: Interbuild Exhibitions Ltd, 11 Manchester Square, London W1M 5AB. (Tel. 01-486 1951).

★ **Remotely Piloted Vehicles 13th to 15th September** *BRISTOL*
Third Bristol International Conference on Remotely Piloted Vehicles jointly sponsored by The Royal Aeronautical Society and the University of Bristol. To be held at the University of Bristol. Information: Dr R. T. Moses, Organizing Secretary, RPV Conference, Faculty of Engineering, Queen's Building, The University, Bristol BS8 1TR. (Tel. (0272) 24161, ext 846)

★ **Safety 14th to 16th September** *MANCHESTER*
A three-day course on Safety of Electrical Instrumentation in Potentially Explosive Atmospheres, organized by SIRA Institute, will be held at UMIST, Manchester. Information: Conferences and Courses Unit, SIRA Institute Ltd, South Hill, Chislehurst, Kent BR7 5EH (Tel. 01-467 2636)

★ **Wescon '82 14th to 16th September** *ANAHEIM*
Show and Convention to be held at the Anaheim Convention Centre and Anaheim Marriott, Anaheim, California. Information: Robert Myers, Electronic Conventions Inc. 999 North Sepulveda Boulevard, El Segundo CA 90245.

★ **Fibre Optics 15th to 17th September** *MANCHESTER*
Conference on Fibre Optics for Instrumentation, organized by the SIRA Institute, will be held at UMIST, Manchester. Information: Conference and Courses Unit, Sira Institute Ltd, South Hill, Chislehurst, Kent

★ **Broadcasting 18th to 21st September** *BRIGHTON*
The ninth International Broadcasting Convention, IBC '82, organized by the IEE, and EEA with the association of IERE, IEEE, RTS and SMPTE, will be held at the Metropole Conference and Exhibition Centre, Brighton. Information: IEE, 2 Savoy Place, London WC2R 0BL (Tel. 01-240 1871).

★ **Non-Destructive Testing 20th to 22nd September** *YORK*
National Non-Destructive Testing Conference, organized by the British Institute of Non-Destructive Testing, to be held in York. Information: Blnst NDT, 1 Spencer Parade, Northampton NN1 5AA. (Tel. (0604) 30124/5).

★ **Electromagnetic Compatibility 21st to 23rd September** *GUILDFORD*
Third conference on Electromagnetic Compatibility, organized by the IERE with the association of the IEE, IEEE, IQA and RAeS, to be held at the University of Surrey, Guildford. Information: Conference Secretariat, IERE, 99 Gower Street, London WC1E 6AZ (Tel. 01-388 3071)

★ **Automatic Testing 21st to 23rd September** *PARIS*
Exhibition and Conference on ATE and Test Systems will be held at C.I.P., Paris. Information: Network, Printers Mews, Market Hill, Buckingham. Tel. (02802) 5226/5227

★ **Telecommunications and Fibre Optics 21st to 24th September** *CANNES*
Eighth European conference on Telecommunication and Fibre Optics organized by the Electronics Industries Group (GIEL), to be held in Cannes. Information: GIEL 11 rue Hamelin, 75783 Paris Cedex 16

★ **Automated Assembly 23rd September** *LONDON*
One day Seminar on 'Automated Assembling: Starting a Project and making it work' organized by the Institution of Production Engineers to be held at the Bowater Conference Centre, London. Information: The Manager, Conferences & Exhibitions, Institution of Production Engineers, Rochester House, 66 Little Ealing Lane, London W5 4XX. Tel. 01-579 9411

★ **Man-Machine Systems 27th to 29th September** *BADEN-BADEN*
Conference on Analysis, Design and Evaluation of Man-Machine Systems sponsored by IFAC in association with the IFIP/IFORS/IEA, to be held in Baden-Baden, Federal Republic of Germany. Information: VDI/VDE-Gesellschaft, Mess- und Regelungstechnik, Postfach 1139, D-4000 Dusseldorf 1. (Tel. (0211) 6214215)

★ **Instrumentation in Flammable Atmospheres 30th September** *LUTON*
A short course on Instrumentation in Flammable Atmospheres, organized by Measurement Technology to be held in Luton. Information: Customer Training Department, Measurement Technology Ltd, Power Court, Luton LU1 3JJ. (Tel. (0582) 236333).

OCTOBER

★ **Electronic Displays 5th to 7th October** *LONDON*
Electronics Displays Exhibition and Conference, to be held at the Kensington Exhibition Centre. Information: Network, Printers Mews, Market Hill, Buckingham. MK18 1JX. (Tel: (0282) 5226).

★ **Defendory Expo '82 11th to 15th October** *ATHENS*
The 4th Exhibition for Defence Systems and Equipment for Land, Sea & Air, organized by the Institute of Industrial Exhibitions in association with the Defence Industries Directorate of The Hellenic Ministry of National Defence to be held in Athens, Greece. Information: Mrs Duda Carr, Westbourne Marketing Services, Crown House, Morden, Surrey SM4 5EB (Tel. 01-540 1101)

★ **Internecon 12th to 14th October** *BRIGHTON*
Internecon Conference and Exhibition, organized by Cahners Exposition Group, to be held at the Metropole Exhibition Hall, Brighton. Information: Cahners Exposition Group, Cavridy House, Ladyhead, Guildford, Surrey, GU1 1BZ. (Tel. (0483) 38083).

★ **Optoelectronics 12th to 14th October** *LAUSANNE*
Conference on Optoelectronics in Telecommunication and Measurements Systems to be held in Lausanne, Switzerland. Information: Secretariat, Journees d'Electronique, EPFL, Ch. de Bellevue 16, CH-1007 Lausanne, Switzerland

★ **CAMPRO '82 13th and 14th October** *LONDON*
Conference on Computer Aided Manufacturing and Productivity organized by Institution of Production Engineers and the Society of Manufacturing Engineers USA, will be held at the Mount Royal Hotel, Marble Arch, London. Information: The Manager, Conferences & Exhibitions, Institution of Production Engineers, Rochester House, 66 Little Ealing Lane, London W5 4XX. Tel. 01-579 9411

★ **RADAR '82 18th to 20th October** *LONDON*
International Conference on Radar, organized by the IEE in association with the IEEE EUREL, IERE, IMA, RAeS and RIN, to be held at the Royal Borough of Kensington and Chelsea Town Hall, Hornton Street, London W8. Information: IEE Conference Department, Savoy Place, London WC2R 0BL. (Tel. 01-240 1871).

★ **Military Microwaves '82 19th to 22nd October** *LONDON*
Third International Conference and Exhibition organized by Microwave Exhibitions and Publishers, to be held at The Cunard International Hotel. Information: Military Microwaves '82 Conference, Temple House, 36 High Street, Sevenoaks, Kent TN13 1JG

★ **Electronics 20th to 22nd October** *HONG KONG*
Second Hong Kong Electronics Fair, sponsored by the Hong Kong Exporters' Association and the Hong Kong Electronics Association, will be held at the Miramar Hotel, Kowloon. Information: Secretary, Hong Kong Electronics Fair Committee, c/o Hong Kong Exporters Association, 1625 Star House, 3 Salisbury Road, Kowloon, Hong Kong.

★ **Multivariable Systems 26th to 28th October** *PLYMOUTH*
Symposium on the Application of Multivariable Systems Theory, organized by the Institute of Measurement and Control to be held at the Royal

Naval Engineering College, Manadon. Information: The Institute of Measurement and Control, 20 Peel Street, London W8 7PD. (Tel. 01-727 0083).

Instrumentation 26th to 28th October LONDON
Electronic Test & Measuring Instrumentation Exhibition and Conference, to be held at the Wembley Conference Centre. Information: Trident International Exhibitions Ltd, 21 Plymouth Road, Tavistock, Devon PL19 8AU. (Tel. (0822) 4671).

Instrumentation in Flammable Atmospheres 28th October LUTON
(See item for 30th September)

Pattern Recognition 19th to 22nd October MUNICH
Sixth International Conference on Pattern Recognition, sponsored by the IEEE in association with the IAPR and DAGM, to be held at the Technical University of Munich. Information: Harry Hayman, P.O. Box 369, Silver Spring, MD 20901 (Tel. (301) 589-3386).

Broadcasting 19th to 21st October SAARBRUCKEN
Conference on Broadcasting Satellite Systems organized by the VDE(NTG) with the association of the specialized groups of the DGLR and the IRT. Information: Herrn Dipl. Ing. Walter Stosser, AEG-Telefunken, Gerberstrasse 33, 7150 Backnang

Manufacturing Technology 26th to 28th October GAITHERSBURG
Fourth IFAC/IFIP Symposium on Information Control Problems in Manufacturing Technology organized by the National Bureau of Standards, US Department of Commerce, in association with IFAC/IFIP will be held in Gaithersburg, Maryland. Information: Mr J. L. Nevins, Vice Chairman, National Organizing Committee, 4th IFAC/IFIP Symposium Charles Stark Draper Labs, Inc. 555 Technology Square Cambridge, MA 02139 USA. (Tel. (617) 258 1347)

NOVEMBER

***Robot 2nd to 4th November LONDON**
International Conference on Robot Vision and Sensory Control—'Intelligent Robot Systems for the Mid Eighties'. Information: Conference Director, IFS (Conferences) Ltd 35-39 High Street, Kempston, Bedford

Computers 16th to 19th November LONDON
Compec Exhibition, to be held at the Olympia Exhibition Centre, London. Information: IPC Exhibitions Ltd, Surrey House, 1 Throwley Way, Sutton, Surrey SM1 4QQ. (Tel. 01-643 8040).

Safety 23rd to 25th November SEVENOAKS
A three-day course on Safety of Electrical Instrumentation in Potentially Explosive Atmospheres, organized by SIRA Institute, will be held at Cudham Hall, Sevenoaks, Kent. Information: Conferences and Courses Unit, SIRA Institute Ltd, South Hill, Chislehurst, Kent BR7 5EH (Tel. 01-467 2636)

Instrumentation in Flammable Atmospheres 25th November LUTON
(See item for 30th September)

DECEMBER

***Electrical Safety 1st to 3rd December LONDON**
Conference Electrical Safety in Hazardous Environments, organized by the IEE. Information: Conference Department, Institution of Electrical Engineers, Savoy Place, London WC2R 0BL. (Tel. 01-240 1871)

ONLINE 7th to 9th December LONDON
The Sixth International Online Information Meeting, organized by *Online Review*, will be held at the Cunard Hotel, London. Information: Organizing Secretary, Online Information Meetings, *Online Review*, Learned Information, Besselsleigh Road, Abingdon, Oxford OX13 6LG. (Tel. 0865-730275)

***INDEX-EL '82 10th to 15th December ATHENS**
Second International Electrical & Electronics Engineering Exhibition, will be held at The Zappio Palace, Athens. British exhibits sponsored by EEA. Information: EEA, 8 Leicester Street, London WC2H 7BN. Tel. 01-437 0678.

1983

JANUARY

***Computer Simulation 27th to 29th January SAN DIEGO**
Multiconference on Modelling and Simulation on Microcomputers organized by The Society for Computer Simulation, will be held at the Holiday Inn, Embarcadero, San Diego. Information: SCS, P.O. Box 2228, La Jolla, California 92038, U.S.A.

FEBRUARY

MECOM '83 7th to 10th February BAHRAIN
Third Middle East Electronic Communications Show and Conference, organized by Arabian Exhibition Management, to be held at the Bahrain Exhibition Centre. Information: Dennis Casson, MECOM '83, 49/50 Calthorpe Road, Edgbaston, Birmingham B15 1TH. (Tel. (021) 454 4416).

MARCH

Component Assembly March BRIGHTON
Brighton Electronics Exhibition on matching components

with insertion, connection and assembly aids and techniques, to be held in Brighton. Information: The Press Officer, Trident International Exhibitions Ltd, 21 Plymouth Road, Tavistock, Devon PL19 8AU. (Tel. (0822) 4671).

●Telecommunications Networks 21st to 25th March BRIGHTON

Second International Network Planning Symposium (Networks '83), organized by the Institution of Electrical Engineers with the association of the IERE, to be held at the University of Sussex, Brighton. Information: IEE Conference Department, Savoy Place, London WC2R 0BL. (Tel. 01-240 1871).

Inspex '83 21st to 25th March BIRMINGHAM
Tenth International Measurement and Inspection Technology Exhibition, sponsored by *Measurement and Inspection Technology* in association with IQA and Gauge and Tool Makers' Association, to be held at the National Exhibition Centre, Birmingham. Information: Exhibition Manager, Inspex '83, IPC Exhibitions Ltd, Surrey House, 1 Throwley Way, Sutton, Surrey SM1 4QQ. (Tel. 01-643 8040).

APRIL

Engineering Education 6th to 8th April PARIS
Second World Conference on Continuing Engineering Education, organized by the European Society for Engineering Education, to be held at UNESCO Headquarters in Paris. Information: Mr N. Krebs Ovesen, Danish Engineering Academy, Building 373, DK 2800, Lyngby, Denmark.

●ICAP '83 12th to 15th April NORWICH

Third International Conference on Antennas and Propagation organized by the IEE in association with the URSI, IEEE, IMA, IoP and the IERE, will be held at the University of East Anglia, Norwich. Information: IEE Conference Department, Savoy Place, London WC2R 0BL. (Tel. 01-240 1871, ext. 222)

MAY

Test and Measurement 2nd to 5th May SAN JOSE
The Second Annual Test and Measurement World Expo will be held at the San Jose Convention Center. Information: Meg Bowen, Test and Measurement World Expo, 215 Brighton Avenue, Boston, MA 02134 U.S.A.

Noise 17th to 20th May MONTPELLIER, FRANCE
Seventh International Conference on Noise in Physical Systems/3rd International Conference on 1/f Noise, will be held in Montpellier, France. Information: Dr B. Jones, Department of Physics, University of Lancaster, (Tel.

Lancaster 65201). or Professor H. Sutcliffe, Department of Electronic & Electrical Engineering, University of Salford.

Electron Tubes 18th to 20th May GARMISCH-PARTENKIRCHEN, WEST GERMANY

Conference on Electron Tubes organized by VDE (NTG) in association with the German Section of the IEEE, will be held in Garmisch-Partenkirchen, Bavaria. Information: Conference Chairman, Dr H. Heynisch, Siemens AG, Werk für Röhren und Sondergebiete, St Martinstrasse 76, D-8000 München 80.

JUNE

IOOC '83 27th to 30th June TOKYO
The Fourth International Conference on Integrated Optics and Optical Fibre Communication, sponsored jointly by the Institute of Electronics and Communication Engineers of Japan and the Institute of Electrical Engineers of Japan, will be held at Keio Plaza Hotel, Tokyo. Information: Y. Suematsu, Department Elec. Phys. Tokyo Institute of Technology, 2-12-1, O-okayama, Meguro-ku, Tokyo, 152 Japan.

JULY

***Reliability '83 6th to 8th July BIRMINGHAM**
Fourth National Reliability Conference organized by the National Centre of Systems Reliability in association with the Institute of Quality Assurance, will be held at the National Exhibition Centre, Birmingham. Information: Mr A. Cross, National Centre of Systems Reliability, UKAEA, Wiggshaw Lane, Culcheth, Warrington WA3 4NE.

SEPTEMBER

***C.A.S.T. '83 13th to 15th September BIRMINGHAM**
First International Conference and Exhibition on Cable and Satellite Television organized by Cable and Satellite Television Exhibitions, will be held at the Birmingham Metropole Hotel. Information: Exhibition, Michael Hyams, Managing Director, Cable & Satellite TV Exhibitions Ltd, 5 Barratt Way, Tudor Road, Harrow HA3 5QG. (Tel. 01-863 7726) Conference, The Economist Conference Unit, 25 St James's Street, London SW1 1HG. (Tel. 01-839 7000)

Simulators 26th to 30th September BRIGHTON
International Conference on Simulators, organized by the IEE, will be held at the University of Sussex. Information: IEE Conference Department, Savoy Place, London WC2R 0BL. (Tel. 01-240 1871) (*Synopses by 4th October.*)

Weightech '83 13th to 15th September LONDON

Third International Industrial and Process Weighing and Force Measurement Exhibition and Conference, organized by Specialist Exhibitions in association with the Institute of Measurement and Control, to be held at the Wembley Conference Centre. Information: Specialist Exhibitions Ltd, Green Dragon House, 64/70 High Street, Croydon, CR9 2UH. (Tel. 01-686 5741) Conference Information: IMC, 20 Peel Street, London W8 7PD. (Tel. 01-727 0083).

OCTOBER

***Computer Graphics '83 4th to 6th October LONDON**
Conference and Exhibition on Computer Graphics organized by Online Conferences. Information: Online Conferences Ltd, Argyle House, Northwood Hills, Middlesex HA6 1TS. (Tel. (09274) 28211).

Security Technology 4th to 6th October ZURICH
17th Carnahan Conference on Security Technology, organized by the Institute for Communication Technology at the Eidg. Technische Hochschule Zurich, in association with the College of Engineering, University of Kentucky, will be held in Zurich. Information: P. de Bruyne, ETH Zentrum-KT, CH-8092 Zurich, Switzerland. (Tel. 411-2562792)

***Viewdata '83 18th to 20th October LONDON**
Conference and Exhibition organized by Online Conferences. Information: Online Conferences Ltd, Argyle House, Northwood Hills, Middlesex HA6 1TS. (Tel. (09274) 28211).

Telecom '83 26th October to 1st November GENEVA
Second World Telecommunication Exhibition, organized by the International Telecommunications Union, to be held at the New Exhibition Conference Centre in Geneva. Information: Telecom '83, ITU, Place des Nations, CH-1211 Genève 20, Switzerland. (Tel. (022) 99 51 11).

Organizers of appropriate events are invited to submit details to the Editor for inclusion in this calendar.